LAURA YLÄ-OUTINEN

Functionality of Human Stem Cell Derived Neuronal Networks

Biomimetic environment and characterization

ACADEMIC DISSERTATION
To be presented, with the permission of the board
of the Institute of Biomedical Technology of the University of Tampere,
for public discussion in the Small Auditorium of Building B,
School of Medicine of the University of Tampere,
Medisiinarinkatu 3, Tampere, on March 30th, 2012, at 12 o'clock.

UNIVERSITY OF TAMPERE

UNIVERSITY
OF TAMPERE

ACADEMIC DISSERTATION
University of Tampere, Institute of Biomedical Technology
Finland

Supervised by
Docent Susanna Narkilahti
University of Tampere
Finland
Professor Jari Hyttinen
University of Tampere
Finland

Reviewed by
Docent Markku Penttonen
University of Jyväskylä
Finland
Assistant Professor Ana Teixeira
Karolinska Institutet
Sweden

Distribution
Bookshop TAJU
P.O. Box 617
33014 University of Tampere
Finland

Tel. +358 40 190 9800
Fax +358 3 3551 7685
taju@uta.fi
www.uta.fi/taju
http://granum.uta.fi

Cover design by
Mikko Reinikka

Acta Universitatis Tamperensis 1714
ISBN 978-951-44-8755-2 (print)
ISSN-L 1455-1616
ISSN 1455-1616

Acta Electronica Universitatis Tamperensis 1184
ISBN 978-951-44-8756-9 (pdf)
ISSN 1456-954X
http://acta.uta.fi

Tampereen Yliopistopaino Oy – Juvenes Print
Tampere 2012

To Ville

Abstract

Cell transplantation therapies provide new hope for central nervous system deficits. In particular, stem cells are a potential source for new regenerative therapies. Human embryonic stem cells (hESC) are considered to be useful for transplantation therapies as they can be successfully differentiated into central nervous system cell types, i.e., neurons, astrocytes, and oligodendrocytes, in sufficient quantities. Another interesting pluripotent cell type, human induced pluripotent stem cells (hiPSCs), was recently identified as a potential source for clinical applications. Both of these pluripotent stem cell types also have rather high potential for *in vitro* platforms. Thus, these cells can be used for toxicology studies, drug screening, developmental research, and patient-specific drug research and diagnostics.

Before the full benefits of these cells can be realized, however, they must be intensively studied in a more *in vivo* like, i.e., biomimetic, environment, in three-dimensional (3D) structures. In 3D, cells interact and behave more like their *in vivo* counterparts. Thus, for *in vitro* models as well as research aimed at regenerative medicine, cells should be tested in a 3D environment. In the present study, a large variety of natural and synthetic biomaterials as growth surfaces or 3D matrices were tested for application to hESC-derived neuronal cells. One synthetic self-assembled peptide hydrogel, PuraMatrix, was also tested in 3D. Human ESC-derived neuronal cells grew and matured in this 3D scaffold.

One of the most important functions of neuronal cells, in addition to their chemical activity, is their electrical activity. Thus, the characteristics of hESC- or hiPSC-derived neuronal cells must be evaluated at the functional, i.e., electrophysiologic level. The electrical activity of hESC-derived neuronal cells at the network level was evaluated using a microelectrode array (MEA) method and the cell culture measurement environment was further improved for that specific cell type. The electrical measurement methods can be used for *in vitro* toxicology studies, as they allow for continuous, noninvasive, and sensitive characterization.

Here, we evaluated and confirmed the validity of hESC-derived neuronal cells and the MEA measurement platform for in vitro neurotoxicity analysis.

The electrical activity of hESC-derived neuronal cells was also evaluated in a 3D scaffold in which cells were encapsulated inside a hydrogel. The cells formed a functional neuronal network in this biomimetic 3D environment, thus providing a platform for *in vitro* toxicology studies the results can be applied to further improve the field of neuronal tissue engineering.

More detailed information about the activity of hESC-derived neuronal cells and their networks are needed before these cells can be reliably used in transplantation therapies. Moreover, further optimization is needed for cell differentiation and maturation processes as well as for data analysis before these cells on MEA can be used as a valid *in vitro* neurotoxicity platform.

Tiivistelmä

Solusiirtohoidot nähdään keskushermoston vakavien sairauksien ja traumojen tulevaisuuden hoitomuotona. Erityisesti kantasoluista erilaistetut solut voisivat olla sopiva solulähde näihin soluterapioihin. Ihmisalkion kantasoluista erilaistetut hermosolut ovat potentiaalisia soluja näihin soluhoitoihin ja niitä onkin saatu onnistuneesti erilaistettua keskushermoston solutyypeiksi: hermosoluiksi, astrosyyteiksi ja oligodendrosyyteiksi. Aivan viimeaikoina toisenkin mielenkiintoisen ihmisperäisen pluripotentin kantasolutyypin, ihmisen indusoitujen pluripotenttien kantasolujen, on todettu erilaistuvan laboratorio-olosuhteissa hermosoluiksi ja hermotukisoluiksi.

Näistä molemmista solutyypeistä erilaistetut hermosolut nähdään potentiaalisiksi solulähteeksi erilaisiin laboratorio-olosuhteissa, *in vitro*, toteutettaviin analyyseihin kuten lääkeainemallinnukseen, toksisuusanalyyseihin, kehitysbiologisiin malleihin sekä potilas-spesifiseen diagnostiikkaan ja lääkeainetutkimukseen.

Lisäksi, ennen kuin alkion kantasoluista erilaistettuja soluja voidaan käyttää soluterapioihin tai *in vitro* malleihin, niiden ominaisuuksia ja toimintaa on tutkittava kudoksen kaltaisessa ympäristössä *in vitro*, mieluiten kolmiulotteisessa, biomimeettisessä, rakenteessa. Siksi on tärkeää tutkia näitä solutyyppejä *in vitro* biomateriaalialustoilla. Tässä työssä tutkittiin ihmisalkion kantasoluista erilaistetuille soluille soveltuvia biomateriaaleja sekä 2D että 3D ympäristössä. Kaupallisen synteettisen PuraMatrix-hydrogeelin soveltuvuutta solujen 3D rakenteeksi tutkittiin tarkemmin.

Lisäksi solujen toiminnallisuus on tärkeä tutkimuskohde, hermosolujen tapauksessa sähköisen aktiivisuuden tutkimus elektrofysiologisten mittausten avulla. Tässä työssä ihmisalkion kantasoluista erilaistettujen hermosolujen sähköistä aktiivisuutta on tutkittu mikroelektrodihila (microelectrode array, MEA)-menetelmällä hermoverkkotasolla. Lisäksi MEA mittausympäristöä parannettiin alkion kantasoluista erilaistetuille soluille paremmin soveltuvaksi polydimetyylisiloksaanista valmistetun solukasvatusrakenteen avulla. Sähköisen

aktiivisuuden mittausta voidaan hyödyntää mm. soluhoitoihin käytettävien solujen *in vitro* tutkimuksessa ja toksikologiamittausalustoina. Tämä työ osoittaa, että ihmisalkion kantasoluista erilaistetut hermosolut soveltuvat MEA-mittaustekniikalla tehtäviin *in vitro*- toksisuusmittauksiin.

Tässä työssä osoitetaan että ihmisalkion kantasoluista erilaistetut hermosolut muodostavat spontaanisti aktiivisen hermoverkon myös kolmiulotteisessa ympäristössä. Solut, joita on kasvatettu hydrogeelimatriisin sisällä, muodostavat sähköisesti aktiivisen hermoverkon, jonka aktiivisuutta pystytään mittaamaan MEA-laitteistolla. Tälläistä 3D solurakennetta voidaan tulevaisuudessa hyödyntää myös *in vitro*-toksisuusmittauksissa.

Tulevaisuudessa ihmisalkion kantasoluista erilaistettuja soluja voidaan käyttää toksismäärityksissä ja jopa soluhoidoissa, mutta ennen tätä soluja tulee tutkia vielä paljon *in vitro*. Lisäksi solujen kasvatus- ja erilaistusmenetelmiä tulee vielä parantaa ennen kuin näitä soluja voidaan käyttää luotettaviin soluterapioihin tai validoituihin toksisuusmalleihin.

Acknowledgements

This study was performed at the Institute of Biomedical Technology (former Regea), at University of Tampere during years 2008-2012.

I owe my deepest gratitude to my supervisor, docent Susanna Narkilahti, for engaging me into her research group, first for bachelor thesis, and further via master thesis to PhD studies. She gave me a great change to adopt into magnificent field of academic research, and I am grateful for her supervising, support, and mentoring during and especially at the final stage of this project.

My second supervisor, Prof. Jari Hyttinen, is acknowledged for his leading and support during this project. Specifically I am grateful for the support in MEA area.

I want to acknowledge the official reviewers for this thesis, Ana Teixeira, PhD, and Adj. Prof. Markku Penttonen for reviewing this book and giving me valuable comments.

The members of follow-up group, docent Heli Skottman, Jarno Mikkonen, PhD, and Prof. Minna Kellomäki are acknowledged for their support during these years, although, mostly unofficially.

I express my gratitude to all my co-authors: Juha Heikkilä, BSc.; Teemu Heikkilä, MSc, BMed; Prof. Jari Hyttinen, Tiina Joki, BSc; Tiina Kaarela, BSc; Prof. Pasi Kallio, Joose Kreutzer, MSc.; Paula Kärnä, BSc; Jarno Mikkonen, PhD; Docent Susanna Narkilahti; Docent Heli Skottman; Prof. Riitta Suuronen; Jarno Tanskanen PhD; Mari Varjola, MSc; and Riikka Äänismaa, PhD.

I want to thank the personnel of IBT, former Regea, for the support in stem cell culturing and research. I owe my deep gratitude to our research group, NeuroGroup. All former and existing lab technicians, students, PhD students, post docs and, of course, group leader Susanna Narkilahti are acknowledged for great working atmosphere, valuable advices, great laughs, and share of the everyday life.

I thank my all dear friends, inside and outside the University, for keeping me in touch with real life.

Last, but not least, I am forever grateful for my parents, my brothers, and my dear husband Ville.

This study was financially supported by the Academy of Finland, Alfred Kordelin Foundation, BioneXt Tampere, Brain Research Society of Finland, Competitive Research Funding of Pirkanmaa Hospital District, Finnish Cultural Foundation: Pirkanmaa Regional Fund, the Finnish Funding Agency for Technology and Innovation, Orion-Farmos Research Foundation, and the Science Foundation of the City of Tampere.

Table of Contents

List of abbreviations

A2B5	Cell surface ganglioside epitope
AFP	Alpha-fetoprotein
BDNF	Brain-derived neurotrophic factor
bFGF	Basic fibroblast growth factor
BLBP	Brain lipid-binding protein
BrdU	Bromodeoxyuridine
BSA	Bovine serum albumin
ChAT	Choline acetyltransferase
CNS	Central nervous system
CNQX	6-cyano-7-nitroquinoxaline-2,3-dione
CNTF	Ciliary neurotrophic factor
DACH1,	Dachshund homolog 1
D-AP5	D-(-)-2-Amino-5-phosphonopentanoic acid
DAPI	4',6-diamidino-2-phenylindole
DMEM	Dulbecco's modified eagle medium
dPBS	Dulbecco's Phosphate Buffered Saline
ECM	Extracellular matrix
EGF	Epidermal growth factor
ELISA	Enzyme-linked immunosorbent assay
EMX2	Homeobox protein-2, transcription factor
EthD-1	Ethidium homodimer-1
GABA	γ-Aminobutyric acid
GalC	Galactosylceramidase
GBx-1	Gastrulation brain homeobox 1, transcription protein
GFAP	Glial fibrillary acidic protein
GLT-1	Glutamate transporter GLT-1 (EAAT2)
hESC	Human embryonic stem cell
hiPSC	Human induced pluripotent stem cell
hNT-3	Human neurotrophin-3
IGF-1	Insulin-like growth factor 1
Klf-4	Krueppel-like factor 4
LED	Light-emitting diode
Lin28	Homolog A, transcription factor, a marker of undifferentiated cells
MAP-2	Microtubule-associated protein 2
MCS	Multichannel Systems Gmbh
MEA	Microelectrode array

MEF	Mouse embryonic fibroblasts
mRNA	Messenger Ribonucleic acid
NCAM	Neural Cell Adhesion Molecule
NDM	Neuronal differentiation medium
NDS	Normal donkey serum
NF-200	Neurofilament 200 kD
NG2	Chondroitin sulfate proteoglycan
NkX2.1	Thyroid transcription factor
nurr-1	Nuclear receptor related protein-1
oct 3/4	Octamer3/4
Olig-2	Oligodendrocyte transcription factor 2
OPC	Oligodendrocyte progenitor cells
Pax-6	Paired box protein-6
PCR	Polymerase chain reaction
PDGF-AA	Human platelet derived growth factor AA
PDMS	Polydimethylsiloxane
PFA	Paraformaldehyde
POM	Poly(oxymethylene)
PTFE	Polytetrafluoroethylene
qRT-PCR	Quantitative real-time PCR
RC-2	Radial glia marker
sox-1/2	Sex determining region Y-box 1, transcription factor
TH	Tyrosine hydroxylase
TTX	Tetrodotoxin

List of original publications

Study I: Heikkilä T, **Ylä-Outinen L**, Tanskanen J, Lappalainen R, Skottman H, Suuronen R, Mikkonen J, Hyttinen J, Narkilahti S. (2009). Human embryonic stem cell-derived neuronal cells form spontaneously active neuronal networks *in vitro*. Exp Neurol. 218(1):109-16.

Study II: Kreutzer J*, **Ylä-Outinen L***, Skottman H, Mikkonen J, Narkilahti S & Kallio P. (2012). Structured PDMS chambers for culturing and monitoring human neuronal cell activity on microelectrode array platforms. J Bionic Eng.9(1):1-10. * equal contribution

Study III: **Ylä-Outinen L,** Heikkilä J, Skottman H, Suuronen R, Äänismaa R, Narkilahti S. (2010). Human cell-based micro electrode array platform for studying neurotoxicity. Front Neuroeng, 3:111

Study IV: **Ylä-Outinen L,** Joki T, Varjola M, Skottman H, Narkilahti S. (2012). Three dimensional growth matrix for human embryonic stem cell-derived neuronal cells. J Tissue Eng Regen Med. *Accepted.*

1. Introduction

Transplantation therapies are considered to be the third potential therapeutic method in modern medicine, after surgery and pharmaceuticals (Lindvall *et al.* 2006) and have raised hopes for the treatment of central nervous system (CNS) deficits. In particular, stem cells are considered a potential source for new regenerative therapies.

Human embryonic stem cells (hESC) have considerable potential for transplantation therapies. They have already been successfully differentiated into CNS cell types: neurons, astrocytes, and oligodendrocytes (Lappalainen *et al.* 2010; Sundberg *et al.* 2010). Human-induced pluripotent stem cells (hiPSCs) are another potential pluripotent stem cell source. They were originally derived from adult human cells, e.g., fibroblasts, by genetic modification (Takahashi *et al.* 2007; Yu *et al.* 2007). Both types of human pluripotent stem cells (e.g., hESCs and hiPSCs) are potential cell sources for transplantation therapies. Human pluripotent stem cells also have potential as *in vitro* toxicity and drug testing models and for use in developmental studies, disease modeling, and patient-specific diagnostics (Bal-Price *et al.* 2009; Johnstone *et al.* 2010; Zeng *et al.* 2006).

The most crucial property of neuronal cells is their ability to receive and transmit electrical signals and to form functional neuronal networks. Thus, the electrophysiologic properties of stem cell-derived neurons are important characteristics that influence their applicability in regenerative medicine and *in vitro* studies. Electrophysiologic properties of neuronal cells are characterized using the patch clamp method, extracellular field recordings (including microelectrode array [MEA] technology), and ratiometric gelator imaging (such as Ca^{2+}-imaging) (Bajpai *et al.* 2009; Cai *et al.* 2004).

Before the full potential benefit of human derived neuronal cells can be realized for these applications, however, the cells must be studied in a more *in vivo* like, i.e., biomimetic, environment, such as in three-dimensional (3D) structures. Neuronal cell cultures are usually two-dimensional (2D), allowing cells to interact in only two

directions, which results in fewer connections between cells, longer neuronal processes, increased proliferation, and decreased maturation compared to those in 3D culture (Geckil *et al.* 2010). *In vivo,* neuronal cells are surrounded by other cells and an extracellular matrix (ECM) and form highly organized neuronal networks. For biomimetic measurements, cells should grow in as natural an environment as possible, and thus the development of a biomimetic 3D structure for neuronal cells is crucial. Biomaterials used as scaffolds for neuronal cells should be biocompatible, support neuronal cell growth, and maintain cell phenotype and/or improve maturation of the formed networks.

In this doctoral thesis, hESC-derived neuronal cells were characterized with MEA technology, which has not been previously applied in studies of these cells. A novel 2D environment for MEA measurements was developed to improve the outcome, and a proof-or-principle study using hESC-derived neuronal cells as a 2D neurotoxicologic platform was performed. Different substrates were tested as possible 2D or 3D matrices for human-derived neuronal cells, and a suitable hydrogel scaffold, a 3D biomimetic environment supporting the growth and functional network formation of these cells, was developed.

2. Literature review

2.1 Stem cells

Stem cells have two unique properties: they can divide in an undifferentiated stage and begin to differentiate into specific cell type(s) depending on their differentiation capacity. Stem cells can divided into three groups based on their differentiation capacity: 1) totipotent cells are able to form a new individual (e.g., fertilized egg and very early embryo); 2) pluripotent cells can differentiate into any cell type of any organ (e.g., inner cell mass embryonic cells); and 3) multipotent stem cells are more limited in their differentiation capacity (e.g., fetal and adult stem cells).

Human ESCs are pluripotent cells that have nearly unlimited developmental potential. Even after months of growth, hESCs continue to replicate and maintain their ability to differentiate into any human body cell type (Thomson *et al.* 1998). Because of these unique properties, hESCs can be used for transplantation therapies or in different *in vitro* models, such as toxicologic, drug screening, and developmental models (Bal-Price *et al.* 2009; Johnstone *et al.* 2010; Rolletschek *et al.* 2004; Zeng *et al.* 2006). Due to their huge potential in medical and pharmacologic fields, much effort has been focused on optimizing hESC culture conditions. Culturing hESCs *in vitro* in an undifferentiated stage requires intensive labor. HESCs grow as colonies, tightly-packed structures that contain thousands of stem cells. Human ESCs are cultured on top of a feeder layer, originally on mouse embryonic fibroblasts (Thomson *et al.* 1998), and more recently on human fibroblasts or ECM-mimicking materials, such as Matrigel, or synthetic ECM-mimicking proteins (Bissonnette *et al.* 2011; Erceg *et al.* 2009; Kim *et al.* 2011). Human ESCs maintain their pluripotency with the support of growth factors; fibroblast growth factor (FGF) is most commonly used (Thomson *et al.* 2006) .

The first hESC lines were derived in 1998 by Thomson and colleagues, and since then there have been at least 650 registered lines derived worldwide (European human embryonic stem cell registry, http://www.hescreg.eu/). The pluripotency of

hESCs is confirmed by gene and protein expression, a germ layer formation test, and a teratoma formation test.

One of the newest pluripotent cell types is the induced pluripotent stem cell (iPSC). These cells are reverted to the stem cell stage from fibroblasts by gene transduction. In 2007, two groups published a new method to produce iPSCs. They transfected fibroblasts with pluripotent genes, including Oct-3/4, Sox-2, Klf-4, and c-Myc (Takahashi *et al.* 2007) or Oct-3/4, Sox-2, Nanog, and Lin28 (Yu *et al.* 2007). These reprogrammed cells act like hESCs, but much more information is needed about their behavior and pluripotent gene-silencing during differentiation before these cells can be used in clinical studies (Kim *et al.* 2011). Nevertheless, hiPSC-differentiated cells, as well as hESC-differentiated cells, show line-specific differences in their differentiation potential (Kim *et al.* 2011; Lappalainen *et al.* 2010). Both human pluripotent stem cell types, however, have been successfully differentiated into neuronal cell types, including electrically functional neuronal cells, astrocytes, and oligodendrocytes.

Multipotent cell types (including fetal stem cells) are also considered to have high potential for different clinical applications because they carry a smaller risk of forming tumors compared to cells of ESC origin (Lindvall *et al.* 2006; Lindvall *et al.* 2010; Sundberg *et al.* 2010). Fetal stem cells have very limited availability and ethical complexities, but can also cause tumor formation (Amariglio *et al.* 2009). Adult stem cells can be harvested from fat tissue, blood, bone marrow, cartilage, and placenta (Ashammakhi *et al.* 2004). These cells have a limited differentiation capacity, so producing sufficient amounts of neuronal cells for transplantation therapies is very challenging (Delcroix *et al.* 2010).

2.2 Neuronal differentiation and network formation

Human ESCs are an excellent source of cells for production of the main cell types of the human brain: neurons, astrocytes, and oligodendrocytes (Erceg *et al.* 2008; Lappalainen *et al.* 2010; Reubinoff *et al.* 2001; Sundberg *et al.* 2010; Zhang *et al.* 2001). Neuronal cells were differentiated from hESCs using specific methods for the first time in 2001 (Carpenter *et al.* 2001; Reubinoff *et al.* 2001; Zhang *et al.* 2001). In these studies, the differentiation protocol began with the embryoid body

formation step. Cells were inducted towards neuronal lineages with bFGF, epidermal growth factor, platelet derived growth factor AA, insulin-like growth factor-1, human neurotrophin-3, or brain-derived neurotrophic factor in either an adherent culture (Carpenter *et al.* 2001; Zhang *et al.* 2001) or suspension culture (Reubinoff *et al.* 2001). These cells were differentiated into neuronal cells, expressing microtubule-associated protein-2 (MAP-2), β-tubulin$_{III}$, and synaptophysin. These cells also showed the electrophysiologic characteristics of neuronal cells, based on the expression of functional Na^{2+} and K^{+}-channels, and evoked action potentials (Carpenter *et al.* 2001).

The developed differentiation methods, adherent or suspension cultures, have been used since with various modifications between laboratories. In principle, both methods produce similar neuronal populations, with phenotypic (e.g., MAP-2, β-tubulin, and PAX-6) and genotypic (e.g., *PAX-6, nestin, β-tubulin, MAP-2*) markers for neuronal cells (Bissonnette *et al.* 2011; Nat *et al.* 2007). These produced neuronal cells have electrical properties that are comparable to their brain counterparts (Carpenter *et al.* 2001; Erceg *et al.* 2008; Itsykson *et al.* 2005; Johnson *et al.* 2007). Further, neuronal cells are targeted to differentiate into region-specific neural tissue subtypes (Liu *et al.* 2011). Most of the research to date has focused on producing spinal cord motoneurons, dopaminergic neurons, and cholinergic neurons (Bissonnette *et al.* 2011; Cimadamore *et al.* 2011; Liu *et al.* 2011; Yuan *et al.* 2011; Zeng *et al.* 2010).

Other neural tissue cell types, namely astrocytes and oligodendrocytes, have been differentiated from hESCs and hiPSCs (Yuan *et al.* 2011). Pluripotent stem cell-derived astrocytes show the typical markers for their *in vivo* counterparts, including glial acidic fibrillary protein (GFAP), astrocyte-specific glutamate transporter-1, and S100β (Krencik *et al.* 2011; Liu *et al.* 2011). They also improve neuronal functions in damaged tissue (Davies *et al.* 2011). Oligodendrocytes, or their progenitors, oligodendrocyte precursor cells (OPCs), have attracted high interest for spinal cord injury transplantation therapies (Keirstead *et al.* 2005). These cells are also differentiated from human pluripotent stem cells, and those cells most typically express NG2, galactocerebroside, and Olig-2 (Sundberg *et al.* 2010; Yuan *et al.* 2011).

Further, the purity of the produced cell populations and a culture environment without animal-derived factors (xeno-free) have become more important issues as

the applications for therapeutic use of these cells nears reality (Nistor *et al.* 2011; Yuan *et al.* 2011). Transplantation therapies are the ultimate potential application for these pluripotent stem cell-derived neuronal or neural cells, and thus the culture and cell material should meet the regulations of clinically used materials (Lindvall *et al.* 2010). The regulative authorities, the Food and Drug Administration in the USA and European Medicines Agency in Europe, have set rules and guidelines for planned transplantation therapies.

2.3 Cell and network characterization

Produced neuronal cell populations must be characterized to verify their characteristics and similarity to the native tissue cell types. Neuronal cells are usually characterized based on genotype, phenotype, morphology, and electrical activity levels.

At the genotype level, the polymerase chain reaction method is most commonly used to evaluate gene expression at the mRNA level. First, silencing the pluripotent markers, such as *oct-4, nanog, sox-2,* and endo- (*AFP*) and mesodermal (*brachyury*) markers are verified (Erceg *et al.* 2010; Kim *et al.* 2011). The early neuronal markers, including three commonly used genes: *PAX-5/6, neural cell adhesion molecule, and Sox-1,* indicate the presence of neuroectodermal/neuronal precursor cells at the beginning of differentiation (Erceg *et al.* 2010; Kim *et al.* 2011). Neuronal markers, including *MAP-2* and *β-tubulin,* show the stages of neuronal cells (Erceg *et al.* 2010; Kim *et al.* 2011; Lappalainen *et al.* 2010). Further, region-specific or cell type-specific markers such as *Dachshund homolog 1, Homeobox protein-2, thyroid transcription factor), and nuclear receptor related protein-1,* shows the maturation of the neuronal cells (Erceg *et al.* 2010; Kim *et al.* 2011) .

Similar patterns of unwanted markers, early markers, neuronal cell markers, and cell type-specific markers can be used for protein level analysis, including immunocytochemical staining, enzyme-linked immunosorbent assay methods, and Western blotting methods. Typical immunocytochemical markers for undifferentiated cells are: Oct-3/4, Nanog, Tra1-60, Stage-specific embryonic antigen-1/4 (Bissonnette *et al.* 2011; Erceg *et al.* 2010; Kim *et al.* 2011; Lappalainen *et al.* 2010). For early neuronal cells, Nestin, musashi, Pax-6, and Sox-

1 are used. For neuronal cells β-tubulin and MAP-2 are widely used markers. Region-specific neuronal cells are stained against: Gbx-1, γ-aminobutyric acid (GABA), serotonin, glutamate, HB-9, choline acetyltransferase, and tyrosine hydroxylase. Common glial cell markers are brain lipid-binding protein, RC-2, O4, A2B5, and GFAP (Bissonnette *et al.* 2011; Erceg *et al.* 2010; Kim *et al.* 2011; Lappalainen *et al.* 2010).

Immunocytochemical imaging as well as other microscopy techniques, either from live or fixed cell cultures, provides morphology information. Pattern recognition methods can be used for automated cell type clustering from phase-contrast imaged cells (Lappalainen *et al.* 2010; Narkilahti *et al.* 2007).

2.4 Electrical activity of the neuronal networks

Electrically active cells, here neuronal cells, have specific electrical properties across the cell membrane that gives them the ability to deliver electrical signals. The potential gradient across the cell membrane is generated via ion channels. These channels control the ion flux through of the cell membrane, which generates the action potentials. In neuronal networks, cell signaling is mediated via synaptic connections, where neurotransmitters and their receptors are involved in propagating the signal over the synaptic cleft (Purves *et al.* 2008).

The electrical properties of the neuronal cells can be measured either intracellularly or extracellularly. In intracellular methods, the electrical potential across the membrane is measured. In extracellular methods, the local differences of extracellular space ion concentrations, e.g., potential, are measured. In intracellular methods, the most important measured parameters are passive membrane potential, ion channel kinetics, and cell excitability. A mature neuron has a membrane potential ranging from -50 to -70 mV; contains ionotrophic sodium, potassium, and calcium channels; and a variety of neurotransmitter-specific receptors (Purves *et al.* 2008). The local field potentials of the neuronal networks are detected extracellularly. This detected electrical potential change can be divided into fast responses (> 200-500 Hz), action potentials, and slow responses (< 200-500 Hz), so-called field potentials. Extracellular methods are concentrated on network activity properties and thus the most important measured parameters are excitability of the

neuronal network (amount of action potentials), responses to pharmaceutical and electrical stimulation, and plasticity of the neuronal network (Purves *et al.* 2008).

2.4.1 Patch clamp

The patch clamp method is used for both intracellular and extracellular measurements, but usually for intracellular measurements. The patch clamp allows for measuring one or, in the hands of a very patient researcher, two or more cells. This method provides excellent information about membrane potential, excitability, and the ion channel composition of the cells. Neuronal cells have specific electrophysiologic properties and thus the cells can be clustered according to these properties. Patch clamp measurement methods can be divided into voltage clamp and current clamp techniques (Hodgkin *et al.* 1952; Purves *et al.* 2008).

Pharmacologic responses are the main focus of patch clamp-techniques, such as tetrodotoxin (TTX, Na-channel blocker), GABA (GABA agonist), bicuculline (GABA-a receptor blocker), D-(-)-2-amino-5-phosphonopentanoic acid (D-AP5, an N-methyl D-aspartate [NMDA] receptor antagonist), 6-cyano-7-nitroquinoxaline-2,3-dione (CNQX, an α-amino-3-hydroxyl-5-methyl-4-isoxazole-propionate [AMPA]/kainate receptor antagonist), and tetraethylammonium (K-channel blocker) (Erceg *et al.* 2009). Based on their responses to these compounds, the properties of the neuronal cells can be determined. Patch clamp methods have been used to characterize murine primary cells; murine neural precursor cells; murine stem cell-derived cells; and human fetal, embryonic, and iPSC-derived neuronal cells (Bibel *et al.* 2004; Erceg *et al.* 2008; Jang *et al.* 2010; Karumbayaram *et al.* 2009; Kiraly *et al.* 2009; Vescovi *et al.* 1999).

2.4.2 Microelectrode array technology (MEA)

MEA technology has been used for cell network studies for decades to examine extracellular properties (Gross *et al.* 1977; Pine 1980; Thomas *et al.* 1972). With MEA, the functional activity of neuronal cell networks can be non-invasively measured *in vitro* for long periods, cultures can be stimulated at the same time, and

real-time monitoring can be performed (Ben-Ari 2001; Illes *et al.* 2007; Pine 1980; Wagenaar *et al.* 2006).

MEA provides a method for analyzing spatiotemporal signaling activity at the neuronal network level. Both spontaneous and stimulated activity can be measured. MEAs are used for monitoring the features of a neuronal network, such as spontaneous activity (Wagenaar *et al.* 2006), response to electrical and pharmacologic stimuli (Illes *et al.* 2007), plasticity (van Pelt *et al.* 2005), and toxicologic screening (Defranchi *et al.* 2011; van Vliet *et al.* 2007). MEA technology also provides information about electrophysiologic properties, developmental changes in activity patterns, and basic learning mechanisms of the nervous system (Ben-Ari 2001; Madhavan *et al.* 2007; Maeda *et al.* 1995; Wagenaar *et al.* 2006; van Pelt *et al.* 2005). Long-term MEA studies can be used to follow the development of the neuronal network: formation of the synaptic connections is followed by synaptic overproduction and thereafter elimination and network stabilization (Corner *et al.* 2002).

As MEA measures the network level activity, analysis of the signal is not straightforward and one electrode can detect signals from several neuronal cells. Nevertheless, the development and maturation of the *in vitro* neuronal network can be characterized based on the MEA signal. Typically, first single spikes occur a couple of days after plating the cells on the MEA. First, single spikes are recorded from *ex vivo* slices, primary cultures, and from stem cell-derived neuronal networks (Illes *et al.* 2007; Mazzoni *et al.* 2007; Wagenaar *et al.* 2006). Thereafter, the signals progress to asynchronous bursts or signal trains (Illes *et al.* 2007; Mazzoni *et al.* 2007; Uroukov *et al.* 2008; Wagenaar *et al.* 2006). At the most mature level, the neuronal network is highly connected and synchronous bursting activity occurs in several electrodes simultaneously (Illes *et al.* 2007; Mazzoni *et al.* 2007; Uroukov *et al.* 2008; Wagenaar *et al.* 2006), and this step is considered to be an *in vitro* mature neuronal network.

Although MEA have been used to analyze spatiotemporal behavior of dissociated rodent cortical or hippocampal slices (Chiappalone *et al.* 2007; Li *et al.* 2007; Madhavan *et al.* 2007; Otto *et al.* 2009; Wagenaar *et al.* 2006; van Pelt *et al.* 2005) or mouse ESC-derived neurons (Ban *et al.* 2006; Illes *et al.* 2007) , no studies have been performed using hESC-derived neuronal networks.

2.5 Controlling neuronal growth in the MEA environment

MEA is a good technology for evaluating network activity from ESC-derived neuronal cells (Illes *et al.* 2007). Nevertheless, network activity monitored randomly in and out of the electrode area-grown networks is not easy to control and to obtain reliable measurements (Shein-Idelson *et al.* 2011). Thus, measurements have been improved by restricting the growth area of the cells using various methods (Erickson *et al.* 2008; Shein-Idelson *et al.* 2011).

Ericson and co-workers built neurocages from Si3N4 to reduce the number of possible connections between dissociated cortical neurons (Erickson *et al.* 2008). These neurons were maintained in single cell cages, and could send their processes only outside of the cage and forming controlled neuronal network between ~16 cells. Possible connections were also reduced by coating only the wires between the electrodes with the cell-attractive material, e.g., protein (Buzanska *et al.* 2009; Erickson *et al.* 2008; Jun *et al.* 2007; Klein *et al.* 1999). This controlled the neuronal networks by limiting their connections from one electrode to each other and provides a method to study cell connectivity and signal propagation.

Poly(dimethylsiloxane) (PDMS) microstructures are also widely used in different cell growth limitation solutions (Adewola *et al.* 2010; Berdichevsky *et al.* 2009; Cimetta *et al.* 2009; Kim *et al.* 2007; Korin *et al.* 2009; Leclerc *et al.* 2003; Rhee *et al.* 2005; Teixeira *et al.* 2009; Tourovskaia *et al.* 2005; van Kooten *et al.* 1998). PDMS is a very good material for laboratory use and is advantageous for inexpensive prototyping applications, even on a nanometric scale (Xia *et al.* 1999). PDMS is also used in different microfluidic channel applications for hESCs or their derivatives (Cimetta *et al.* 2009; Kamei *et al.* 2009; Korin *et al.* 2009).

2.6 Neural network modulation

With MEAs, cell activity can be measured not only in native networks but also in modulated networks. Chemical modulation means basically the use of neurotransmitter receptor agonists or antagonists. With MEA technology, the

neurotransmitter modulator acts on the whole network and is thus a rapid and sensitive method of examining the effect at the network level. Based on the network response to specific neurotransmitter modulation, it is possible to identify the types of neurons and signaling pathways present in the cultures.

Glutamatergic signaling is the most important excitatory pathway of neuronal network signaling. Glutamatergic signaling can be modulated with AMPA/kainate receptor antagonists (such as CNQX) or by inhibiting NMDA-receptors (e.g., with D-AP5), which reduces the network activity. Another very relevant pathway is the main inhibitory circuit, GABAergic signaling. GABAergic signaling can be inhibited by bicuculline, a selective GABA-A antagonist. Bicuculline induces excitatory activity in a neuronal network by blocking the effect of inhibitory GABAergic signaling. Adding GABA, on the other hand, inhibits the neuronal network activity (Illes *et al.* 2007). Other signaling pathways, such as serotonergic and dopaminergic, can be studied similarly by selecting fast-acting agonists and antagonists for these receptors (Purves *et al.* 2008). The use of mouse ESC-derived neuronal networks has demonstrated that neurotransmitter modulation occurs as in other *in vitro* neuronal networks (Illes *et al.* 2007).

Neuronal networks can also be modulated by electrical stimulation. The effect of electrical stimulation to the network is either excitatory or inhibitory, depending on the amplitude, frequency, and pattern of the stimulation (Fields *et al.* 1990; Wagenaar *et al.* 2004; Yamada *et al.* 2006). Responses to the electrical stimulation reveal that the network is capable of plastic changes and has the capacity to learn.

2.7 Neurotoxicity

Neurotoxicity of different compounds is traditionally examined in whole animals. Animal testing is widely used, but it is both costly and time-consuming, and interpolation of the results to humans is not straightforward. Based on the 2005 EU figures, one million animals are used for toxicology testing in Europe annually (the Commission on the Statistics 2007) and the new EU regulations are aimed at reducing, refining, and replacing animal testing (Directive 2010/63/EU). Currently, most chemical tests for neurotoxicity, however, continue to be performed with animals and the OECD regulations are still based on animal testing (Bal-Price et al.

2010, Coecke, 2005, Bremer and Hartung, 2004, OECD Guidelines for the Testing of Chemicals http://www.oecd.org/document/7/0,3343 ,en_2649_34377_37051368 _1 _1_1_1,00. html).

Alternative methods for *in vivo* animal tests are based largely on the use of animal cells and end-point analyses. Results of tests using animal cells cannot always be interpolated to humans in a straightforward manner, and end-point analyses do not provide dynamic information during the exposure. REACH (Regulation of Chemical use by the European Chemical Agency, ECHA, http://echa.europa.eu/reach_en.asp) states that testing of chemical hazardous effects should be performed with a minimal amount of animal testing. Nevertheless, REACH statements emphasize that the safety of new testing methods should be as reliable as previous methods. Thus, more suitable animal or human cell-based models must be developed. Rodent primary cell cultures (Harry et al., 1998; van Vliet et al., 2007; Bal-Price et al., 2009; Hogberg et al., 2009) and human cell-based neurotoxicity platforms (Zeng et al., 2006; Buzanska et al., 2009a,b; Moors et al., 2009; Bal-Price et al., 2010) have either been developed or are under development for *in vitro* neurotoxicity platforms. In these studies, human umbilical cord blood cells are used as the cell source. Currently, human pluripotent stem cell-derived neuronal cells are available, and these cells are considered to be good material for neurotoxicity assays (Bal-Price *et al.* 2010).

A second challenge is to develop these neurotoxicity assays further so that they cover all of the necessary parameters that are crucial for neurospecific assays. Therefore, in addition to the traditional end-point analysis parameters, such as cell survival, cell division, and neurite length, these assays should also include neuronal functionality. The use of MEA is a potential system for neurotoxicologic applications due to the fact that it allows for fast, sensitive, and cost-effective measurements. Reliable information is provided about the modulation of signaling and cell-cell interactions in networks (Johnstone *et al.* 2010). The use of MEA technology as a neurotoxicity assay have been reported in several studies (Bal-Price *et al.* 2009; Johnstone *et al.* 2010; Melani *et al.* 2005; van Vliet *et al.* 2007) and several companies provide these services (e.g., http://www.neuroproof.com/eng/ Company/Aboutus.html). The use of human pluripotent stem cell-derived neuronal networks in MEA applications for neurotoxicity assays has not yet been addressed.

2.8 Applications of hESC-derived neurons

Human ESC-derived neuronal cells have been intensively studied for transplantation therapies applications and *in vitro* applications (Bal-Price *et al.* 2010; Bal-Price *et al.* 2009; Gaspard *et al.* 2010; Harry *et al.* 1998; Hess *et al.* 2008; Johnstone *et al.* 2010; Lindvall *et al.* 2006; Lindvall *et al.* 2010; Nisbet *et al.* 2008; Reier 2004; Toh *et al.* 2011; Webber *et al.* 2004). In this study, we examined cell differentiation of hESCs into a pure and robust cell population, culturing of the cells in 2D and/or 3D matrices *in vitro*, and characterized the cell cultures in detail (Figure 1).

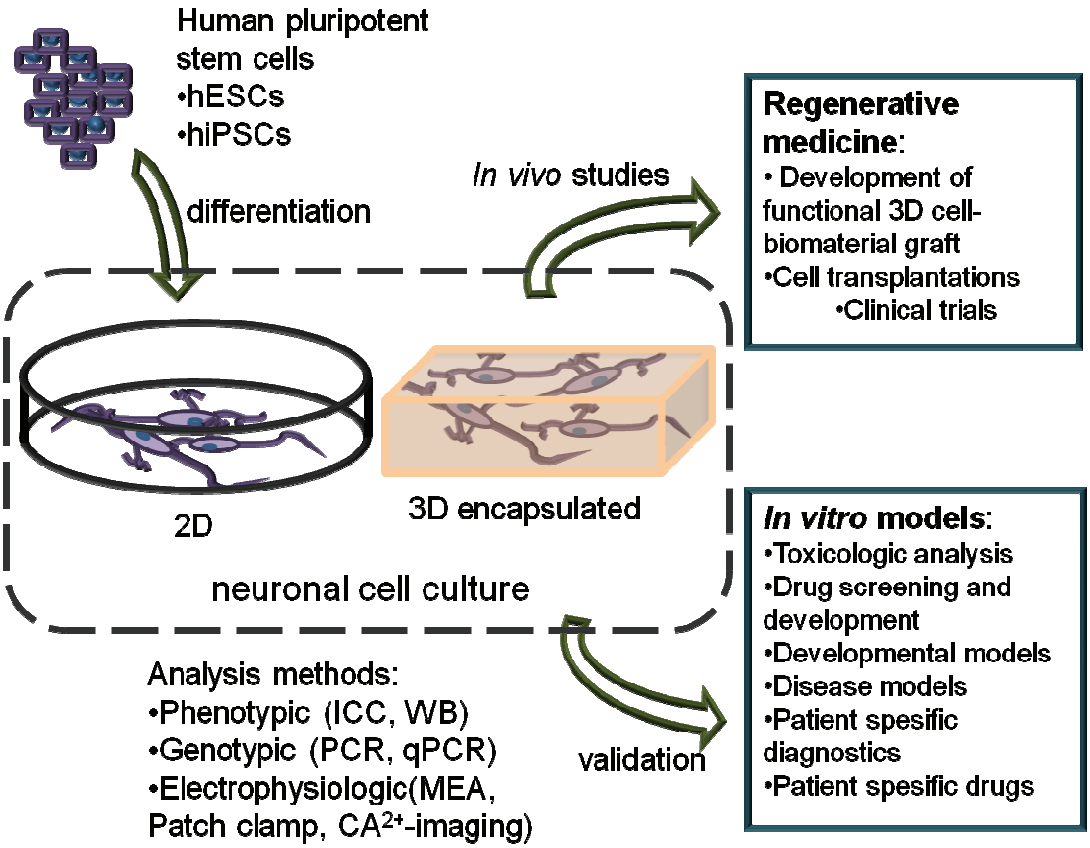

Figure 1. Human pluripotent stem cells can potentially be used for various applications. Human ESC-derived cells can be differentiated into neuronal lineages in 2D or in 3D cultures. These cells can be further used for transplantation therapies or for *in vitro* modeling.

Before these cells can be applied for regenerative therapies, extensive animal studies are needed. The number of animal studies required can be minimized, however, by performing properly designed *in vitro* tests (e.g., cellular responses and

network formation in 3D scaffold *in vitro*). *In vitro* models using stem cell-derived neuronal cells are useful in various areas, such as toxicologic analysis, drug screening and development, developmental studies, disease models, and patient-specific drug screening and diagnostics (Figure 1).

2.8.1 Neuronal culture

Two-dimensional neuronal cultures are easier to handle but do not mimic the *in vivo* situation in which cells interact with each other and with the surrounding environment as in 3D cultures, e.g., tissue-specific architecture is missing in 2D cultures (Geckil *et al.* 2010; Nisbet *et al.* 2008). Moreover, neuronal cells have a more complex morphology in 3D, and 3D structures may enhance the maturation and inhibit the proliferation of stem cell-derived neuronal cells (Geckil *et al.* 2010; Nisbet *et al.* 2008). Thus, when *in vivo* mimicking *in vitro* models or cell products for transplantation therapies are developed, it is very important to study cells in 3D.

Three dimensional structures for cells can be created using biomaterials. Biomaterials are materials that interact with living organisms, tissue, cells, or organs. All biomaterials can be classified into natural or synthetic materials based on their origin (Delcroix *et al.* 2010). Based on the structure of the material, biomaterials can comprise sponges, engineered structures (e.g., guidance channels), fibers, spheres, or gels (Delcroix *et al.* 2010). In general, the desired properties for biomaterials used with neuronal cells aimed for use in transplantation therapies or *in vitro* models are as follows: 1) allows for cell encapsulation and nutrient flow, 2) (controlled) biodegradation, 3) allows for cell adhesion, 4) supports neuronal phenotype, 5) has suitable (*in vivo* like) mechanical properties, 6) guides cell growth, and 7), is injectable (especially for transplantable solutions) (Straley *et al.* 2010).

2.8.2 Used/tested biomaterials for neuronal cells

Neuronal tissue engineering is a promising new therapeutic method and thus many biomaterials have been tested for neuronal applications. In tissue engineering, biomaterials are designed to improve the function of the tissue or organ in the

human body. Neuronal tissue engineering is an area in which combining cells, biomaterials, and growth factors is aimed at assembling a product that can be transplanted into patients suffering neurotrauma or diseases of the central or peripheral nervous system. In neuronal tissue engineering, biomaterials can support cell growth, support tissue structure, or improve the tissue/cell function. Biomaterials for neural tissue engineering should be non-toxic, 3D, support the growth of the desired cell type, and allow for nutrition flow (Holmes *et al.* 2000; Thonhoff *et al.* 2008).

Extracellular matrix-based materials, such as collagen, laminin, and fibronectin, are most commonly used for neural guidance structures. In addition, hyaluronic acid- and alginate-based materials are widely used natural material groups for peripheral nerve guidance. Even more commonly used materials are synthetic polymers. Examples of those are poly(lactic acid) (PLA), polyglygolide, poly(ε-caprolactone) (PCL), and their co-polymers, biodegradable glass, and poly(ethyleneterephthalate) (PTFE) (Schmidt *et al.* 2003). Table 1 lists the most commonly used materials with reported potential for neuronal tissue engineering. These materials have been tested in vitro or in vivo for neuronal cells, including chicken dorsal root ganglion cells, murine neuronal precursor and ESCs, and hESCs. Nevertheless, only a few studies have used human pluripotent stem cell-derived neuronal cells as a cell source. The most commonly used material is hydrogel (Turunen et al. 2011), although polyaliphatic esters, including PLA and PCL (Ashammakhi et al. 2007; Subbiah et al. 2005; Yang et al. 2004), and polyamide are also widely tested. Although the experiments listed in Table 1 are aimed at clinical usage of cell/biomaterial combinations, not all of the experiments were performed in 3D cultures.

Table 1. Biomaterials that have been tested *in vitro* or *in vivo* for neural tissue engineering or regenerative medicine purposes.

Material	Origin	Origin of tested cell type	Tested in vitro(2D/3D) /in vivo	Amenable to modification	Final use/target	Reference
gels						
fibrin	Nat.	mESC	3D in vitro	yes, aprotinin to retard the degradation	spinal cord injury	(Willerth *et al.* 2006)
IKVAV	Synt.	mNPC	3D	n.a.	spinal cord injury	(Silva *et al.* 2004)
MITCHs	Synt.	HUVEC, mNPCs, PC-12	3D in vitro	yes, gelator basement modifications, RGDS etc. Functional groups	experimental and clinical use in 3D cell encapsulation	(Wong Po Foo *et al.* 2009)
HA	Nat.	cDGR	3D in vitro, in vivo SCI-model	n.a.	spinal cord injury	(Horn *et al.* 2007)
Matrigel	Nat.	hESC	in vivo stroke-model	n.a.	cerebral ischemia	(Jin *et al.* 2010)
Pura Matrix	Synt.	hNSC	2d/3D in vitro	yes, functional groups, not tested in this study	stroke, spinal cord injury	(Thonhoff *et al.* 2008)
collagen type I	Nat.	mNPC	3D in vitro, bioreactor	n.a.	transplantation therapies	(Lin *et al.* 2004)
electrospun mesh						
PA	Synt.	hESC	2D mesh in vitro	n.a.	transplantation therapies	(Shahbazi *et al.* 2011)
PCL-gelatin	Synt./ nat.	C17.2	in vitro 2D mesh	n.a.	nerve TE	(Ghasemi-Mobarakeh *et al.* 2008)
PCL-collagen	Synt.	hMSC	3D multilayered electrospun structure	n.a.	neural TE	(Srouji *et al.* 2008)
sponges						
PLGA-co-PLGA-PLL	Synt.	mNPC	in vivo	yes, PLL functionalization	Spinal cord injury	(Teng *et al.* 2002)
PLA sponge	Synt.	hESC	3D in vitro, in vivo	n.a.	transplantation therapies	(Levenberg *et al.* 2003)
electrospun PLA	Synt.	mCSC	2D/3D	n.a.	neural TE	(Yang *et al.* 2004)
PSDB	Synt.	TERA2. cl.SP12	3D sponge	yes, protein functionalization	in vitro models and cell culture	(Hayman *et al.* 2005)
PCL-EEP	Synt.	hEBD	3D in vitro	n.a.		(Yim *et al.* 2006)
PLGA	Synt.	mNPC	3D	n.a.	neural TE	(Xiong *et al.* 2009)
others						
PDMS	Synt.	UCB-hMSCs	2D in vitro, Micropatterned	n.a.	regenerative medicine, preconditioning of the cells on PDMS	(Kim *et al.* 2008)

PSDB, poly(styrene/divinylbenzene); PA, polyamide; IKVAV, isoleucine-lysine-valine-alanine-valine; MITCHs, WW and PPxY containing mixing-induced, two-component hydrogels; PCL-EEP, poly(epsilon-caprolactone-co-ethyl ethylene phosphate) scaffold; mESC, mouse embryonic stem cell, mNPC, murine neural progenitos cells, PC-12, PC-12 rat tumor cell line; cDRG, chicken dorsal root ganglion cells; hNSC, human neural stem cells; fetal origin, C17.2, neonatal mouse cerebellum cell line; hMSC, human mesenchymal stem cells; mCSC, neonatal mouse cerebellum stem cells; TE, tissue engineering; TERA2.cl.SP12, human pluripotent embryonal carcinoma stem cells; hEBD, human embryoid body derived cells; hUCB-MSC, human umbilical cord blood – mesenchymal stem cells

2.8.2.1 Three dimensional culture platforms

Cells are conventionally cultured in 2D on top of a suitable coating. With this method, cells are easy to observe and manipulate. Nevertheless, 2D cultures in which cells interact with each other only laterally do not mimic the *in vivo* situation. Thus, a 3D matrix provides a more natural growth environment. For transplantation therapies, cells should adapt to an *in vivo* like environment, that is, a 3D environment, to increase cell survival. Moreover, a 3D biomaterial matrix can fill the cavity at the lesion site and thus provide better conditions for transplanted cells to migrate towards the host tissue (Hejcl *et al.* 2008; Nisbet *et al.* 2008) .

Few hydrogels in 3D format, such as Matrigel (Thonhoff *et al.* 2008), PuraMatrix™ (Gelain *et al.* 2006; Thonhoff *et al.* 2008), hyaluronic acid (Brännvall *et al.* 2007), poly(ethylene glygolide)-derivatives (Freudenberg *et al.* 2009), and chitosan (Leipzig *et al.* 2010), have been studied in combination with neuronal cells. Although these materials support the growth of neuronal cells, not all of them are suitable for clinical use. For example, Matrigel is of mouse origin and is not a defined product. Hyaluronic acid and chitosan have only been tested with animal-derived neural cells, so the suitability of these materials in combination with human-derived neuronal cells can not be directly extrapolated (Brännvall *et al.* 2007; Leipzig *et al.* 2010). PuraMatrix and Matrigel, on the other hand, are biocompatible with human fetal stem cell-derived neuronal cells (Thonhoff *et al.* 2008).

Most potential 3D materials for stem cell-derived neuronal cells aimed for transplantation therapies or functional models according to published reports are synthetic hydrogels (Table 1). These products contain only known components that are not harmful to stem cells or their derivatives and do not cause harmful side effects after transplantation (Imreh *et al.* 2006; Mitalipova *et al.* 2005). A good

example of a material meeting these requirements is the commercially available PuraMatrix, a synthetic, peptide nanofibrous hydrogel for which the composition is completely known and controlled, and the structure allows for modifications with functional groups (Zhang 2002; Zhang *et al.* 2005)

2.8.3 Regenerative medicine

The greatest hope for stem cell research is related to transplantation cell therapies. In these therapies, the *in vitro* differentiated cells are transplanted into the injured site of the human CNS and the cells are assumed to restore the function of lost or damaged tissue (Hejcl *et al.* 2008; Nisbet *et al.* 2008; Zhong *et al.* 2008). The research and development of these types of therapies requires multidisciplinary knowledge in areas of molecular biology, cell biology, biomaterials, and different technical areas. Central nervous system traumas, disorders, and dysfunctions currently without curative treatment, may be ameliorated in the future with tissue engineering-therapy (Jain 2009). Many aspects that must be carefully considered, however, remain before such therapies can be applied.

First, cells need to be delivered to the injured site. The simplest method of cell transplantation is intravenous injection. The accumulation of the cells at the injury site, especially in the CNS, however, can be very poor (Lappalainen *et al.* 2008). Thus, the most relevant way to perform cell transplantations is *in situ*, i.e., via focal injection(s) in or near the injury site (Lindvall *et al.* 2010). Second, cells must remain viable in the damaged area (Hejcl *et al.* 2008). In *in vivo* studies, the survival of the transplanted cells is often poor (Hicks *et al.* 2009; Oizumi *et al.* 2008). This survival rate may be enhanced by supportive biomaterial (Hejcl *et al.* 2008; Nisbet *et al.* 2008; Park *et al.* 2009). Moreover, biomaterials can also support cell migration (transplanted or host cells), reduce immune reactions, and support the maturation of transplanted cells (Lindvall *et al.* 2010; Wu *et al.* 2010; Zhong *et al.* 2008). Third, cells should act in the tissue as native cells. That can be evaluated beforehand *in vitro* or *in vivo* in animal models. For neuronal cells, electrical activity and the ability to form neuronal networks are crucial properties that transplanted cells should demonstrate in the host tissue.

One way to increase the survival of transplanted cells is to seed the cells in a biomaterial matrix that promotes viability, proliferation, and differentiation of transplanted neural cells (Thonhoff *et al.* 2008). Thus, mixed technologies, such as cell-biomaterial based tissue engineered-transplants are needed to develop efficient treatments for CNS deficits (Zhang *et al.* 2005). Polypeptides or other hydrogels, either natural or synthetic, are a potential supportive scaffold material for transplanted cells (Table 1, (Shin *et al.* 2003). For example, Levenberg and colleagues (2003) studied salt-leaching-processed porous poly(lactide-co-glycolide) (PLGA) scaffolds and concluded that hESCs differentiated into neural lineages in the scaffold. In addition to acting as the growth matrix, therefore, the scaffold could also support neural differentiation *in vitro* and *in vivo* (Levenberg *et al.* 2003)

There are also other strategies to treat CNS injuries by tissue engineering besides cell therapy. Willerth *et al.* are focused on controlled drug delivery in nervous system therapy instead of cell transplantation therapy. The aim of the controlled drug therapy is to add suitable drugs to a biomaterial and by controlling the degradation of the material, the drug is released in a controlled manner. The aim is to promote the tissue's own regeneration process with a suitable drug implanted into the target tissue composed of the biomaterial. This could be a new area of neural tissue engineering with or without cell therapy (Willerth *et al.* 2007).

Human ESC-derived neuronal cells are already in clinical phase trials. Very recently, Geron (www.geron.com), a US company, started the first Phase I trial with hESC-derived OPCs for patients suffering from spinal cord injury. This study has, however, been halted due to the poor global economic situation. Currently, Stem Cells Inc. (www.stemcellsinc.com/) began conducting clinical trials with human fetal neural stem cells for spinal cord injury patients, and ReNeuron is conducting phase I safety trials with human fetal brain stem cell-derived cells for stroke (www.reneuron.com).

2.8.4 *In vitro* models

Human ESCs and hiPSCs provide a mechanism for evaluating the functionality of human cell-derived neuronal cells using *in vitro* models, such as by toxicology tests, drug screening, human developmental models, disease models, and patient-specific

diagnostics and drugs (Figure 1). Improvement of the *in vitro* environment suitable for each cell type and application is crucial, because *in vitro* models must be validated and stable to give reliable information (Shein-Idelson *et al.* 2011). The 3D cell culture matrix can also be useful for *in vitro* platforms as neuronal cells are able to form electrically active neuronal networks in 3D scaffolds, which then provide a good *in vitro* model for neurotoxicity and developmental studies (Pautot *et al.* 2008).

2.8.4.1 Toxicology

In vitro toxicity models have been intensively studied in recent years (see section 2.7.). Traditionally used toxicity analyses are based on one, or at most two, end-point analyses. Using these methods, however, the analysis of mechanisms and kinetics is limited. Recently, multipoint analyses were suggested to provide more information, not only on the lethal toxicity, e.g., viability, but also on dynamics of the cells and their networks (Bal-Price *et al.* 2010; van Vliet *et al.* 2007).

Neurotoxicity models now benefit from the evaluation of neuronal cell functionality (Johnstone *et al.* 2010). These neurotoxicity models usually rely on MEA-based methods that provide continuous data about the neuronal activity that can be evaluated, even in subtoxic levels. The validation of these models, however, requires more work (Bal-Price *et al.* 2010). Lead, mercury, and commonly used drugs, e.g., paracetamol, are commonly used neurotoxicants for validation purposes (Castoldi *et al.* 2001; Kaur *et al.* 2006). Although toxicologic analysis is based on evaluation of cell signaling pathways and mechanisms and cell-cell interactions, 3D culturing may be a crucial parameter to create as good an *in vitro* model as possible (Kang *et al.* 2011).

2.8.4.2 Drug screening and development

Drug screening studies will benefit from well-validated *in vitro* models. These studies will make screening of suitable drug candidates faster and, when the model is based on well-characterized human cells, more reliable (Kiris *et al.* 2011). Especially in drug screening applications, the large-scale production of cells for

high-throughput analyses is important (Kiris *et al.* 2011; McNeish 2007). Many pharmacologic companies are very interested in these new technologies and have invested in their own research and development (Lou *et al.* 2011; McKernan *et al.* 2010).

2.8.4.3 Developmental models

Stem cells may provide clues to unknown developmental pathways via *in vitro* studies (Toh *et al.* 2011; Vallier *et al.* 2005) . Cell differentiation, migration, or death can be monitored in detail via *in vitro* stem cell models (Smits *et al.* 2009). With human stem cell technology, new information about human early brain development, which is inconvenient to study *in vivo* or with other methods, becomes accessible (Petros *et al.* 2011).

2.8.4.4 Disease models and patient specific drugs

The new iPSC technology (for details, see section 2.1.) provides a totally new research area for disease modeling. This technique allows the culture of cells bearing genetic disorders *in vitro,* e.g., the development of genetic disease models. Human iPSCs are differentiated into neuronal cells, and further, when the starting material is from a patient carrying a genetic disease, "diseased" *in vitro* neuronal cultures are generated (Durnaoglu *et al.* 2011; Kerkis *et al.* 2011). Induced pluripotent stem cell-technology also allows for screening patient specific drugs (Aalto-Setälä *et al.* 2009), but that area is not yet active in the field of neurology.

3. Aims of the study

The aims of this study were to evaluate the electrical activity of hESC-derived neuronal cells at the network level and to develop a culturing environment for the growth of functional network and measurements. The second aim was to screen suitable 2D and 3D growth matrices for hESC-derived neuronal cells. Third, we evaluated the usability of the functional hESC-derived neuronal cells in 2D toxicology screening and in 3D structure studies.

The studies addressed four specific aims:

1) Evaluation of the functionality of the hESC-derived neuronal cells utilizing the MEA system

2) Improving the cell culture and measurement environment with a structured PDMS culture chamber

3) Demonstration of the use of the functional 2D hESC-derived neuronal cells in *in vitro* toxicity evaluation of the effect of low-dose methyl mercury exposure on neuronal network activity of the neuronal networks.

4) Culturing hESC-derived neuronal cells on a suitable 3D scaffold and evaluating the electrical activity of the cells in 3D.

4. Materials and methods

4.1 Human embryonic stem cell culture and differentiation

The hESCs used in this study were derived either at the Regea – Institute for Regenerative Medicine, University of Tampere (Regea 08/023, Regea 06/040, Regea 06/015 (used in **Studies I, II, III, and IV**), or at the Karolinska Institute, Hospital Huddinge, Stockholm Sweden (HS181, HS360, HS362, used in **Study I**). Regea has approval from the Pirkanmaa Hospital District to derive, culture, and differentiate hESCs (Skottman, R05116) and permission from Valvira (1426/32/300/05) to conduct human stem cell research.

The hESCs were routinely confirmed to have a normal karyotype, be mycoplasma free, and have a normal undifferentiated phenotype based on immunocytochemical staining (against SSEA3, SSEA4, Nanog, Oct 3/4, and Tra-1-60) and embryoid body formation testing.

Human ESCs were grown in colonies on top of a human feeder cell layer (human foreskin feeders, line CRL-2429, ATCC, Manassas, VA) in stem cell medium containing Knockout Dulbecco's modified eagle medium (DMEM, Invitrogen, Carlsbad, CA) with 20% serum replacement, 2 mM GlutaMax (Invitrogen), 1% non-essential amino acids (Cambrex Bio Science, Allendale, NJ), 50 U/ml penicillin/streptomycin (Lonza Group Ltd, Switzerland), 0.1 mM 2-mercaptoethanol (Invitrogen), and 8 ng/ml bFGF (R&D Systems, Minneapolis, MN) as previously described (Rajala *et al.* 2007).

4.1.1 Neural differentiation

In **Studies I, II, III, and IV**, we used neural cells differentiated from hESCs. For neuronal differentiation, hESC colonies were mechanically cut into small pieces that were placed into neuronal differentiation medium (NDM) for suspension culture in

low attachment cell culture wells (Nunc). The NDM contained 1:1 DMEM/F12 and Neurobasal media supplemented with 2 mM GlutaMax, 1×B27, and 1×N2 (all from Gibco), 25 U/ml penicillin/streptomycin (Cambrex, Belgium), and 20 ng/ml bFGF. The small cell aggregates formed small spheres, so-called neurospheres. The spheres were differentiated in suspension culture for 6 to 10 weeks and cut into smaller pieces weekly for good nutrient transfer into the inner parts of the spheres. The workflow of neuronal cell differentiation is presented in Figure 1. A prolonged neuronal differentiation period guides the cells into an astroglial fate, as shown by Lappalainen and colleagues (Lappalainen *et al.* 2010). Thus, 20 to 30-week differentiated spheres were used for the astroglial experiments in **Study IV**. For all suspension cultures, the culture medium was changed three times per week.

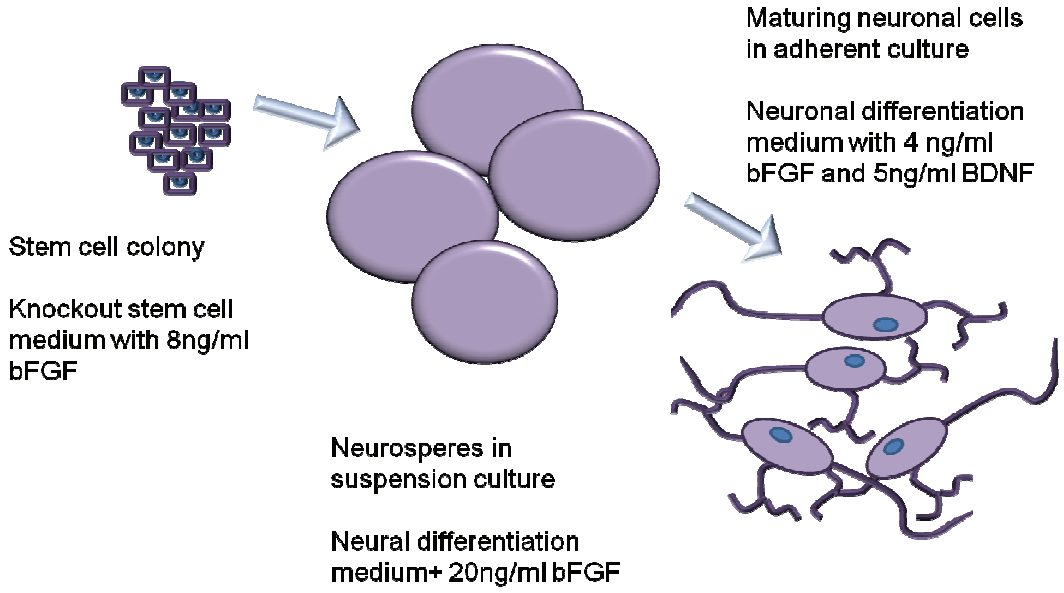

Figure 2. Neuronal cell differentiation from hESCs.

In addition to neuronal cells and astrocytes, in **Study IV**, oligodendrocyte precursor cells were used. For oligodendroglial differentiation, hESCs were cut in aggregates as described above. OPC differentiation was initiated with medium containing N2 medium [DMEM/F-12 medium with 1× N2, 2 mM GlutaMax (Gibco), 0.6% glucose, 5 mM HEPES, 2 µg/ml heparin (Sigma-Aldrich, St. Louis, MO), 25 U/ml penicillin/streptomycin] supplemented with 10 ng/ml human ciliary neurotrophic factor (CNTF), 20 ng/ml human epidermal growth factor (all R&D

Systems, Europe), and 20 ng/ml bFGF for 4 weeks. Thereafter, for the following 3 weeks, the cells were cultured in N2 medium containing 10 ng/ml CNTF, 20 ng/ml epidermal growth factor, 10 ng/ml bFGF, 100 ng/ml insulin-like growth factor-1 (Sigma-Aldrich), 20 ng/ml platelet-derived growth factor-AA (Peprotech Inc., Rocky Hill, NJ), and 1 µg/ml laminin (Sigma-Aldrich). In that stage (stage 2), cells are OPCs and can be used for analysis or further experiments. The cells were differentiated into oligodendrocytes in medium containing N2 medium supplemented with 200 µM L-ascorbic acid 2-phosphate (Sigma-Aldrich), 10 ng/ml CNTF, and 40 ng/ml 3,3′,5-triiodo-L-thyronine (Sigma-Aldrich) was used as previously described by Sundberg et al. (Sundberg 2010). The workflow for OPC-differentiation is presented in Figure 3.

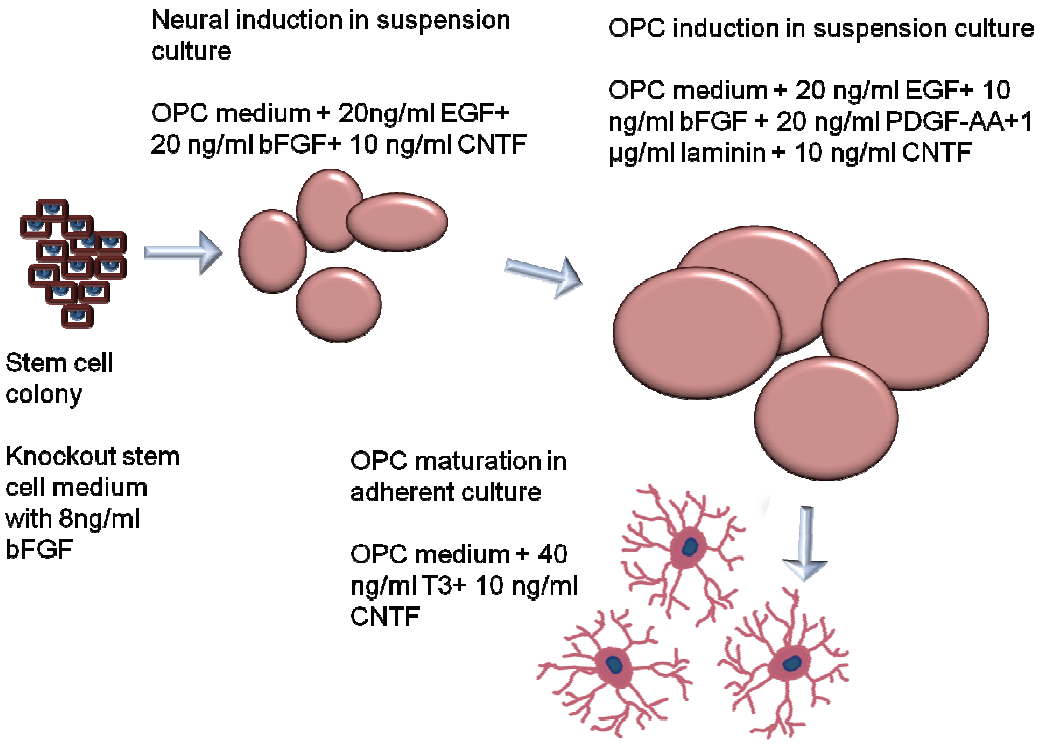

Figure 3. Oligodendrocyte precursor cell differentiation from hESCs.

4.1.2 Maturation/network formation of hESC-derived neuronal cells

For *in vitro* maturation of neuronal cells and network formation, cells were plated to adherent cultures (cell culture plastic, MEA plates, or cover slips) after 6 to 8 weeks differentiation as neurospheres. A laminin coating solution was used for the cell culture plastic. Cell culture wells were coated with 10 µg/ml human or mouse laminin (Sigma) diluted in Dulbecco's phosphate buffered saline (dPBS) and incubated overnight (+4 °C) or for 2 hours in +37°C. Thereafter, the coating solution was removed and cells and the appropriate cell culture medium were added.

Two different cell-seeding strategies were used throughout the experiments. In the aggregate method, cell spheres were cut into smaller aggregates (Ø 50-300 µm, containing ~ 1000-100 000 cells/aggregate) and plated on a laminin-coated surface.

For the single cell suspension method, cells were enzymatically dissociated into single cells. TryLE Select (1x, Invitrogen) or trypsin (1x, Lonza) was added to the cells. Cells were incubated with the enzymes for 5 to 15 minutes, and then washed with 5% human serum and cell culture medium (after trypsin), or 2× cell culture medium (after TrypLE Select). The single cell suspension was plated into laminin-coated cell culture wells at a density of ~0.5-1×10^5 per cm^2.

Neuronal cells were plated with medium that did not contain bFGF to initiate neuronal maturation. Three to 5 days later, 4 ng/ml bFGF and brain-derived neurotrophic factor (5 ng/ml, Gibco) were added to the medium to enhance cell growth and maturation. The medium was changed three times per week.

Cells attached to the laminin in 1 to 2 days and began to migrate along the surface.

4.2 Characterization and analysis of produced neuronal networks

4.2.1 Morphology

During the adherent culturing, cells were routinely observed with a phase contrast microscope (Nikon T2000S). The normal morphology of the neuronal cells is presented in Figure 4.

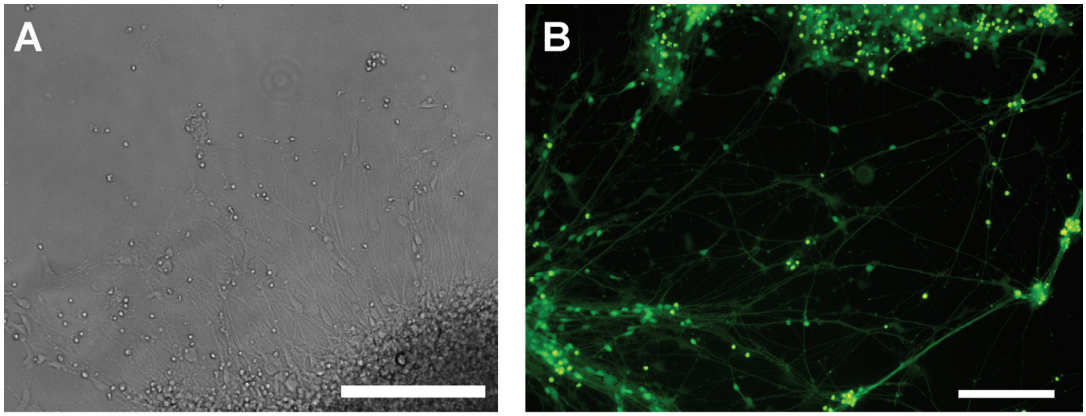

Figure 4. Normal morphology of hESC-derived neuronal cells. Neuronal cells were differentiated for 8 week in suspension culture and thereafter cultured in adherent culture for 1 week (A). Live/dead analysis shows that those cells remained viable for 1 week culture in the adherent culture (B). Scalebars 100 µm.

4.2.2 Time-lapse imaging

In **Study III,** time-lapse imaging was used for more careful morphologic analysis (Cell-IQ®, Chip-man Technologies Ltd, Tampere, Finland). The system comprises a cell culture environment (controlled temperature and gas flow in a sterile environment) and microscope setup with an LED light source, 10× phase contrast optics, and camera. The whole setup is controlled with Cell-IQ® Imagen (Chip-Man Technologies) software. The system obtains repeated images in the same position over a long time. Further, images can be analyzed with analysis software, and neuronal cells, astrocytes, and non-neuronal cells can be tracked and analyzed from the image data, as previously described (Narkilahti *et al.* 2007; Toimela *et al.* 2008).

4.2.3 Viability

In **Studies I, III**, and **IV**, cell viability was observed using the LIVE/DEAD Viability/Cytotoxicity Kit for mammalian cells (Molecular Probes, #L3224, Invitrogen). The kit has two fluorescent components, calcein-AM and ethidium homodimer-1 (EthD-1). Calcein AM is virtually non-fluorescent outside the cell, but can enter the cells in a polyanionic form and emits green fluorescence at ~515 nm, and is used to detect live, metabolically active cells. EthD-1 attaches to nucleic acid and can only penetrate a disturbed cell membrane, and emits red fluorescence at 635 nm, and thus is used for dead cell detection.

Cells were stained with solution containing cell culture medium and 0.1 μM calcein AM and 0.5 μM EthD-1 for 30 minutes. The cells were imaged immediately after incubation in the staining solution with an Olympus IX 51 inverted fluorescence microscope and an Olympus DB71 digital camera (both Olympus, Finland).

4.2.4 Genotypic analysis

The neuronal cell genotype was characterized with quantitative real-time polymerase chain reaction in **Study III**. Samples from adherent cell cultures were collected into lysis buffer. RNA was extracted from the samples using the NucleoSpin® RNA XS kit (Machery-Nagel GmbH & Co, Düren, Germany). The cDNA was then transcribed from RNA. Quantitative real-time polymerase chain reaction was performed With TaqMan® Gene Expression assays (Applied Biosystems) with ABI Prism 7300 instrument (Applied Biosystems, Foster, City, CA). The following genes were analyzed: *musashi* (ID Hs01045894), *neurofilament-68* (ID Hs00196245), and *glyceraldehyde 3-phosphate dehydrogenase* (ID 4331182). All samples had four technical replicates and expression of *musashi*, *GFAP,* and *neurofilament-68* was compared by using *glyceraldehyde 3-phosphate dehydrogenase* as an internal reference.

4.2.5 Proliferation

In Study III, cell proliferation capacity was evaluated using two quantitative colorimetric methods, 5-bromo-2′-deoxyuridine (BrdU) and Wst-1 analyses. The BrdU method is based on an enzyme-linked immunosorbent assay for BrdU (Roche, Basel, Switzerland), which is based on the BrdU linkage to the DNA during strand synthesis. Briefly, neuronal cell cultures were incubated with BrdU labeling reagent for 20 hours at +37°C. The cells were then collected and re-plated at a density of 5000 cells/well in 96-well plates. Thereafter, cells were centrifuged (300 ×g), dried, and fixed with FixDenat solution. Anti-BrdU monoclonal antibody conjugated with peroxidase was added to the wells. Unattached antibody was washed off, and the substrate solution was added for 5 minutes. The reaction was stopped with H_2SO_4 and the absorbance was detected at 450 nm using a Viktor2 1420 Multilabel Counter (PerkinElmer-Wallac, Waltham, MA). Background absorbance was measured from non-cell containing samples, and the background absorbance was subtracted from the measured samples. Altogether, 10 parallel samples from each group were analyzed.

The Wst-1 analysis is based on succinate-tetrazolium reductase activity. A Wst-1 Cell proliferation Assay (Takara Bio Inc., Shiga, Japan) was used. In the method, ready-to-use solution was used according the manufacturer's instruction. Briefly, cells cultured in 96-well plates were washed with dPBS. Diluted reagent was added to the cells and the cells were incubated 4 hours at +37°C. Absorbance from the samples was measured using a Viktor2 1420 Multilabel Counter at 450 nm. The background absorbance (measured from negative controls) was subtracted from the measured sample absorbance. A total of 12 parallel samples was measured from each group.

4.2.6 Immunocytochemical characterization

In **Studies III and IV**, cell cultures were analyzed with immunocytochemistry. First, adherent cell cultures were fixed with 4% paraformaldehyde for 20 minutes. Samples were washed three times with dPBS. Then, nonspecific staining was blocked with a mixture containing 10% normal donkey serum (Sigma-Aldrich),

0.1% Triton-X 100 (Sigma-Aldrich), and 1% bovine serum albumin (BSA, Sigma-Aldrich) for 45 minutes at room temperature. The cells were then washed with buffer containing 1% normal donkey serum, 0.1% Triton X-100, and 1% BSA in dPBS and incubated overnight at 4°C with primary antibodies diluted in the same buffer. The primary antibodies are listed in Table 2.

Table 2. Antibodies used for immunocytochemical staining. Immunocytochemical characterization of common neural cell type markers was performed in **Studies III** and **IV**.

antibody	*full name*	*origin*	*dilution*	*manufacturer*	*used secondary antibody*	*manufacturer of secondary antibody*
MAP-2	microtubule associated protein, for neuronal cells	rabbit	1:600-800	Chemicon	Donkey anti-rabbit488	Molecular Probes
NF-200	neurofilament 200 kD, for neuronal cells	mouse	1:600	Sigma	Goat anti-mouse 488	Molecular Probes
β-tub	β-tubulin isotype III, for neuronal cells	mouse	1:1000	Sigma	Goat anti-mouse568	Molecular Probes
GFAP	glial fibrillary acidic protein antibody, for astrocytes	sheep	1:800	R&D systems	Donkey anti-sheep568	Molecular Probes
GalC	Galactocerebroside, for OPCs	Mouse	1:400	Chemicon	Donkey anti-mouse 568	Molecular Probes
K-i67	Ki-67 protein, for proliferating cells	rabbit	1:800	chemicon	Donkey anti-rabbit 488	Molecular Probes

After primary antibody incubation, the samples were washed with 1% BSA in PBS and incubated with secondary antibody solution (the secondary antibodies are listed in Table 2) diluted in washing buffer. The incubation time for the secondary antibodies was 2 hours at room temperature. Finally, the samples were washed 2× with dPBS and 2× with phosphate buffer and mounted with Vectashield with 4′6-diamidino-2-phenylindole (Vector Laboratories, Peterborough, UK). Immunocytochemical samples were imaged with an Olympus microscope (IX51, Olympus) equipped with a fluorescence unit and camera (DP30BW, Olympus).

When primary antibodies were omitted (negative control), no positive labeling was detected. Some modifications of the protocol were performed with the hydrogel samples in **Study IV**.

4.2.7 Confocal microscopy

In **Study IV**, confocal imaging was performed using immunocytochemically-stained samples. Confocal images were taken with an LSM 700 setup (Carl Zeiss Oy, Jena, Germany). The stacked images were taken with a 40 × air objective, in 1 µm range, in a total thickness of 70 µm. Visualization of the confocal data was performed with Zen2009 (Carl Zeiss) or BioImageXD (www.bioimagexd.net).

4.3 Scaffolds for neuronal cells

Neuronal cells are traditionally cultured on protein surfaces. Nevertheless, those surfaces are not always suitable for specific applications. Thus, suitable 2D and 3D growth matrices for hESC-derived neuronal cells were evaluated.

4.3.1 Two-dimensional scaffolds

The 2D scaffolds we tested were 1) coating solutions, for which the standard cell culture polystyrene was coated by incubating 2 to 24 hours at +20 to +37°C, 2) nanofibrous materials, or 3) thin gel surfaces. In 2D scaffolds, neuronal cells were plated on top of the biomaterial surfaces either as a single cell suspension or as small aggregates. Laminin, and collagen I, II, III, and IV, were used as the coating surfaces. In brief, the proteins were diluted to various concentrations and incubated on polystyrene cell culture wells for 2 to 24 hours at +20 to +37°C. Electrospun PCL scaffolds were processed from a polymeric solution in solvent via an electrospinning process (Ylä-Outinen, 2010) by Prof. Tan and colleagues (Nanyang Technological University, Singapore).

Table 3. Biomaterials tested as a 2D growth matrix for hESC-derived neuronal cells.

Material	*Form*	*Manufacturer*	*2D/3D*	*Analysis method*
Fibers				
Biactive glass	Fibers	Inion Oyj, Tampere, Finland	3D fibers	Immuno/LD/SEM
Poly lactide	Electrospun fibers	TUT/BME, Tampere, Finland	2D/3D fibrous mat	Immuno/LD/SEM
Poly(e-caprolactone)	Electrospun mat	NTU/MSE, Singapore	2D/3D fibrous mat	Immuno
Protein surfaces				
Collagen I	Protein surface	Fibrogen, Helsinki, Finland 10 µg/ml	coated surface	LD/immuno/phC
Collagen II	Protein surface	Fibrogen, Helsinki, Finland 10 µg/ml	coated surface	LD/immuno/phC
Collagen III	Protein surface	Fibrogen, Helsinki, Finland 10 µg/ml	coated surface	LD/immuno/phC
Collagen IV	Protein surface	Sigma, 10 µg/ml	coated surface	LD/immuno/phC
Laminin	Protein surface	Sigma, 10 µg/ml	coated surface	LD/immuno/phC
Engineered surfaces				
PDMS	Surface	TUT/ASE, Tampere, Finland	2D	immuno
Corning cell bind surface	Surface	Corning	2D	LD/immuno
Surmodics	Surface	SurModics, Eden Prairie, MN, USA	2D	LD/immuno
TiO	Surface	Vivoxid, Turku, Finland	2D	LD/immuno
Patterns/guidance channels				
Fibronectin surface	Patterned surface	NTU/MSE, Singapore	2D/ patterns	PhC
Ormocomp	Structured neurocages	TUT/BME, Tampere, Finland	3D structures	Immuno/LD
Gels				
CellStart TM	Gel	Invitrogen	2D gel surface	Immuno/LD
PuraMatrix	Gel	3DM Inc.	2D gel surface	LD/immuno/confo
OG2	Gel	Nano Fiber Matrices B.V., Groningen, Netherlands	2D gel surface	LD/immuno/confo
Particles				
PLGA particles	Microspheres	NTU/MSE, Singapore	particles	LD

LD, live/dead viability/cytotoxicity analysis; phC, imaging with phase contrast microscope; immuno, immunocytochemical analysis; confo, confocal microscopy of immunocytochemically-stained samples; SEM, scanning electron microscopy

Gel-like materials were tested as a surface (thin coating) so that cells were embedded in the gel layer. 1) Cells were cultured on the top of the material. 2) Cells were first plated on the laminin surface, and after the cells became attached, the gel layer was applied over the cells.

4.3.2 Three-dimensional scaffolds

Growth, survival, maturation, and signaling of the neuronal networks in a 3D growth matrix were evaluated in **Study IV**, PuraMatrix (BD Bioscience, Sparks, MD), and in OG-2 -gels (manufactured by Metselaar and DeJong, Nano Fiber Matrices B.V. Netherland). All tested materials were synthetic, self-assembled hydrogels.

PuraMatrix was gelated into four final concentrations: 0.25, 0.15, 0.10, and 0.05 % (w/v). In general, PuraMatrix was gelated according to manufacturer's instructions. PuraMatrix solution was mixed with 10% sucrose solution (w/v in sterile distilled water) to the appropriate concentration. The solution was then added to a cell culture chamber or well (140 µl/cm^2) and gelation was initiated by adding cell culture medium and incubating at +37°C for 30 minutes. During the gelation period, the medium was changed 3 times.

OG-2 gel stock solution was prepared as 133.3 mg/ml in HCl (0.21 M). The cells were suspended in sucrose solution as described earlier, and the cell solution was quickly mixed with gel stock solution and added to the cell culture well. Stock solution gelated immediately and the cell culture medium was added on the top of the cell-gel-mixture.

Cells were encapsulated inside the hydrogel. In addition to these cell/hydrogel compositions, cells were cultured in laminin-coated polystyrene (positive control) as described earlier and non-coated (negative control) cell culture polystyrene.

For hydrogel encapsulation experiments, the cells were inside the gel either as aggregates or as a single cell suspension. For encapsulation, hydrogel solution was processed and mixed with a single cell suspension made in 10% sucrose. This hydrogel/cell mixture was then gelated by cell culture medium.

4.3.3 Analysis

Cell/gel combinations were characterized using a viability assay, immunocytochemical staining with fluorescence, and confocal microscopy and with MEA measurements. Cells required prolonged culture periods in 3D cultures to form connected networks, thus culture periods were 2 to 6 weeks for 3D scaffolds. Electrical activity from 3D cultures was measured 3 to 5 weeks after plating.

4.4 Electrical measurement

4.4.1 Set-up and settings

The extracellular electrical activity of the neuronal cells was measured with a MEA (Multichannel Systems [MCS] GmbH, Reutlingen, Germany) system. The system contains cell culture dishes with substrate-embedded microelectrodes, a preamplifier with dish holder and heater element, filter, AD converter, and computer for controlling the system. The recording system is presented in Figure 5. The recording system and measurements were controlled and acquired with MC_Rack and MEA_Select softwares (MCS).

Prior to the measurements, the MEA-plates were sealed in a laminar hood with a semi-permeable membrane (ALA MEA-MEM, ALA Scientific Instruments Inc., Westbury, NY) or PDMS gap. Both materials are permeable to gas, but microbes or other larger particles cannot pass through. Measurements were performed using an MEA amplifier placed on top of the microscope (Olympus IX 51, Olympus, Finland). The temperature (+37ºC) of the cell cultures during the measurement was controlled using a TC02 temperature controller (MCS) connected to a heating element in the MEA amplifier.

Samples were allowed to stabilize for 3 to 5 minutes before the 5 to 10-minute measurement period. During or after the measurement, the cells were imaged with the microscope's camera (ALTRA 20, Olympus) connected to CellD software (version 2.6, build 1210, Olympus Soft Imaging Solutions GmbH, Munich, Germany) or with the Andor camera (Andor Technology plc., Belfast, Northern Ireland) and TillVision (Till Photonics, Gräfelfing, Germany) software.

The samples were then placed back into the incubator and cultured normally. Thus, measurement of a particular network could be repeated several times over days or even months.

Signals from the cells were amplified ×1100 and sampled at 20 kHz. Post-recorded signals were filtered with a high-pass filter (2nd order Butterworth filter) at 200 Hz to remove the background fluctuations. In addition, the quality of the measurement was assessed using the non-filtered raw data. Background noise of less than 10 μV_{rms} was allowed.

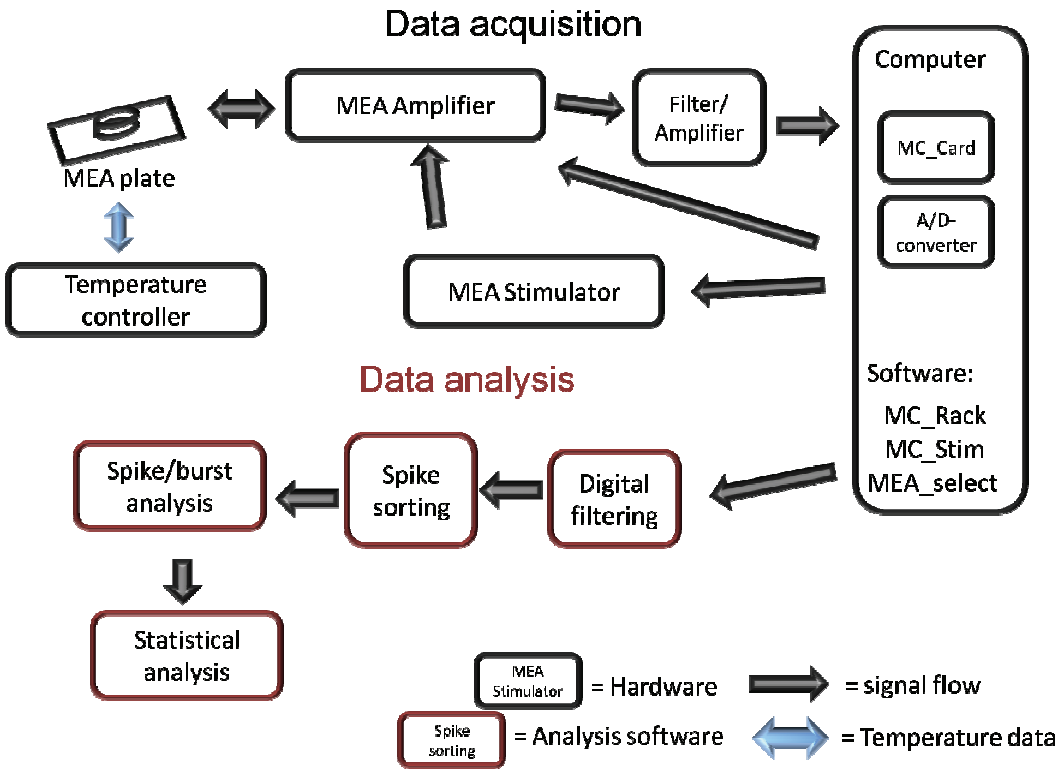

Figure 5. Workflow in MEA experiments. Data was acquired by the measurement computer, and then processed and analyzed.

4.4.2 MEA plate designs

In these experiments (**Studies I, II, II, and IV**), commercial MEA plates (MCS) were used. In the standard MEA plate, 59 substrate-embedded measurement electrodes were arranged in a square array in an 8×8 layout with 200-µm inter-electrode distance (Figure 6A). A glass dish (49×49 mm) substrate was the basement material, and electrode wires were insulated with a Si_3N_4-layer that was

also the surface material of the MEA plate. The electrodes were 30 µm in diameter and made from titanium nitride. The electrode wires and amplifier contact pads were made from titanium. One larger electrode in the MEA dish was used as the internal reference electrode (www.multichannelsystems.com). These 8×8 layouts were made with and without a permanently attached glass ring. The glass ring was used as a medium reservoir for cell culture.

In another layout **(Study III)**, the electrodes were divided into 6 separate areas, each area containing 9 measurement electrodes in a 3×3 grid and one reference electrode of the same size and distance as in the standard layout (6-well MEA, MCS). With this layout, one MEA plate contained 6 separate cell culture and measurement areas, as shown in Figure 6B.

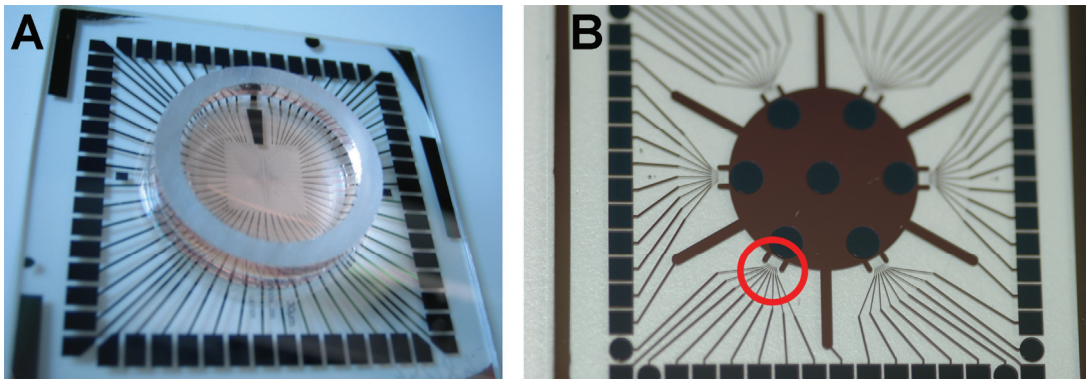

Figure 6. MEA layouts. (A) Standard 8×8 electrode layout on MEA plate with glass ring (MCS). (B) 6well MEA layout (MCS) without culturing chamber. One electrode area is indicated with a red circle.

4.4.3 Structured PDMS chambers

In **Study II**, PDMS was used for a new MEA culture chamber design. To reduce the area in which the cells grow in MEA plates, a structured chamber was designed. These chambers were attached to the top of standard MEA plates or 6-well MEA plates without a glass ring. The designed chamber was manufactured from PDMS (Sylgard® 184, Dow Corning, Corning, NY), which is widely used in fast prototyping, mold casting, and is easy to process (Cimetta *et al.* 2009; Kamei *et al.* 2009; Korin *et al.* 2009).

The design has a large (1000 µl) medium reservoir and limited (∅ 4 mm) cell attachment area around the electrode grid area. This design allows cells seeded only on electrode area, but still retain large medium volume for rare (three time per week) medium change. Also, the reference electrode area is open. The chamber was molded from PDMS elastomer in a polytetrafluoroethylene mold. In brief, the mold was fabricated by lathe machining of two separate parts. A support was made from polytetrafluoroethylene and the insert for tiny structures was made from polyoxymethylene. The two-part mold makes it easier to create variations in the design. The mold support can contain either a one-chamber mold, or nine parallel chamber molds.

The PDMS components were then mixed in a ratio 10:1 (rubber : curing agent) and the liquid was strained into the mold and incubated in a vacuum chamber (~100 mbar absolute) for 20 minutes to remove air bubbles. Full curing occurred within 2 hours at 70°C.

The 6 well-design chambers were manufactured without a mold from thick (6.5 mm) and thin (0.5 mm) polytetrafluoroethylene sheets by punching holes. The thicker sheet formed the medium reservoir (punch ∅ 6-8 mm), and the thinner sheet formed the cell attachment area (punch ∅ 3-4 mm). These two parts were bonded irreversibly together using an oxygen plasma treatment (Vision 320 Mk II, Advanced Vacuum Scandinavia AB, Sweden).

Also, a common medium reservoir for 6-well design was fabricated. This was constructed similarly to the 6-well chamber, but the upper part contained only one large (punch ∅ 22 mm) hole as a medium reservoir.

All structured PDMS chambers are reversibly bonded to MEA plates by van der Waals interaction and the bond was watertight for long-term cell culture and MEA measurements. The PDMS chambers were re-usable as MEA plates. They were cleaned and could be re-used up to 6 times.

These structures were designed, manufactured and tested in collaboration with Prof. Pasi Kallio and MSc (Tech.) Joose Kreutzer from Tampere University of Technology, Department of Automation and Science.

4.4.4 Cell plating and culture

In **Studies I, II, III,** and **IV**, cells were plated in MEAs as 2D cultures. Prior to cell seeding, MEA plates were treated with two coating solutions. Clean and sterile MEA plates were treated with 0.05% polyethyleneimine (Fluka, Italy) in sterile water solution for 2 hours at +37°C or overnight at +4°C. The polyethyleneimine solution was rinsed and MEA plates were dried under a laminar hood. Laminin solution (20 µg/ml) was added drop-by-drop in the electrode area or to the whole bottom area. After incubation (2 hours at +37°C or overnight at +4°C), the solution was removed and cells were plated in NDM cell culture medium.

Two different cell-seeding strategies were used. First, in the aggregate method, neurospheres cultured in suspension culture were cut into very small aggregates (~50-100 µm). The aggregates were plated (~10 aggregates, ~100 000-500 000 cells, in ∅ 2 mm electrode area, and less, <100 000 cells to smaller areas). For the single cell suspension method, the cells were dissociated into a single cell suspension as described earlier with TrypLE Select or Trypsin.

Cell cultured in MEA plates were maintained in petri dishes in a controlled environment at +37°C, 5% CO_2, humidified air, between the MEA recordings. Medium (NDM supplemented with 5 ng/ml brain-derived neurotrophic factor and 4 ng/ml bFGF) was changed three times per week. In **Study IV**, neuronal cells encapsulated into a hydrogel matrix (described in chapter 4.7) were plated onto standard layout MEA plates with structured PDMS chambers.

4.4.5 Reuse of MEA plates

The MEA plates can be reused several times. Prior to re-use, discarded cells were washed off the dish with distilled water and the MEA plates were washed with a neutral detergent (0.1% Terg-A-Zyme, Sigma-Aldrich, in distilled water) solution overnight. Thereafter, the plates were rinsed with distilled water and air dried. Finally, the plate was sterilized with either 70% ethanol and 10-minute UV-light exposure or an autoclave.

4.4.6 Analysis

For analysis, spike detection was performed with MC_Rack software (MCS). For the analysis and visualization of the data MC_DataTool (MCS), NeuroExplorer (Nex Technologies, Littleton, MA), MATLAB (MathWorks, Natick, MA), and Microsoft Excel (Microsoft Corporation, Redmond, WA) software were used.

Selection criteria for the experiment were the same as that used in **Study III**. These criteria were defined as follows: train-like activity (over 300 spikes/300-second measurement period) at least in one channel and spiking activity from at least four other channels. In all studies, spikes were sorted using MC_Rack software and the detection threshold was defined as follows:

$$spike\_amplitude \geq -5 \times STD_{rms}$$

In **Study III,** spike data was normalized with respect to baseline activity of each MEA.

4.4.7 Pharmacology

In **Studies I** and **III**, spontaneously active neuronal networks were modulated with known pharmacologic substances to verify the neuronal origin of the signaling. For pharmacologic stimulation, the drugs were first diluted to the appropriate concentration in cell culture medium, the cell medium was then changed, and the culture was stabilized for 5 minutes before recording 5 minutes of signal.

The Na^{2+}-channel blocker TTX (50 μM, Sigma) was used to evaluate the sodium-channel activity in the neuronal networks. First, baseline activity was measured from the MEAs in this experiment (n=2). Then, the cell medium was exchanged for fresh medium and activity was measured. Next, TTX solution was added to the MEAs and activity was measured. Finally, the medium was again exchanged for fresh medium, and restored signaling was measured.

The effects on glutamatergic and GABAergic signaling were evaluated with the following experimental design. The baseline and fresh medium effects were first measured. Then, the AMPA/kainate receptor antagonist CNQX (30 μM, Sigma) was added to the MEA plates and the signals were measured. In addition to CNQX, the

NMDA-receptor antagonist DAP5 (20 μM, Sigma) was added to inhibit glutamatergic signaling. Thereafter, fresh medium was added and recovery was measured. GABA (100 μm, Sigma-Aldrich) was used to stimulate GABA receptors. Finally, the $GABA_A$ antagonist [(-)-bicuculline methiodide; 10-30 μM, Sigma-Aldrich] added and the effects were measured.

4.4.8 Electrical stimulation

The electrical stimulation protocol was designed with MC_stim (MCS) software and the networks were stimulated in MEA plates using a STG2004 stimulus generator (MCS). In **Study I,** the following stimulus protocol was used: a train of 50 biphasic voltage pulses (± 800 mV, 400 μs per phase), followed by a 4 to 56 second latent period, and repeated for a total of 10 minutes for the MEA measurement period. One measurement electrode was stimulated at a time. Stimulation blanking was also used, meaning that the stimulated electrode was blanked for 20 ms after the stimulation to reduce the size of the stimulation artifacts. In addition, all the electrodes were grounded for ± 8 ms around each stimulation time point.

4.4.9 Toxicity

In **Study III**, the effect of the known neurotoxicant methyl mercury chloride (MeHgCl, Sigma) was evaluated. First, the acute response of 0, 0.5, 50, and 500 nM MeHgCl was measured for 1 hour immediately after adding the MeHgCl. The delayed effect was then measured at 24, 48, and 72 hours after exposure. At each time point, all MEAs (n=4 for each group) were measured for 5 minutes. After 72 hours of exposure, the medium was changed and recovery was measured for 24, 48, and 72 hours.

A similar exposure protocol was applied to neuronal networks cultured in 48- and 96-well plates. Viability, proliferation, and gene expression were analyzed and immunocytochemical stainings of the cell cultures were performed.

4.5 Statistical analysis

For statistical analysis in **Study IV**, cells were calculated from at least 3 parallel samples, and from at least 5 images of each. Cells were counted from the images and at least 50 cells were counted per figure (except for the negative control, in which the cells did not attach and cell counts were extremely small). Statistical analysis was performed using SPSS 19 software (SPSS Inc., Chicago, IL). A non-parametric Kruskal-Wallis test followed by *post-hoc* comparison by Mann-Whitney U-test was performed on all datasets. An alpha-corrected p-value of less than 0.05 was considered significant.

5. Results

5.1 Spontaneous activity of the neuronal network

Neuronal cell activity was measured (**Studies I, II, III,** and **IV**) using the MEA system (Figure 7 A). Differentiated viable neuronal cells (Figure 7 **B)** cultured on MEA plates (Figure 7 **C**) were measured repeatedly, and survived for long culturing periods (up to 20 weeks). Those cells formed spontaneously active neuronal networks.

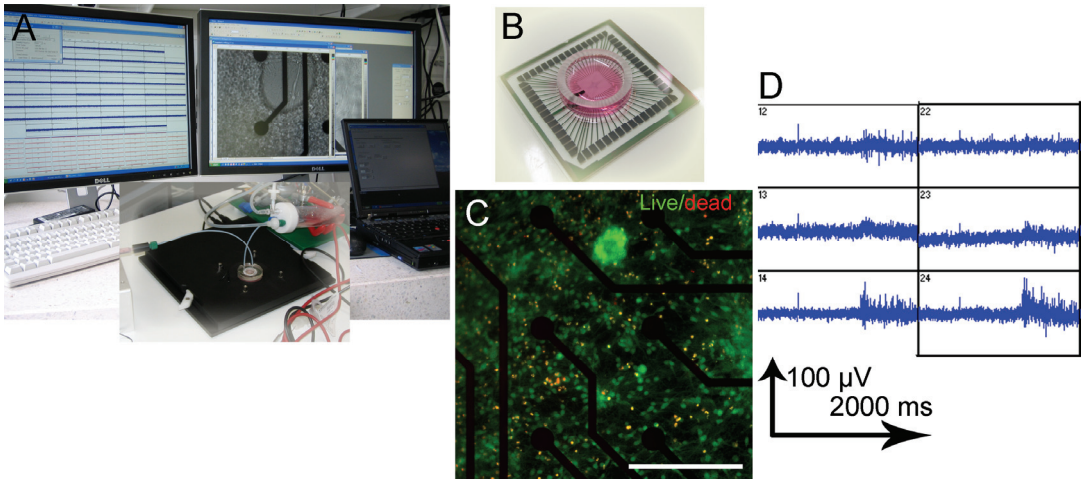

Figure 7. MEA recording system and measurement of the hESC-derived neuronal cells with the device. (A) The MEA recording system is composed of an MEA amplifier, computer, and heater. (B) MEA plate with glass ring culture chamber. (C) Human ESC-derived neuronal cells remain viable on MEA plates, based on live/dead analysis (live cells are seen in green and dead are seen in red). Scale bar is 100 µm (D) Mature (days on MEA > 30) neuronal network shows bursting activity on MEA plates.

The first step in spontaneous activity is single spiking activity. Here, single action potentials were generated by single neurons (Figure 7A). These first spikes occurred within 2 to 7 days after plating the cells on the MEA. Thereafter, the signals developed spike train-like activity (Mazzoni *et al.* 2007; Uroukov *et al.* 2008), during which several single spikes form a simple signal pattern (Figure 7B). This spike train-like activity is usually observed after 1 to 2 weeks of culturing on MEA. Finally, in the most developed phase, the spikes were organized into synchronous complex bursts (Figure 7 C), e.g., occurring in several electrodes at the same time (Figure 7 D). In bursts, the network is interconnected and the signal spread quickly from one cell to another.

5.2 Improvement of the measurement environment

In **Study II**, we aimed to improve the measurement environment for hESC-derived neuronal cells. We designed a structured PDMS chamber for MEA plates. The cells were able to grow in only a limited area (Ø 4 mm) on top of the electrodes (Figure 8 A, B). The chamber has a large (1000 µl) medium reservoir, allowing us to change the medium only 3 times/week. Improvement was evaluated by examining the success rate of cell attachment and measuring spontaneous cell activity. The limited cell growth area resulted in equally good cell attachment to the MEA plates compared to standard glass ring plates (Figure 4 in **Study II**) and better signaling development of the neuronal network. Spontaneous activity was analyzed based on two parameters: mean spiking activity/MEA and mean spikes/active channel. Both parameters revealed that cell cultures with a restricted culture area develop faster and spike more actively compared to cells cultured in a larger area (Figure 8 C, D).

Moreover, the same idea of a limited cell growth area was used to design a specific chamber for the 6-well MEA chambers. With this MEA plate type, 6 parallel cultures (9 measurement electrodes/culture) could be measured at the same time in one MEA plate. In these 6-well plates, the cells were still able to form active neuronal networks (Figures 5 and 6 in **Study II**), despite the limited growth area (Ø 2-3 mm).

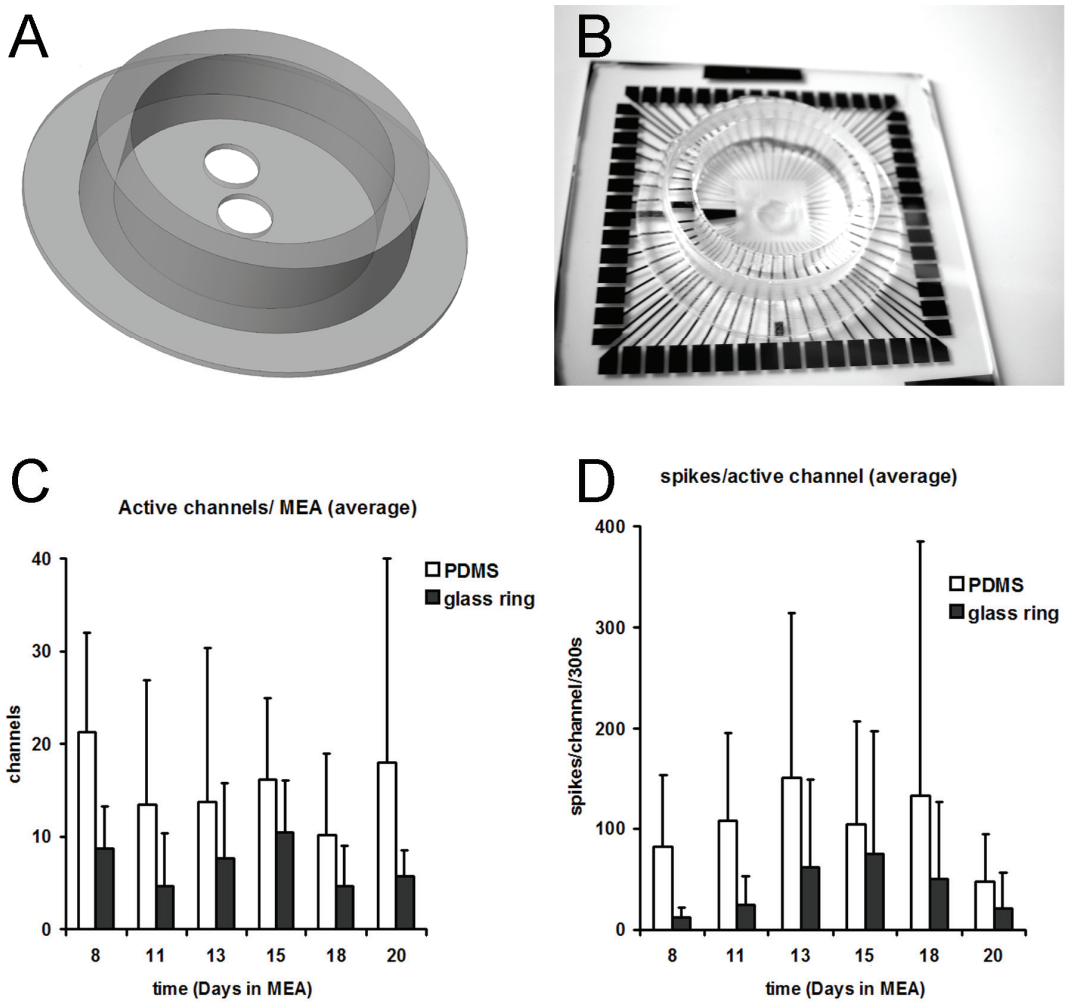

Figure 8. A structured PDMS chamber improved the electrical activity of the hESC-derived neuronal cells. Image of the PDMS chamber (A) and the chamber attached to the MEA plate (B). The PDMS chamber improved the electrical activity of the neuronal cells, based on measurements of active channels/MEA (C) and spikes/active channel (D). For (C) and (D), the bar represents the mean (n= 13) and the error bars represent the standard deviation.

5.3 Chemical modulation of the neuronal network

Chemical modulation of the neuronal networks can be used to evaluate the neuronal origin and receptor expression in neuronal networks, and the neurotoxic or pharmaceutical effects of the substances.

The Na^{2+}-channel blocker TTX was first applied to the neuronal networks (Figure 2G-H in **Study I**). TTX (50 μM) reversibly silenced the whole network, indicating that cell signaling is neuronally based, i.e., Na^{2+}-mediated.

The expression and functionality of certain neuron-specific receptors were characterized with CNQX, D-AP5, GABA, and bicuculline. CNQX and D-AP5 are well-known glutamate signaling inhibitors that block AMPA/kainate and NMDA receptors, respectively. CNQX decreased the spontaneous activity of the neuronal networks and the addition of both CNQX and D-AP5 almost completely blocked signaling. The effect was reversible, and activity recovered to near the baseline level after washout (Figure 4 in **Study I**). The network was silenced by the addition of GABA. On the other hand, activity recovered to baseline or was even higher after the addition of bicuculline (a $GABA_A$ antagonist; Figure 4 in **Study I**, and Figure 3B in **Study III**). Interestingly, in some cases, bicuculline caused prominent bursting activity (Figure 4G-H in **Study I**), whereas in other cases it only restored the signaling back to the baseline level (Figure 3B, 0 mM MeHgCl in **Study III**).

Well-characterized spontaneously active neuronal networks can be used for *in vitro* toxicity research. The toxicant MeHgCl was used at different concentrations to evaluate the suitability of the hESC-derived neuronal networks on MEA for toxicologic analysis. In the acute phase (0-1 hour after exposure), none of the networks (exposure concentration 0-500 nM) responded to the addition of MeHgCl (Figure 2 in **Study III**). After a delay, MeHgCl exposure showed some concentration-dependent effects (Figure 3 in **Study IV**). A clear decrease in activity was observed at the highest concentration (500 nM MeHgCl), affecting signaling. Native cells acted similarly and were equally viable (Figures 4 and 5 in **Study III**).

5.4 Cell culture scaffolds

5.4.1 Tested cell cultured platforms for 2D and 3D cultures

Several different cell culture scaffolds in 2D were tested for hESC-derived neuronal networks (Table 4). Bioactive glass fibers allowed for some attachment of the neuronal cells, but did not largely support the viability, outgrowth, or maturation of the attached cells (Table 4, Figure 9C). Electrospun PLA and PCL were tested as electrospun mats containing tiny (Ø 100-1000 µm) fibers. Cells attached to both electrospun mats, but slightly better attachment was observed on the PLA scaffolds.

Cell viability, outgrowth, and maturation were prominent in PLA scaffolds, whereas PCL scaffolds provided poor neuronal cell support (Table 4, Figure 9A).

All tested coated protein surfaces (collagen I-IV, laminin) supported neuronal cell attachment. Laminin (Figure 9E) and collagen IV were the most suitable for neuronal cells, whereas collagen I, II, and III did not provide an optimal protein surface for neuronal cells (Table 4, Figure 9B for collagen III).

PDMS seemed to have potential as a cell growth surface. The attachment and outgrowth of the cells was prominent, but the PDMS surface did not provide optimal support for the neuronal phenotype. Neither Cell Bind- surface (Corning, Figure 9D) nor SurModics were very good surfaces for neuronal cells. Titanium monoxide did not support cell growth at all (Table 4).

I also examined guidance channels, aimed at controlling cell growth. μ-Contact printed fibronectin patterns on a PCL surface seemed promising for cell guidance. Cells attached to the fibronectin cues well, and growth along the guidance structures was moderate. Two-photon polymerized Ormocomp neurocages did not restrict the cell growth as well as fibronectin patterns. Still, the cells seemed to mature in the Ormocomp neurocages moderately well (Table 4).

Gel surfaces were satisfactory for hESC-derived neuronal cell growth. All studied gels supported cell attachment, viability, outgrowth, and maturation very well or moderately well. The gel surface with the most potential was the OG-2 (Biomade) gel (Table 4).

Tested PLGA particles supported cell attachment (Table 4).

Table 4. Attachment, viability, outgrowth, and maturation of hESC-derived neuronal cells on various 2D biomaterials.

Material	*Attachment*	*Viability*	*Outgrowth*	*Maturation*	*(PD) / (UP)*
Fibers					
Biactive glass	+	-	-	-	UP
Poly lactide	++	++	++	++	PD
Poly(e-caprolactone)	+	-	-	-	UP
Protein surfaces					
Collagen I	++	-	-	-	UP
Collagen II	++	+	+	-	UP
Collagen III	+	+	+	+	UP
Collagen IV	++	++	++	+	UP
laminin	++	++	++	++	PD
Engineered surfaces					
PDMS	++	+	++	+	UP
Corning Cell Bind - surface	+	+	+	-	UP
SurModics	+	+	+	+	UP
Titanium Oxide	+	-	-	-	UP
Patterns/guidance channels					
Fibronectin surface	++	+	+	+	UP
Ormocomp	+	+	-	+	UP
Gels					
CellStart TM	++	+	+	+	UP
PuraMatrix	++	+	++	++	PD
OG2	++	++	++	++	UP
Particles					
PLGA particles	-	-	-	-	UP

++= very good, += moderate suitability, -= poor suitability. UP= Unpublished data, PD= published data

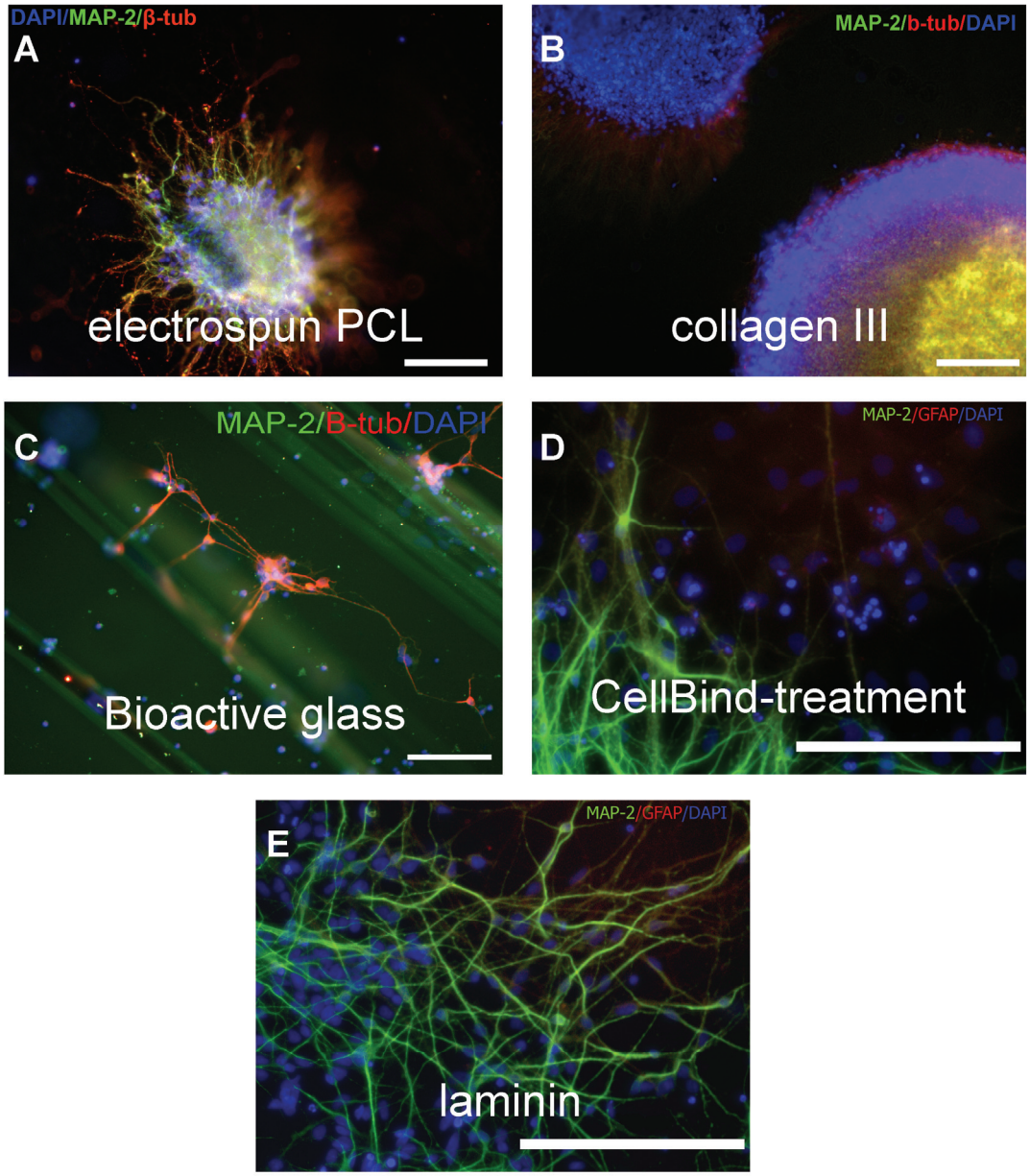

Figure 9. Maturation of hESC-derived neuronal cells on biomaterial surfaces. Cultured cells were immunostained after 2-week culture on the top of the biomaterials. Electrospun polycaprolactone (PCL, A) comprises a randomly oriented mat. Collagen III (B) and laminin (E) were used to coat the top of the cell culture plastic. Bioactive glass fibers had approximate diameters of 100 µm (C). Cell Bind-treated culture wells were commercially available treated cell culture wells (Corning, D). Scale bars for A, B, C= 100 µm, scale bars for D, E= 200 µm

5.4.2 Neuronal network formation and electrical activity in 3D

The optimal PuraMatrix gel concentration for encapsulation of neuronal cells was 0.10% to 0.15% (Figure 3 in **Study IV)**. At this concentration, cell survival was good, and migration and maturation were sufficient (Figure 10 A). Because neuronal cells (MAP-2 positive cells) comprised the majority of cells at a concentration of 0.10% (Figure 10 B), this concentration was selected for further experiments. Neuronal cells showed a more branched morphology in 3D culture (encapsulated inside the 0.10 % PuraMatrix gel) compared to the 2D laminin surface (Figure 10C for 3D, and D for 2D cultures). Neuronal cells formed a dense MAP-2 and β-tubulin positive neuronal network in 3D culture that was analyzed by confocal microscopy (Figure 10E).

Neuronal cells encapsulated inside the 0.10% PuraMatrix gel had the potential to form functionally active neuronal network. These cells matured into a training network similarly to their 2D counterparts grown on a laminin surface, but the maturation was slower on 3D cultured networks (Figure 4 in **Study IV**).

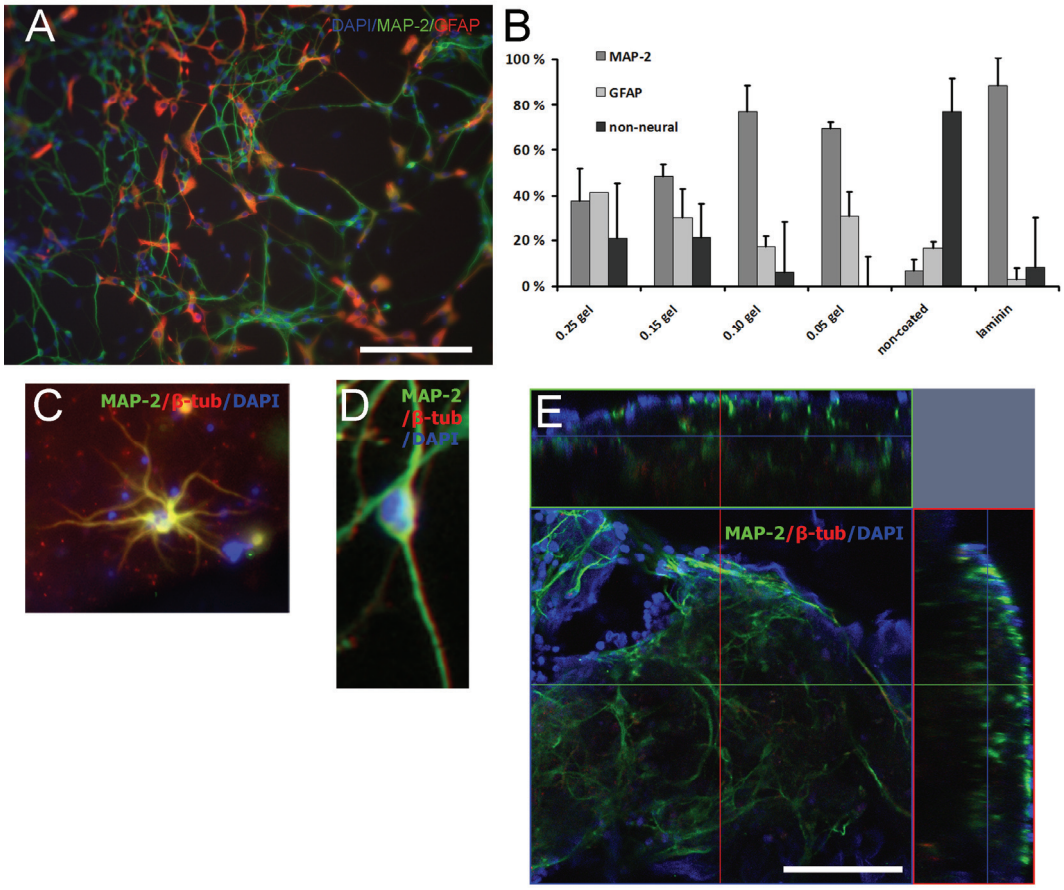

Figure 10. Human ESC-derived neuronal cells inside the PuraMatrix hydrogel. (A) Cells are able to form neuronal networks inside the gel supported by astroglial cells. (B) A 0.10% gel matrix seems optimal for neuronal (MAP-2 positive) cells. (C) Cells inside the hydrogel form a more complex morphology compared to those cultured on a laminin surface (D). (E) Orthogonal section from confocal images shows that cells spread all over the 3D gel structure, whereas the cell somata localized on the surface areas.

6. Discussion

In this thesis, the aim was to produce electrically active human neuronal networks in 2D and 3D that could serve as a platform to study their applicability for transplantation therapies and *in vitro* neurotoxicity analysis.

6.1 Spontaneous activity of stem cell-derived neuronal networks

Human ESC-derived neuronal cells were previously characterized using patch clamp techniques at the single cell level *in vitro* (Carpenter *et al.* 2001; Erceg *et al.* 2008; Johnson *et al.* 2007) and after transplantation *in vivo* (Reubinoff *et al.* 2001). Here, for the first time, the activity of those cells was demonstrated using MEA technique *in vitro* at the network level (**Study I**). While culturing these cells on top of the MEA, it is possible to monitor the spatial and temporal distribution of network formation. These hESC-derived neuronal cells are thus able to form spontaneously active neuronal networks *in vitro*. The activity development resembles that of rodent primary and mouse ESC-derived neuronal cultures (Illes *et al.* 2007; Wagenaar *et al.* 2006). Our differentiation method using suspension culture (described in more detail in (Lappalainen *et al.* 2010)) seems to be suitable for forming spontaneously active and mature neuronal networks. The adherent neural differentiation method, used by many research groups (Hoffman *et al.* 2005; Nat *et al.* 2007), may not be suitable for the production of active neuronal networks, at least according to the study results from mouse ESC-derived neuronal cells (Illes *et al.* 2009). This may be caused by a lack of glial cells in adherently differentiated homogenous cultures (Illes *et al.* 2009). Nevertheless, our laboratory has demonstrated that a purified neural cell adhesion molecule-positive neuronal population (100% of cells are neuronal precursor cells) can form a spontaneously

active network (Sundberg 2011). Thus, hESC-derived neuronal cells are able to form a spontaneously active neuronal network in at least the spike train-like activity phase without the presence of glial cells. Nevertheless, the differentiation method (suspension culture vs. adherent differentiation method), may have a crucial effect on spontaneous activity development in human-stem cell derived neuronal networks.

Compared to mouse ESCs, the development of hESC-derived functional neuronal networks is slower. While in mouse ESC-derived neuronal networks the signaling matures to the bursting phase (5 ± 2 spikes within a 300-ms time period) within 7 days (Illes *et al.* 2007), hESC-derived neuronal cells required 4 to 5 weeks. Nevertheless, the development followed similar schema in both cell types, despite the different time scale, as discussed in **Study I**. Moreover, some of the hESC-derived networks did not develop to the bursting phase at all, but continued to have spike train-like activity instead. Overall, human pluripotent stem cells, both hESC-(**Study 1**, (Lappalainen *et al.* 2010)) and hiPSC (Äänismaa *et al.* 2011)-derived neuronal networks, reached similar activity levels shown for ESC- or primary cell-derived *in vitro* neuronal cultures and thus are valid for various applications in which neuronal activity is considered to be a crucial factor.

6.2 MEA analysis

MEA technology has been used for almost four decades with many types of neuronal cells. Nevertheless, in this study, for the first time, hESC-derived neuronal cells were measured using the MEA method. All previous electrophysiologic studies of hESC-derived neuronal cells have been performed using patch clamp technology (Carpenter *et al.* 2001; Erceg *et al.* 2008; Johnson *et al.* 2007). Patch clamp technology is a widely used, but time-consuming technique, and thus fast screening for drug responses or electrical stimulations can be more easily performed with MEA technology.

One of the biggest challenges in using MEA technology as a measurement tool is the data analysis. Previous studies were performed mostly with primary rodent cultures, in which activity is prominent and at least 50% of MEA electrodes detect

bursting activity (Potter *et al.* 2001; Wagenaar *et al.* 2006). Thus, the network proceeds quickly and reliably to a bursting level, and most of the cells in the electrode area are involved in the formation of an active network. This kind of network-wide signaling is rather easy to analyze based on existing analysis tools (Chiappalone *et al.* 2007; Wagenaar *et al.* 2006; van Pelt *et al.* 2005). These methods are based on the detection of bursts, defined as a cluster of single spikes occurring within a short time interval and followed by a long latency stage. The exact definitions of bursts vary from laboratory to laboratory, but at least 3 to 5 spikes with a spike-to-spike interval of less than 100 ms or comparable is most common (Hogberg *et al.* 2011; Illes *et al.* 2007; Wagenaar *et al.* 2004). Calculating parameters, such as burst-to-burst interval, spikes-in-burst, and burst duration, can be assessed and compared between the neuronal networks.

Human ESC-derived neuronal networks seem, however, to form such immature networks that only rare networks show prominent bursting activity (**Studies I** and **III**), which is standard in rodent primary cell data analysis. Thus, previously developed burst analysis tools are not suitable for hESC-derived neuronal network activity analysis. In **Studies I, II,** and **III,** we used very simple parameters based on spiking activity but not bursting activity. The number of active electrodes, total number of spikes/MEA, and number of spikes/active electrodes were calculated. These values are simple and yet show the overall activity of the network. The drawbacks of these parameters is that a large MEA-to-MEA variation occurs and thus a relatively large number of parallel MEAs per experiment are needed for valid statistical analysis.

The second big challenge in MEA technology is random and uncontrolled network formation. Neurons are usually seeded on MEA plates as aggregates (**Studies I, II,** and **III**) or as homogenous single cell suspensions (**Study II**, (Illes *et al.* 2007; Wagenaar *et al.* 2006)). Nevertheless, cells migrate freely and randomly form networks. The development of a random network complicates the signaling analysis, e.g., burst leader and signal propagation analyses. Thus, reducing the possible connections makes analysis simpler and easier than the use of neurocages (Erickson *et al.* 2008), PDMS guidance channels (Kanagasabapathi *et al.* 2011), or protein patterns (Shein-Idelson *et al.* 2011). Here, the protein guidance channels and Ormocomp neurocages were tested for guiding the hESC-derived neuronal cell growth (unpublished data, Table 4). Both methods appear promising but require

further optimization, especially with regard to restricting the spread of the cells. Moreover, guidance structures have not yet been tested in the MEA environment with hESC-derived neuronal cells.

In the standard commercially available MEA electrode layout, only a small portion of the whole growth area is covered by the measurement electrodes, increasing the possibility that the network will form outside the electrode area. Therefore, in **Study II**, we reduced the cell growth area by creating a structured PDMS culture chamber in which the cells grew only in a limited area just on top of the electrodes, but the medium reservoir is still large (1 ml). The reduced growth area resulted in better activity and faster signal development than the standard growth area, which allows for more stable and robust MEA measurements from hESC-derived neuronal networks, and is important for their *in vitro* applications.

In the future, more reliable and robust analysis tools should be developed specifically for hESC-derived neuronal networks. Burst analysis tools optimized for hESC-derived neuronal cell activity data would provide more possibilities for statistical analysis and thus strengthen the analyses. Moreover, the controlled growth of neuronal networks makes analysis more straightforward and a restricted growth area produces more active and reliable networks. Altogether, improvement in the analysis tools and MEA culture environment would facilitate the development of valid and standardized analysis tools for neurotoxicologic screening.

6.3 Toxicology studies

Most toxicology studies are performed using animal cells. Although the availability of animal cells is good, they may differ from human cells and thus human cells are more relevant for human neurotoxicity platforms (Breier *et al.* 2008; Johnstone *et al.* 2010). There is a clear need for human cell-based neurotoxicologic *in vitro* platforms. These platforms could be used for rapid, reliable, and targeted toxicologic analysis. New *in vitro* platforms could provide information about toxicity and harmful effects without killing the cells, and these *in vitro* methods could be scaled to high-throughput and high-content analyses. High-throughput

analysis methods are a key aim in developing toxicity platforms (Bal-Price *et al.* 2009) as multiple samples can be analyzed simultaneously in both a time- and cost-effective manner. Another aim is high content screening, where multiple parameters are evaluated simultaneously to obtain more detailed information, e.g., toxic mechanisms (Giuliano *et al.* 2003). Traditionally, molecular biologic and viability analyses have been used for human cell based platforms (Buzanska *et al.* 2009; Fritsche *et al.* 2005; Moors *et al.* 2009), but these analyses provide only endpoint information. Electrophysiologic methods provide a new interesting analysis method for neurotoxicity assays. MEA technology allows for both high content and throughput screening in a sequential manner. Many companies already sell devices allowing for MEA measurements, multiparametric data analysis, and imaging with multiple cell culture wells (e.g., 3-Brain, Alpha MED Sciences/Panasonic, Axion Biosystems, MultiChannel Systems, Plexon, Qwane Biosciences SA, and Tucker-Davis Technologies) for toxicologic analysis.

Study III showed a proof-of-principle that MEA technology could be utilized with human-derived neuronal networks for a human *in vitro* toxicity platform using methyl mercury as the toxicant. We found that even small doses (500 nM) of methyl mercury decreased the network activity without affecting other evaluated parameters (viability, cell division, and gene and protein expression) of the cells. These findings suggest an even bigger role for MEA-based analysis parameters in neurotoxicology, as it is the only reliable method for showing the subtoxic level effect of methyl mercury on human-derived neuronal cultures. Thus, in the future, more precise neurotoxicologic analyses can be performed using MEA technology and human pluripotent stem cell-derived neuronal cells.

6.4 Biomaterial studies

Human ESCs have high potential as a cell source for transplantation therapies and in combination with supportive biomaterials in tissue-engineered products (Lindvall *et al.* 2010; Nisbet *et al.* 2008). Before developing tissue-engineered products, the establishment of a supportive *in vitro* model platform is crucial.

Here, various 2D surfaces and 3D scaffolds for hESCs were tested. The tested materials were selected according to the results of previous studies using animal-

derived neuronal cells (Brännvall *et al.* 2007; Cullen *et al.* 2007; Holmes *et al.* 2000; Yang *et al.* 2005) and based on the materials that were available commercially or via research collaboration. Poly(L-lysine), laminin, and Matrigel are widely used 2D-coating surfaces for various neuronal cells, including primary cells, murine neural progenitor cells, and hESC-derived neuronal cells (Erceg *et al.* 2008; Kim *et al.* 2010; Lappalainen *et al.* 2010; Reubinoff *et al.* 2000; Thonhoff *et al.* 2008; Uemura *et al.* 2010). We tested collagens (types I-IV) and laminin as 2D-coating materials for hESC-derived neuronal cells. Human laminin (derived from human placenta) seemed to provide the best surface for neurons (Table 4) and it was also used in **Studies I, II, III,** and **IV** as a coating material for cell culture plastic wells and coverslips. In addition, mouse laminin (derived from sarcoma cell basement membrane) was used in **Study III**. For MEA platforms, laminin did not provide adequate long-term attachment by itself (unpublished data). Thus, in **Study I**, PEI was added to the coating procedure to improve the surface charge and thus attachment of the laminin (Illes *et al.* 2007; Robinette *et al.* 2011).

In **Study II**, PDMS was used as cell culture chamber material, but it was also been tested as a growth surface. It provided a good surface for attachment, but not for the support for the neuronal maturation. That might be improved by varying the mechanical properties of the PDMS as reported earlier with rat neural stem cells (Teixeira *et al.* 2009).

For 3D scaffolds, hydrogels seem to have the most potential in combination with neuronal cells for transplantation therapies or neuronal tissue engineering. These materials are soft and mimic the mechanical properties of the ECM of nervous tissue (Geckil *et al.* 2010). They also form uniform or aligned 3D structures and cells are easy to encapsulate inside these structures (Geckil *et al.* 2010; Nisbet *et al.* 2008). The most commonly used natural hydrogels for neurologic applications are collagen and fibrinogen (Willerth *et al.* 2007; Xu *et al.* 2009). The better studied hydrogels are synthetic, peptide-mimicking hydrogels (Brännvall *et al.* 2007; Holmes *et al.* 2000). In **Study IV**, we demonstrated that PuraMatrix is suitable for 3D culturing of human derived neurons, astrocytes, and oligodendrocytes. Previous reports indicated that fibrin, hyaluronic acid, collagen, and Matrigel as well as PuraMatrix form a suitable growth matrix for human fetal stem cells, murine neural progenitors, or primary cell-derived neuronal cells in 3D (Brännvall *et al.* 2007; Holmes *et al.* 2000; Willerth *et al.* 2007; Xu *et al.* 2009).

Besides the hydrogels, a variety of electrospun, microspheric, and sponge-like materials have been tested (Jin *et al.* 2009; Silva *et al.* 2004; Thonhoff *et al.* 2008). For hESC-derived neuronal cells, fiber-like electrospun meshes were supportive (Shahbazi *et al.* 2011; Ylä-Outinen *et al.* 2010). These electrospun meshes seemed to support the growth of the cells nicely, but the materials used were not injectable and thus not optimal for future transplantation therapies (Nisbet *et al.* 2008). The same drawbacks were observed when using the salt-leached PLA sponge, which also supports hESC-derived neuronal cell differentiation and maturation (Levenberg *et al.* 2003).

6.5 Differences between 2D and 3D cultures

The 3D environment seems to support neurons in a different way from the 2D environment at genotypical, phenotypical, as well as functional levels (Crompton *et al.* 2007; Li *et al.* 2007; Ortinau *et al.* 2011; Sarig-Nadir *et al.* 2010; Thonhoff *et al.* 2008); Mahoney *et al.* 2006; Xu *et al.* 2009). Both the expression of neuron-specific genes and amount of mature neurons, based on immunocytochemical characterization, are increased in a 3D environment compared to a 2D environment (Ortinau *et al.* 2010). Electrophysiologic characterization of hippocampal neuronal cells in 3D culture shows improvement of spontaneously evoked signaling compared to that in 2D (Xu *et al.* 2009). Similar effects were detected in 3D cultured hESC-derived neuronal cells at morphologic and immunologic levels in **Study IV,** as neurons had a more typical *in vivo*-like morphology in 3D than in 2D culture**.** At the functional level, however, more time was required for neurons to develop functional networks in 3D than in 2D, but that is expected as neurons undergo drastic changes when transferred into an encapsulated 3D culture that likely slows their maturation. To date, only Pautot and colleagues have studied 3D neuronal networks *in vitro* with prolonged follow-up times (Pautot *et al.* 2008). As we demonstrated in our study, a prolonged follow-up time revealed the formation of functional neuronal networks in 3D, and thus these types of studies are needed, both

for evaluating the characteristics and behavior of possible 3D cell grafts and for validating the contribution of 3D *in vitro* models for various purposes.

6.6 Stem cell therapies in the present and in the future

Additional detailed information about the activity of the hESC-derived neuronal cells and networks are needed before these cells can be reliably used in transplantation therapies. Studies of stem cell transplantation therapies have faced both drawbacks and promising advances during recent years. Stem cell technology raises high hopes for patients suffering from neuronal dysfunction and therefore already a few companies have managed to take these applications into clinical phase trials. Stem Cells Inc. (www.stemcellsinc.com) has conducted a Phase I/II study on the safety of neural stem cell transplantation for children with Batten disease. The report from this clinical trial with human fetal stem cell-derived cells indicates that the transplanted cells caused no harmful effects and the cells remained alive in the host tissue for a long time (up to 3 years). This clinical trial was the first approved clinical trial with human neural stem cells worldwide. Now the company has focused on conducting a Phase I trial with these same cell transplants for the treatment of spinal cord injuries. ReNeuron (www.reneuron.com) aims to treat stroke patients in a similar manner with human fetal stem cell-derived neuronal cells in their Phase I trials. A total of 12 patients are included in the first Phase I safety trial and 6 of these patients have already been treated. The first report will be released by the company in early 2012. In contrast, Geron (www.geron.com), the third company performing approved clinical trials with human stem cell-derived cells, recently discontinued their clinical trial for treatment of spinal cord injury after treating 4 of 12 patients before halting the trial for economic reasons. Geron's trial led to increased tension worldwide as it was the first approved clinical trial with hESC-derived neural cells. Some other global companies sell stem cell treatments for a variety of patients, and have performed un-approved, un-documented, or unreported treatments for individual patients. These treatments place patients at great risk, as recently demonstrated in the case of XCell-Center GmbH (http://www.xcell-center.com/) in Germany. Hopefully, clinical phase studies will

soon become more common and will provide reliable information about the advantages of stem cell therapies. Nevertheless, transplantation therapies will only be applied for select CNS dysfunctions in select patients.

7. Conclusions

This project aimed to clarify the applicability of hESC-derived neuronal networks for *in vitro* modeling purposes and future transplantation therapies. Pluripotent stem cell technology and especially the applications of these cells are exciting new research areas.

Based on the findings of the present study, we conclude the following:

1) Human ESC-derived neuronal networks form spontaneously active neuronal networks *in vitro*. These neuronal networks develop signaling systems comparable to those of animal-derived cell networks. Signaling can be modulated by neurotransmitter agonists or antagonists.
2) Human ESC-derived neuronal networks form spontaneously active neuronal network faster and signaling develops faster when the cells are cultured in a structured PDMS cell cultivation chamber.
3) Human ESC-derived neuronal networks and the MEA measurement platform are a suitable system for toxicologic studies.
4) PuraMatrix is a suitable 3D growth matrix for hESC-derived neuronal networks. These cells grow and mature inside the hydrogel scaffold and form spontaneously active neuronal 3D networks.

References

Aalto-Setälä K, Conklin BR and Lo B. (2009): Obtaining consent for future research with induced pluripotent cells: opportunities and challenges. *PLoS Biol* 7: e42.

Adewola AF, Lee D, Harvat T, Mohammed J, Eddington DT, Oberholzer J and Wang Y. (2010): Microfluidic perifusion and imaging device for multi-parametric islet function assessment. *Biomed Microdevices* 12: 409-17.

Amariglio N, Hirshberg A, Scheithauer BW, Cohen Y, Loewenthal R, Trakhtenbrot L, Paz N, Koren-Michowitz M, Waldman D, Leider-Trejo L, Toren A, Constantini S and Rechavi G. (2009): Donor-derived brain tumor following neural stem cell transplantation in an ataxia telangiectasia patient. *PLoS Med* 6: e1000029.

Ashammakhi N, Ndreu A, Piras AM, Nikkola L, Sindelar T, Ylikauppila H, Harlin A, Gomes ME, Neves NM, Chiellini E, Chiellini F, Hasirci V, Redl H and Reis RL. (2007): Biodegradable nanomats produced by electrospinning: expanding multifunctionality and potential for tissue engineering. *J Nanosci Nanotechnol* 7: 862-82.

Ashammakhi N, Renier D, Arnaud E, Marchac D, Ninkovic M, Donaway D, Jones B, Serlo W, Laurikainen K, Törmälä P and Waris T. (2004): Clinical Notes: Successful Use of Biosorb Osteofixation Devices in 165 Cranial and Maxillofacial Cases: A Multicenter Report. *Journal of Craniofacial Surgery* 15: 1-10.

Bajpai R, Coppola G, Kaul M, Talantova M, Cimadamore F, Nilbratt M, Geschwind DH, Lipton SA and Terskikh AV. (2009): Molecular stages of rapid and uniform neuralization of human embryonic stem cells. *Cell Death Differ* 16: 807-25.

Bal-Price AK, Hogberg HT, Buzanska L and Coecke S. (2010): Relevance of in vitro neurotoxicity testing for regulatory requirements: challenges to be considered. *Neurotoxicol Teratol* 32: 36-41.

Bal-Price AK, Hogberg HT, Buzanska L, Lenas P, van Vliet E and Hartung T. (2009): In vitro developmental neurotoxicity (DNT) testing: Relevant models and endpoints. *Neurotoxicology*.

Ban J, Bonifazi P, Pinato G, Broccard F, Studer L, Torre V and Ruaro ME. (2006): ES-derived neurons form functional networks in vitro. *Stem Cells*.

Ben-Ari Y. (2001): Developing networks play a similar melody. *Trends Neurosci* 24: 353-60.

Berdichevsky Y, Sabolek H, Levine JB, Staley KJ and Yarmush ML. (2009): Microfluidics and multielectrode array-compatible organotypic slice culture method. *J Neurosci Methods* 178: 59-64.

Bibel M, Richter J, Schrenk K, Tucker KL, Staiger V, Korte M, Goetz M and Barde YA. (2004): Differentiation of mouse embryonic stem cells into a defined neuronal lineage. *Nat Neurosci* 7: 1003-9.

Bissonnette CJ, Lyass L, Bhattacharyya BJ, Belmadani A, Miller RJ and Kessler JA. (2011): The controlled generation of functional basal forebrain cholinergic neurons from human embryonic stem cells. *Stem Cells* 29: 802-11.

Breier JM, Radio NM, Mundy WR and Shafer TJ. (2008): Development of a high-throughput screening assay for chemical effects on proliferation and viability of immortalized human neural progenitor cells. *Toxicol Sci* 105: 119-33.

Brännvall K, Bergman K, Wallenquist U, Svahn S, Bowden T, Hilborn J and Forsberg-Nilsson K. (2007): Enhanced neuronal differentiation in a three-dimensional collagen-hyaluronan matrix. *J Neurosci Res* 85: 2138-46.

Buzanska L, Ruiz A, Zychowicz M, Rauscher H, Ceriotti L, Rossi F, Colpo P, Domanska-Janik K and Coecke S. (2009): Patterned growth and differentiation of human cord blood-derived neural stem cells on bio-functionalized surfaces. *Acta Neurobiol Exp (Wars)* 69: 24-36.

Buzanska L, Sypecka J, Nerini-Molteni S, Compagnoni A, Hogberg HT, del Torchio R, Domanska-Janik K, Zimmer J and Coecke S. (2009): A human stem cell-based model for identifying adverse effects of organic and inorganic chemicals on the developing nervous system. *Stem Cells* 27: 2591-601.

Cai J, Cheng A, Luo Y, Lu C, Mattson MP, Rao MS and Furukawa K. (2004): Membrane properties of rat embryonic multipotent neural stem cells. *Journal of neurochemistry* 88: 212-26.

Carpenter MK, Inokuma MS, Denham J, Mujtaba T, Chiu CP and Rao MS. (2001): Enrichment of neurons and neural precursors from human embryonic stem cells. *Exp Neurol* 172: 383-97.

Castoldi AF, Coccini T, Ceccatelli S and Manzo L. (2001): Neurotoxicity and molecular effects of methylmercury. *Brain Res Bull* 55: 197-203.

Chiappalone M, Vato A, Berdondini L, Koudelka-Hep M and Martinoia S. (2007): Network dynamics and synchronous activity in cultured cortical neurons. *Int J Neural Syst* 17: 87-103.

Cimadamore F, Fishwick K, Giusto E, Gnedeva K, Cattarossi G, Miller A, Pluchino S, Brill LM, Bronner-Fraser M and Terskikh AV. (2011): Human ESC-derived neural crest model reveals a key role for SOX2 in sensory neurogenesis. *Cell Stem Cell* 8: 538-51.

Cimetta E, Figallo E, Cannizzaro C, Elvassore N and Vunjak-Novakovic G. (2009): Micro-bioreactor arrays for controlling cellular environments: design principles for human embryonic stem cell applications. *Methods* 47: 81-9.

Corner MA, van Pelt J, Wolters PS, Baker RE and Nuytinck RH. (2002): Physiological effects of sustained blockade of excitatory synaptic transmission on spontaneously active developing neuronal networks--an inquiry into the reciprocal linkage between intrinsic biorhythms and neuroplasticity in early ontogeny. *Neurosci Biobehav Rev* 26: 127-85.

Crompton KE, Goud JD, Bellamkonda RV, Gengenbach TR, Finkelstein DI, Horne MK and Forsythe JS. (2007): Polylysine-functionalised thermoresponsive chitosan hydrogel for neural tissue engineering. *Biomaterials* 28: 441-9.

Cullen DK, Lessing MC and LaPlaca MC. (2007): Collagen-dependent neurite outgrowth and response to dynamic deformation in three-dimensional neuronal cultures. *Ann Biomed Eng* 35: 835-46.

Davies SJ, Shih CH, Noble M, Mayer-Proschel M, Davies JE and Proschel C. (2011): Transplantation of specific human astrocytes promotes functional recovery after spinal cord injury. *PLoS One* 6: e17328.

Defranchi E, Novellino A, Whelan M, Vogel S, Ramirez T, van Ravenzwaay B and Landsiedel R. (2011): Feasibility Assessment of Micro-Electrode Chip Assay as a Method of Detecting Neurotoxicity in vitro. *Front Neuroeng* 4: 6.

Delcroix GJ, Schiller PC, Benoit JP and Montero-Menei CN. (2010): Adult cell therapy for brain neuronal damages and the role of tissue engineering. *Biomaterials* 31: 2105-20.

Durnaoglu S, Genc S and Genc K. (2011): Patient-specific pluripotent stem cells in neurological diseases. *Stem Cells Int* 2011: 212487.

Erceg S, Lainez S, Ronaghi M, Stojkovic P, Perez-Arago MA, Moreno-Manzano V, Moreno-Palanques R, Planells-Cases R and Stojkovic M. (2008): Differentiation of human embryonic stem cells to regional specific neural precursors in chemically defined medium conditions. *PLoS ONE* 3: e2122.

Erceg S, Ronaghi M, Zipancic I, Lainez S, Rosello MG, Xiong C, Moreno-Manzano V, Rodriguez-Jimenez FJ, Planells R, Alvarez-Dolado M, Bhattacharya SS and Stojkovic M. (2010): Efficient differentiation of human embryonic stem cells into functional cerebellar-like cells. *Stem Cells Dev* 19: 1745-56.

Erceg S, Ronaghia M and Stojkovica M. (2009): Human Embryonic Stem Cell Differentiation Toward Regional Specific Neural Precursors. *Stem Cells* 27: 78-87.

Erickson J, Tooker A, Tai YC and Pine J. (2008): Caged neuron MEA: a system for long-term investigation of cultured neural network connectivity. *J Neurosci Methods* 175: 1-16.

Fields RD, Neale EA and Nelson PG. (1990): Effects of patterned electrical activity on neurite outgrowth from mouse sensory neurons. *J Neurosci* 10: 2950-64.

Freudenberg U, Hermann A, Welzel PB, Stirl K, Schwarz SC, Grimmer M, Zieris A, Panyanuwat W, Zschoche S, Meinhold D, Storch A and Werner C. (2009): A star-PEG-heparin hydrogel platform to aid cell replacement therapies for neurodegenerative diseases. *Biomaterials* 30: 5049-60.

Fritsche E, Cline JE, Nguyen NH, Scanlan TS and Abel J. (2005): Polychlorinated biphenyls disturb differentiation of normal human neural progenitor cells: clue for involvement of thyroid hormone receptors. *Environ Health Perspect* 113: 871-6.

Gaspard N and Vanderhaeghen P. (2010): From stem cells to neural networks: recent advances and perspectives for neurodevelopmental disorders. *Dev Med Child Neurol* 53: 13-7.

Geckil H, Xu F, Zhang X, Moon S and Demirci U. (2010): Engineering hydrogels as extracellular matrix mimics. *Nanomedicine (Lond)* 5: 469-84.

Gelain F, Bottai D, Vescovi A and Zhang S. (2006): Designer self-assembling peptide nanofiber scaffolds for adult mouse neural stem cell 3-dimensional cultures. *PLoS One* 1: e119.

Ghasemi-Mobarakeh L, Prabhakaran MP, Morshed M, Nasr-Esfahani MH and Ramakrishna S. (2008): Electrospun poly(epsilon-caprolactone)/gelatin nanofibrous scaffolds for nerve tissue engineering. *Biomaterials* 29: 4532-9.

Giuliano KA, Haskins JR and Taylor DL. (2003): Advances in high content screening for drug discovery. *Assay Drug Dev Technol* 1: 565-77.

Gross GW, Rieske E, Kreutzberg GW and Meyer A. (1977): A new fixed-array multi-microelectrode system designed for long-term monitoring of extracellular single unit neuronal activity in vitro. *Neurosci Lett* 6: 101-5.

Harry GJ, Billingsley M, Bruinink A, Campbell IL, Classen W, Dorman DC, Galli C, Ray D, Smith RA and Tilson HA. (1998): In vitro techniques for the assessment of neurotoxicity. *Environ Health Perspect* 106 Suppl 1: 131-58.

Hayman MW, Smith KH, Cameron NR and Przyborski SA. (2005): Growth of human stem cell-derived neurons on solid three-dimensional polymers. *J Biochem Biophys Methods* 62: 231-40.

Hejcl A, Lesny P, Pradny M, Michalek J, Jendelova P, Stulik J and Sykova E. (2008): Biocompatible hydrogels in spinal cord injury repair. *Physiol Res* 57 Suppl 3: S121-32.

Hess DC and Borlongan CV. (2008): Stem cells and neurological diseases. *Cell Prolif* 41 Suppl 1: 94-114.

Hicks AU, Lappalainen RS, Narkilahti S, Suuronen R, Corbett D, Sivenius J, Hovatta O and Jolkkonen J. (2009): Transplantation of human embryonic stem cell-derived neural precursor cells and enriched environment after cortical stroke in rats: cell survival and functional recovery. *Eur J Neurosci* 29: 562-74.

Hodgkin AL, Huxley AF and Katz B. (1952): Measurement of current-voltage relations in the membrane of the giant axon of Loligo. *J Physiol* 116: 424-48.

Hoffman LM and Carpenter MK. (2005): Characterization and culture of human embryonic stem cells. *Nat Biotechnol* 23: 699-708.

Hogberg HT, Sobanski T, Novellino A, Whelan M, Weiss DG and Bal-Price AK. (2011): Application of micro-electrode arrays (MEAs) as an emerging technology for developmental neurotoxicity: evaluation of domoic acid-induced effects in primary cultures of rat cortical neurons. *Neurotoxicology* 32: 158-68.

Holmes TC, de Lacalle S, Su X, Liu G, Rich A and Zhang S. (2000): Extensive neurite outgrowth and active synapse formation on self-assembling peptide scaffolds. *Proc Natl Acad Sci U S A* 97: 6728-33.

Horn EM, Beaumont M, Shu XZ, Harvey A, Prestwich GD, Horn KM, Gibson AR, Preul MC and Panitch A. (2007): Influence of cross-linked hyaluronic acid hydrogels on neurite outgrowth and recovery from spinal cord injury. *J Neurosurg Spine* 6: 133-40.

Illes S, Fleischer W, Siebler M, Hartung HP and Dihne M. (2007): Development and pharmacological modulation of embryonic stem cell-derived neuronal network activity. *Exp Neurol* 207: 171-6.

Illes S, Theiss S, Hartung HP, Siebler M and Dihne M. (2009): Niche-dependent development of functional neuronal networks from embryonic stem cell-derived neural populations. *BMC Neurosci* 10: 93.

Imreh MP, Gertow K, Cedervall J, Unger C, Holmberg K, Szoke K, Csoregh L, Fried G, Dilber S, Blennow E and Ahrlund-Richter L. (2006): In vitro culture conditions favoring selection of chromosomal abnormalities in human ES cells. *J Cell Biochem* 99: 508-16.

Itsykson P, Ilouz N, Turetsky T, Goldstein RS, Pera MF, Fishbein I, Segal M and Reubinoff BE. (2005): Derivation of neural precursors from human embryonic stem cells in the presence of noggin. *Mol Cell Neurosci* 30: 24-36.

Jain KK. (2009): Cell therapy for CNS trauma. *Mol Biotechnol* 42: 367-76.

Jang S, Cho HH, Cho YB, Park JS and Jeong HS. (2010): Functional neural differentiation of human adipose tissue-derived stem cells using bFGF and forskolin. *BMC Cell Biol* 11: 25.

Jin K, Mao X, Xie L, Galvan V, Lai B, Wang Y, Gorostiza O, Wang X and Greenberg DA. (2009): Transplantation of human neural precursor cells in Matrigel

scaffolding improves outcome from focal cerebral ischemia after delayed postischemic treatment in rats. *J Cereb Blood Flow Metab* 30: 534-44.

(2010): Transplantation of human neural precursor cells in Matrigel scaffolding improves outcome from focal cerebral ischemia after delayed postischemic treatment in rats. *J Cereb Blood Flow Metab* 30: 534-44.

Johnson MA, Weick JP, Pearce RA and Zhang SC. (2007): Functional neural development from human embryonic stem cells: accelerated synaptic activity via astrocyte coculture. *J Neurosci* 27: 3069-77.

Johnstone AF, Gross GW, Weiss DG, Schroeder OH, Gramowski A and Shafer TJ. (2010): Microelectrode arrays: a physiologically based neurotoxicity testing platform for the 21st century. *Neurotoxicology* 31: 331-50.

Jun SB, Hynd MR, Dowell-Mesfin N, Smith KL, Turner JN, Shain W and Kim SJ. (2007): Low-density neuronal networks cultured using patterned poly-l-lysine on microelectrode arrays. *J Neurosci Methods* 160: 317-26.

Kamei K-i, Guo S, Yu ZTF, Takahashi H, Gschweng E, Suh C, Wang X, Tang J, McLaughlin J, Witte ON, Lee K-B and Tseng H-R. (2009): An integrated microfluidic culture device for quantitative analysis of human embryonic stem cells. *Lab on a Chip* 9: 555-563.

Kanagasabapathi TT, Ciliberti D, Martinoia S, Wadman WJ and Decre MM. (2011): Dual-compartment neurofluidic system for electrophysiological measurements in physically segregated and functionally connected neuronal cell culture. *Front Neuroeng* 4: 13.

Kang KS and Trosko JE. (2011): Stem cells in toxicology: fundamental biology and practical considerations. *Toxicol Sci* 120 Suppl 1: S269-89.

Karumbayaram S, Novitch BG, Patterson M, Umbach JA, Richter L, Lindgren A, Conway AE, Clark AT, Goldman SA, Plath K, Wiedau-Pazos M, Kornblum HI and Lowry WE. (2009): Directed differentiation of human-induced pluripotent stem cells generates active motor neurons. *Stem Cells* 27: 806-11.

Kaur P, Aschner M and Syversen T. (2006): Glutathione modulation influences methyl mercury induced neurotoxicity in primary cell cultures of neurons and astrocytes. *Neurotoxicology* 27: 492-500.

Keirstead HS, Nistor G, Bernal G, Totoiu M, Cloutier F, Sharp K and Steward O. (2005): Human embryonic stem cell-derived oligodendrocyte progenitor cell transplants remyelinate and restore locomotion after spinal cord injury. *J Neurosci* 25: 4694-705.

Kerkis I, Hayashi MAF, Lizier NF, Cassola AC, Pereira LV and A. K. (2011): Pluripotent Stem Cells as an In Vitro Model of Neuronal Differentiation, . *Embryonic Stem Cells - Differentiation and Pluripotent Alternatives, Michael S. Kallos (Ed.)*.

Kim DS, Lee JS, Leem JW, Huh YJ, Kim JY, Kim HS, Park IH, Daley GQ, Hwang DY and Kim DW. (2010): Robust enhancement of neural differentiation from human ES and iPS cells regardless of their innate difference in differentiation propensity. *Stem Cell Rev* 6: 270-81.

Kim JE, O'Sullivan ML, Sanchez CA, Hwang M, Israel MA, Brennand K, Deerinck TJ, Goldstein LS, Gage FH, Ellisman MH and Ghosh A. (2011): Investigating synapse formation and function using human pluripotent stem cell-derived neurons. *Proc Natl Acad Sci U S A* 108: 3005-10.

Kim SJ, Lee JK, Kim JW, Jung JW, Seo K, Park SB, Roh KH, Lee SR, Hong YH, Kim SJ, Lee YS, Kim SJ and Kang KS. (2008): Surface modification of polydimethylsiloxane (PDMS) induced proliferation and neural-like cells differentiation of umbilical cord blood-derived mesenchymal stem cells. *J Mater Sci Mater Med* 19: 2953-62.

Kim YC, Kang JH, Park S-J, Yoon E-S and Park J-K. (2007): Microfluidic biomechanical device for compressive cell stimulation and lysis. *Sensors and Actuators B: Chemical* 128: 108-116.

Kiraly M, Porcsalmy B, Pataki A, Kadar K, Jelitai M, Molnar B, Hermann P, Gera I, Grimm WD, Ganss B, Zsembery A and Varga G. (2009): Simultaneous PKC and cAMP activation induces differentiation of human dental pulp stem cells into functionally active neurons. *Neurochem Int* 55: 323-32.

Kiris E, Nuss JE, Burnett JC, Kota KP, Koh DC, Wanner LM, Torres-Melendez E, Gussio R, Tessarollo L and Bavari S. (2011): Embryonic stem cell-derived motoneurons provide a highly sensitive cell culture model for botulinum neurotoxin studies, with implications for high-throughput drug discovery. *Stem Cell Res* 6: 195-205.

Klein CL, Scholl M and Maelicke A. (1999): Neuronal networks in vitro: formation and organization on biofunctionalized surfaces. *J Mater Sci Mater Med* 10: 721-7.

Korin N, Bransky A, Dinnar U and Levenberg S. (2009): Periodic "flow-stop" perfusion microchannel bioreactors for mammalian and human embryonic stem cell long-term culture. *Biomed Microdevices* 11: 87-94.

Krencik R and Zhang SC. (2011): Directed differentiation of functional astroglial subtypes from human pluripotent stem cells. *Nat Protoc* 6: 1710-7.

Lappalainen RS, Narkilahti S, Huhtala T, Liimatainen T, Suuronen T, Narvanen A, Suuronen R, Hovatta O and Jolkkonen J. (2008): The SPECT imaging shows the accumulation of neural progenitor cells into internal organs after systemic administration in middle cerebral artery occlusion rats. *Neurosci Lett* 440: 246-50.

Lappalainen RS, Salomaki M, Yla-Outinen L, Heikkila TJ, Hyttinen JA, Pihlajamaki H, Suuronen R, Skottman H and Narkilahti S. (2010): Similarly derived

and cultured hESC lines show variation in their developmental potential towards neuronal cells in long-term culture. *Regen Med* 5: 749-62.

Leclerc E, Sakai Y and Fujii T. (2003): Cell culture in 3-dimensional microfluidic structure of PDMS (polydimethylsiloxane). *Biomedical Microdevices* 5: 109-114.

Leipzig ND, Wylie RG, Kim H and Shoichet MS. (2010): Differentiation of neural stem cells in three-dimensional growth factor-immobilized chitosan hydrogel scaffolds. *Biomaterials* 32: 57-64.

Levenberg S, Huang NF, Lavik E, Rogers AB, Itskovitz-Eldor J and Langer R. (2003): Differentiation of human embryonic stem cells on three-dimensional polymer scaffolds. *Proc Natl Acad Sci U S A* 100: 12741-6.

Li GN, Livi LL, Gourd CM, Deweerd ES and Hoffman-Kim D. (2007): Genomic and morphological changes of neuroblastoma cells in response to three-dimensional matrices. *Tissue Eng* 13: 1035-47.

Lin HJ, O'Shaughnessy TJ, Kelly J and Ma W. (2004): Neural stem cell differentiation in a cell-collagen-bioreactor culture system. *Brain Res Dev Brain Res* 153: 163-73.

Lindvall O and Kokaia Z. (2006): Stem cells for the treatment of neurological disorders. *Nature* 441: 1094-6.

(2010): Stem cells in human neurodegenerative disorders--time for clinical translation? *J Clin Invest* 120: 29-40.

Liu H and Zhang SC. (2011): Specification of neuronal and glial subtypes from human pluripotent stem cells. *Cell Mol Life Sci* 68: 3995-4008.

Lou YJ and Liang XG. (2011): Embryonic stem cell application in drug discovery. *Acta Pharmacol Sin* 32: 152-9.

Madhavan R, Chao ZC and Potter SM. (2007): Plasticity of recurring spatiotemporal activity patterns in cortical networks. *Phys Biol* 4: 181-93.

Maeda E, Robinson HP and Kawana A. (1995): The mechanisms of generation and propagation of synchronized bursting in developing networks of cortical neurons. *J Neurosci* 15: 6834-45.

Mazzoni A, Broccard FD, Garcia-Perez E, Bonifazi P, Ruaro ME and Torre V. (2007): On the dynamics of the spontaneous activity in neuronal networks. *PLoS One* 2: e439.

McKernan R, McNeish J and Smith D. (2010): Pharma's developing interest in stem cells. *Cell Stem Cell* 6: 517-20.

McNeish JD. (2007): Stem cells as screening tools in drug discovery. *Curr Opin Pharmacol* 7: 515-20.

Melani R, Rebaudo R, Noraberg J, Zimmer J and Balestrino M. (2005): Changes in extracellular action potential detect kainic acid and trimethyltin toxicity in hippocampal slice preparations earlier than do MAP2 density measurements. *Altern Lab Anim* 33: 379-86.

Mitalipova MM, Rao RR, Hoyer DM, Johnson JA, Meisner LF, Jones KL, Dalton S and Stice SL. (2005): Preserving the genetic integrity of human embryonic stem cells. *Nat Biotechnol* 23: 19-20.

Moors M, Rockel TD, Abel J, Cline JE, Gassmann K, Schreiber T, Schuwald J, Weinmann N and Fritsche E. (2009): Human neurospheres as three-dimensional cellular systems for developmental neurotoxicity testing. *Environ Health Perspect* 117: 1131-8.

Narkilahti S, Rajala K, Pihlajamaki H, Suuronen R, Hovatta O and Skottman H. (2007): Monitoring and analysis of dynamic growth of human embryonic stem cells: comparison of automated instrumentation and conventional culturing methods. *Biomed Eng Online* 6: 11.

Nat R, Nilbratt M, Narkilahti S, Winblad B, Hovatta O and Nordberg A. (2007): Neurogenic neuroepithelial and radial glial cells generated from six human embryonic stem cell lines in serum-free suspension and adherent cultures. *Glia* 55: 385-99.

Nisbet DR, Crompton KE, Horne MK, Finkelstein DI and Forsythe JS. (2008): Neural tissue engineering of the CNS using hydrogels. *J Biomed Mater Res B Appl Biomater* 87: 251-63.

Nistor G, Siegenthaler MM, Poirier SN, Rossi S, Poole AJ, Charlton ME, McNeish JD, Airriess CN and Keirstead HS. (2011): Derivation of high purity neuronal progenitors from human embryonic stem cells. *PLoS One* 6: e20692.

Oizumi H, Hayashita-Kinoh H, Hayakawa H, Arai H, Furuya T, Ren YR, Yasuda T, Seki T, Mizuno Y and Mochizuki H. (2008): Alteration in the differentiation-related molecular expression in the subventricular zone in a mouse model of Parkinson's disease. *Neurosci Res* 60: 15-21.

Ortinau S, Schmich J, Block S, Liedmann A, Jonas L, Weiss DG, Helm CA, Rolfs A and Frech MJ. (2011): Effect of 3D-scaffold formation on differentiation and survival in human neural progenitor cells. *Biomed Eng Online* 9: 70.

Otto F, Illes S, Opatz J, Laryea M, Theiss S, Hartung HP, Schnitzler A, Siebler M and Dihne M. (2009): Cerebrospinal fluid of brain trauma patients inhibits in vitro neuronal network function via NMDA receptors. *Ann Neurol* 66: 546-55.

Park DH and Eve DJ. (2009): Regenerative medicine: advances in new methods and technologies. *Med Sci Monit* 15: RA233-51.

Pautot S, Wyart C and Isacoff EY. (2008): Colloid-guided assembly of oriented 3D neuronal networks. *Nat Methods* 5: 735-40.

Petros TJ, Tyson JA and Anderson SA. (2011): Pluripotent stem cells for the study of CNS development. *Front Mol Neurosci* 4: 30.

Pine J. (1980): Recording action potentials from cultured neurons with extracellular microcircuit electrodes. *J Neurosci Methods* 2: 19-31.

Potter SM and DeMarse TB. (2001): A new approach to neural cell culture for long-term studies. *J Neurosci Methods* 110: 17-24.

Purves D, Augustine GJ, Fitzpatrick D, Hall WC, LaMantia A-S, McNamara JO and White LE. (2008). Neuroscience. Sunderland, MA, Sinauer Associates, Inc.

Rajala K, Hakala H, Panula S, Aivio S, Pihlajamaki H, Suuronen R, Hovatta O and Skottman H. (2007): Testing of nine different xeno-free culture media for human embryonic stem cell cultures. *Human reproduction (Oxford, England)* 22: 1231-8.

Reier PJ. (2004): Cellular Transplantation Strategies for Spinal Cord Injury and Translational Neurobiology. *Neurorx* 1: 424-451.

Reubinoff BE, Itsykson P, Turetsky T, Pera MF, Reinhartz E, Itzik A and Ben-Hur T. (2001): Neural progenitors from human embryonic stem cells. *Nat Biotechnol* 19: 1134-40.

Reubinoff BE, Pera MF, Fong CY, Trounson A and Bongso A. (2000): Embryonic stem cell lines from human blastocysts: somatic differentiation in vitro. *Nat Biotechnol* 18: 399-404.

Rhee SW, Taylor AM, Tu CH, Cribbs DH, Cotman CW and Jeon NL. (2005): Patterned cell culture inside microfluidic devices. *Lab Chip* 5: 102-7.

Robinette BL, Harrill JA, Mundy WR and Shafer TJ. (2011): In vitro assessment of developmental neurotoxicity: use of microelectrode arrays to measure functional changes in neuronal network ontogeny. *Front Neuroeng* 4: 1.

Rolletschek A, Blyszczuk P and Wobus AM. (2004): Embryonic stem cell-derived cardiac, neuronal and pancreatic cells as model systems to study toxicological effects. *Toxicology letters* 149: 361-9.

Sarig-Nadir O and Seliktar D. (2010): The role of matrix metalloproteinases in regulating neuronal and nonneuronal cell invasion into PEGylated fibrinogen hydrogels. *Biomaterials* 31: 6411-6.

Schmidt CE and Leach JB. (2003): Neural tissue engineering: strategies for repair and regeneration. *Annu Rev Biomed Eng* 5: 293-347.

Shahbazi E, Kiani S, Gourabi H and Baharvand H. (2011): Electrospun nanofibrillar surfaces promote neuronal differentiation and function from human embryonic stem cells. *Tissue Eng Part A* 17: 3021-31.

Shein-Idelson M, Ben-Jacob E and Hanein Y. (2011): Engineered neuronal circuits: a new platform for studying the role of modular topology. *Front Neuroeng* 4: 10.

Shin H, Jo S and Mikos AG. (2003): Biomimetic materials for tissue engineering. *Biomaterials* 24: 4353-64.

Silva GA, Czeisler C, Niece KL, Beniash E, Harrington DA, Kessler JA and Stupp SI. (2004): Selective differentiation of neural progenitor cells by high-epitope density nanofibers. *Science* 303: 1352-5.

Smits AM, van den Hengel LG, van den Brink S, Metz CH, Doevendans PA and Goumans MJ. (2009): A new in vitro model for stem cell differentiation and interaction. *Stem Cell Res* 2: 108-12.

Srouji S, Kizhner T, Suss-Tobi E, Livne E and Zussman E. (2008): 3-D Nanofibrous electrospun multilayered construct is an alternative ECM mimicking scaffold. *J Mater Sci Mater Med* 19: 1249-55.

Straley KS, Foo CW and Heilshorn SC. (2010): Biomaterial design strategies for the treatment of spinal cord injuries. *J Neurotrauma* 27: 1-19.

Subbiah T, Bhat GS, Tock RW, Parameswaran S and Ramkumar SS. (2005): Electrospinning of Nanofibers. *Journal of Applied Polymer Science* 96: 557-569.

Sundberg M (2011). Differentiation and Purification of Human Pluripotent Stem Cell-derived Neuronal and Glial Cells - graft designing for spinal cord injury repair. http://acta.uta.fi/teos.php?id=11421, Tampere University Press, Acta Universitatis Tamperensis; 1593.

Sundberg M, Andersson PH, Akesson E, Odeberg J, Holmberg L, Inzunza J, Falci S, Ohman J, Suuronen R, Skottman H, Lehtimaki K, Hovatta O, Narkilahti S and Sundstrom E. (2010): Markers of pluripotency and differentiation in human neural precursor cells derived from embryonic stem cells and CNS tissue. *Cell Transplant* 20: 177-91.

Sundberg M, Skottman H, Suuronen R and Narkilahti S. (2010): Production and isolation of NG2+ oligodendrocyte precursors from human embryonic stem cells in defined serum-free medium. *Stem Cell Res* 5: 91-103.

Takahashi K, Tanabe K, Ohnuki M, Narita M, Ichisaka T, Tomoda K and Yamanaka S. (2007): Induction of pluripotent stem cells from adult human fibroblasts by defined factors. *Cell* 131: 861-72.

Teixeira AI, Ilkhanizadeh S, Wigenius JA, Duckworth JK, Inganas O and Hermanson O. (2009): The promotion of neuronal maturation on soft substrates. *Biomaterials* 30: 4567-72.

Teng YD, Lavik EB, Qu X, Park KI, Ourednik J, Zurakowski D, Langer R and Snyder EY. (2002): Functional recovery following traumatic spinal cord injury mediated by a unique polymer scaffold seeded with neural stem cells. *Proc Natl Acad Sci U S A* 99: 3024-9.

the Commission on the Statistics tEU (2007). Fifth Report from the Commission on the Statistics on the number of animals used for experimental and other scientific purposes in the member states of the European Union COM/2007/675 final. COM/2007/675.

Thomas CA, Jr., Springer PA, Loeb GE, Berwald-Netter Y and Okun LM. (1972): A miniature microelectrode array to monitor the bioelectric activity of cultured cells. *Exp Cell Res* 74: 61-6.

Thomson JA, Itskovitz-Eldor J, Shapiro SS, Waknitz MA, Swiergiel JJ, Marshall VS and Jones JM. (1998): Embryonic stem cell lines derived from human blastocysts. *Science* 282: 1145-7.

Thomson JA and Ludwig T (2006). Medium and culture of embryonic stem cells. International patent application. **US20060084168**.

Thonhoff JR, Lou DI, Jordan PM, Zhao X and Wu P. (2008): Compatibility of human fetal neural stem cells with hydrogel biomaterials in vitro. *Brain Res* 1187: 42-51.

Toh YC, Blagovic K, Yu H and Voldman J. (2011): Spatially organized in vitro models instruct asymmetric stem cell differentiation. *Integr Biol (Camb)* 3: 1179-87.

Toimela T, Tahti H and Ylikomi T. (2008): Comparison of an automated pattern analysis machine vision time-lapse system with traditional endpoint measurements in the analysis of cell growth and cytotoxicity. *Altern Lab Anim* 36: 313-25.

Tourovskaia A, Figueroa-Masot X and Folch A. (2005): Differentiation-on-a-chip: a microfluidic platform for long-term cell culture studies. *Lab Chip* 5: 14-9.

Uemura M, Refaat MM, Shinoyama M, Hayashi H, Hashimoto N and Takahashi J. (2010): Matrigel supports survival and neuronal differentiation of grafted embryonic stem cell-derived neural precursor cells. *J Neurosci Res* 88: 542-51.

Uroukov IS and Bull L. (2008): On the effect of long-term electrical stimulation on three-dimensional cell cultures: Hen embryo brain spheroids. *Medical Devices: Evidence and Research* 1: 1-12.

Wagenaar DA, Pine J and Potter SM. (2004): Effective parameters for stimulation of dissociated cultures using multi-electrode arrays. *J Neurosci Methods* 138: 27-37.

(2006): An extremely rich repertoire of bursting patterns during the development of cortical cultures. *BMC Neurosci* 7: 151–156.

Vallier L, Alexander M and Pedersen RA. (2005): Activin/Nodal and FGF pathways cooperate to maintain pluripotency of human embryonic stem cells. *Journal of cell science* 118: 4495-509.

van Kooten TG, Whitesides JF and von Recum A. (1998): Influence of silicone (PDMS) surface texture on human skin fibroblast proliferation as determined by cell cycle analysis. *J Biomed Mater Res* 43: 1-14.

van Pelt J, Vajda I, Wolters PS, Corner MA and Ramakers GJ. (2005): Dynamics and plasticity in developing neuronal networks in vitro. *Prog Brain Res* 147: 173-88.

van Vliet E, Stoppini L, Balestrino M, Eskes C, Griesinger C, Sobanski T, Whelan M, Hartung T and Coecke S. (2007): Electrophysiological recording of re-aggregating brain cell cultures on multi-electrode arrays to detect acute neurotoxic effects. *Neurotoxicology* 28: 1136-46.

Webber DJ and Minger SL. (2004): Therapeutic potential of stem cells in central nervous system regeneration. *Curr Opin Investig Drugs* 5: 714-9.

Vescovi AL, Parati EA, Gritti A, Poulin P, Ferrario M, Wanke E, Frolichsthal-Schoeller P, Cova L, Arcellana-Panlilio M, Colombo A and Galli R. (1999): Isolation and cloning of multipotential stem cells from the embryonic human CNS and establishment of transplantable human neural stem cell lines by epigenetic stimulation. *Exp Neurol* 156: 71-83.

Willerth SM, Arendas KJ, Gottlieb DI and Sakiyama-Elbert SE. (2006): Optimization of fibrin scaffolds for differentiation of murine embryonic stem cells into neural lineage cells. *Biomaterials* 27: 5990-6003.

Willerth SM and Sakiyama-Elbert SE. (2007): Approaches to neural tissue engineering using scaffolds for drug delivery. *Adv Drug Deliv Rev* 59: 325-38.

Wong Po Foo CT, Lee JS, Mulyasasmita W, Parisi-Amon A and Heilshorn SC. (2009): Two-component protein-engineered physical hydrogels for cell encapsulation. *Proc Natl Acad Sci U S A* 106: 22067-72.

Wu Y-P, Chen W-S, Teng C and Zhang N. (2010): Stem Cells for the Treatment of Neurodegenerative Diseases. *Molecules* 15: 6743-6758.

Xia Y, Rogers JA, Paul KE and Whitesides GM. (1999): Unconventional Methods for Fabricating and Patterning Nanostructures. *Chem Rev* 99: 1823-1848.

Xiong Y, Zeng YS, Zeng CG, Du BL, He LM, Quan DP, Zhang W, Wang JM, Wu JL, Li Y and Li J. (2009): Synaptic transmission of neural stem cells seeded in 3-dimensional PLGA scaffolds. *Biomaterials* 30: 3711-22.

Xu T, Molnar P, Gregory C, Das M, Boland T and Hickman JJ. (2009): Electrophysiological characterization of embryonic hippocampal neurons cultured in a 3D collagen hydrogel. *Biomaterials* 30: 4377-83.

Yamada M, Tanemura K, Okada S, Iwanami A, Nakamura M, Mizuno H, Ozawa M, Ohyama-Goto R, Kitamura N, Kawano M, Tan-Takeuchi K, Ohtsuka C, Miyawaki A, Takashima A, Ogawa M, Toyama Y, Okano H and Kondo T. (2006): Electrical stimulation modulates fate determination of differentiating embryonic stem cells. *Stem Cells*.

Yang F, Murugan R, Wang S and Ramakrishna S. (2005): Electrospinning of nano/micro scale poly(L-lactic acid) aligned fibers and their potential in neural tissue engineering. *Biomaterials* 26: 2603-10.

Yang F, Xu CY, Kotaki M, Wang S and Ramakrishna S. (2004): Characterization of neural stem cells on electrospun poly(L-lactic acid) nanofibrous scaffold. *J Biomater Sci Polym Ed* 15: 1483-97.

Yim EK, Wen J and Leong KW. (2006): Enhanced extracellular matrix production and differentiation of human embryonic germ cell derivatives in biodegradable poly(epsilon-caprolactone-co-ethyl ethylene phosphate) scaffold. *Acta Biomater* 2: 365-76.

Ylä-Outinen L, Mariani C, Skottman H, Suuronen R, Harlin A and Narkilahti S. (2010): Electrospun Poly(L,D-lactide) Scaffolds Support the Growth of Human Embryonic Stem Cell-derived Neuronal Cells. *The Open Tissue Engineering and Regenerative Medicine Journal* 3: 1-9.

Yu J, Vodyanik MA, Smuga-Otto K, Antosiewicz-Bourget J, Frane JL, Tian S, Nie J, Jonsdottir GA, Ruotti V, Stewart R, Slukvin, II and Thomson JA. (2007): Induced pluripotent stem cell lines derived from human somatic cells. *Science* 318: 1917-20.

Yuan SH, Martin J, Elia J, Flippin J, Paramban RI, Hefferan MP, Vidal JG, Mu Y, Killian RL, Israel MA, Emre N, Marsala S, Marsala M, Gage FH, Goldstein LS and Carson CT. (2011): Cell-surface marker signatures for the isolation of neural stem cells, glia and neurons derived from human pluripotent stem cells. *PLoS One* 6: e17540.

Zeng H, Guo M, Martins-Taylor K, Wang X, Zhang Z, Park JW, Zhan S, Kronenberg MS, Lichtler A, Liu HX, Chen FP, Yue L, Li XJ and Xu RH. (2010): Specification of region-specific neurons including forebrain glutamatergic neurons from human induced pluripotent stem cells. *PLoS One* 5: e11853.

Zeng X, Chen J, Deng X, Liu Y, Rao MS, Cadet JL and Freed WJ. (2006): An in vitro model of human dopaminergic neurons derived from embryonic stem cells: MPP+ toxicity and GDNF neuroprotection. *Neuropsychopharmacology* 31: 2708-15.

Zhang N, Yan H and Wen X. (2005): Tissue-engineering approaches for axonal guidance. *Brain Res Brain Res Rev* 49: 48-64.

Zhang S. (2002): Emerging biological materials through molecular self-assembly. *Biotechnol Adv* 20: 321-39.

Zhang S, Gelain F and Zhao X. (2005): Designer self-assembling peptide nanofiber scaffolds for 3D tissue cell cultures. *Semin Cancer Biol* 15: 413-20.

Zhang SC, Wernig M, Duncan ID, Brustle O and Thomson JA. (2001): In vitro differentiation of transplantable neural precursors from human embryonic stem cells. *Nat Biotechnol* 19: 1129-33.

Zhong Y and Bellamkonda RV. (2008): Biomaterials for the central nervous system. *J R Soc Interface* 5: 957-75.

Äänismaa R, Ylä-Outinen L, Mikkonen JE and Narkilahti S. (2011). Human pluripotent stem cell-derived neuronal networks: their electrical functionality and usability for modelling and toxicology, InTech.

Experimental Neurology 218 (2009) 109–116

Contents lists available at ScienceDirect

Experimental Neurology

journal homepage: www.elsevier.com/locate/yexnr

Human embryonic stem cell-derived neuronal cells form spontaneously active neuronal networks *in vitro*

Teemu J. Heikkilä [a,b], Laura Ylä-Outinen [a,b], Jarno M.A. Tanskanen [a], Riikka S. Lappalainen [b], Heli Skottman [b], Riitta Suuronen [a,b,c], Jarno E. Mikkonen [b], Jari A.K. Hyttinen [a], Susanna Narkilahti [b,*]

[a] *Department of Biomedical Engineering, Tampere University of Technology, Tampere, Finland*
[b] *Regea–Institute for Regenerative Medicine, University of Tampere and Tampere University Hospital, Tampere, Finland*
[c] *Department of Eye, Ear, and Oral Diseases, Tampere University Hospital, Tampere, Finland*

ARTICLE INFO

Article history:
Received 5 July 2008
Revised 23 February 2009
Accepted 14 April 2009
Available online 22 April 2009

Keywords:
Human embryonic stem cell-derived neurons
hESC-derived neuronal networks
MEA
Microelectrode array
Neuronal differentiation
Neuronal network
Polyethyleneimine
Spike train
Stem cells
Synchronous bursting

ABSTRACT

The production of functional human embryonic stem cell (hESC)-derived neuronal cells is critical for the application of hESCs in treating neurodegenerative disorders. To study the potential functionality of hESC-derived neurons, we cultured and monitored the development of hESC-derived neuronal networks on microelectrode arrays. Immunocytochemical studies revealed that these networks were positive for the neuronal marker proteins β-tubulin$_{III}$ and microtubule-associated protein 2 (MAP-2). The hESC-derived neuronal networks were spontaneously active and exhibited a multitude of electrical impulse firing patterns. Synchronous bursts of electrical activity similar to those reported for hippocampal neurons and rodent embryonic stem cell-derived neuronal networks were recorded from the differentiated cultures until up to 4 months. The dependence of the observed neuronal network activity on sodium ion channels was examined using tetrodotoxin (TTX). Antagonists for the glutamate receptors NMDA [D(−)-2-amino-5-phosphonopentanoic acid] and AMPA/kainate [6-cyano-7-nitroquinoxaline-2,3-dione], and for GABA$_A$ receptors [(−)-bicuculline methiodide] modulated the spontaneous electrical activity, indicating that pharmacologically susceptible neuronal networks with functional synapses had been generated. The findings indicate that hESC-derived neuronal cells can generate spontaneously active networks with synchronous communication *in vitro*, and are therefore suitable for use in developmental and drug screening studies, as well as for regenerative medicine.

Introduction

Human embryonic stem cells (hESCs) are pluripotent cells that have nearly unlimited developmental potential. Even after months of growth, hESCs continue to replicate and maintain the ability to differentiate into any human body cell type (Thomson et al., 1998). Their developmental potential makes hESCs a promising and essentially unlimited supply of numerous cell types for basic research and cell transplantation therapies for the treatment of a wide range of degenerative diseases, such as Parkinson's disease (Wang et al., 2007), Alzheimer's disease (Wu et al., 2007), and diabetes (Lock and Tzanakakis, 2007). Large amounts of functional neuronal cells, however, are needed to treat neurodegenerative disorders (Hess and Borlongan, 2008). To date, no reported studies have focused on developing functional neuronal networks of hESC-derived cells that act *in vitro* as they should *in vivo*. Thus, much more *in vitro* study-based information about the characteristics of hESC-derived neuronal cells is required before viable, safe, and functional cell grafts can be developed for successful transplantation and integration into the nervous system. In addition to the potential applications of hESCs in regenerative medicine, hESC-derived cells can be used in other medical, biological, and pharmaceutical applications (Rolletschek et al. 2004; Stummann and Bremer, 2008). Furthermore, more detailed studies of hESCs will contribute valuable information about early human development.

To better understand how single cell activity combines to form network-level functions, it is essential to study how neurons work in concert. Microelectrode array (MEA) technology (Gross et al., 1977; Pine, 1980) allows measuring the electrical activity of a neuronal system at the network-level. The electrical activity of a cell population can be measured while the cells grow *in vitro* on a growth plate with embedded recording electrodes. MEA recordings reveal the spatial and temporal distribution of electrical activity generated by neuronal populations near the microelectrodes. Despite the simplified level of organization of planar cell cultures on MEAs, this system reveals general information about electrophysiological properties, developmental changes in the activity patterns, and basic learning mechanisms of the nervous system (Ben-Ari, 2001; Katz and Shatz, 1996; Madhavan et al., 2007; Maeda et al., 1995; Van Pelt et al., 2005; Wagenaar et al., 2006; Yvert et al., 2004). MEA cultures can be followed for long periods of time over which the populations develop

* Corresponding author.
E-mail address: susanna.narkilahti@regea.fi (S. Narkilahti).

0014-4886/$ – see front matter © 2009 Elsevier Inc. All rights reserved.
doi:10.1016/j.expneurol.2009.04.011

from isolated neurons into fully connected neuronal networks, during which they pass through the phases of overproduction of synaptic connections and subsequent synaptic elimination and stabilization (Corner et al., 2002). Spatiotemporal analyses of multi-channel recordings on dissociated rodent cortical or hippocampal slices (Chiappalone et al., 2007; Li et al., 2007; Madhavan et al., 2007; Otto et al., 2003; Van Pelt et al., 2005; Wagenaar et al., 2006) or mouse embryonic stem cell-derived neurons (Ban et al., 2007; Illes et al., 2007) have been performed. Neuronal cell populations derived from hESCs, however, have not been previously studied.

Here, we describe the functional development of hESC-derived neuronal networks cultured for up to 4 months on MEAs. We followed the maturation of the neuronal network activity towards synchronous bursting and observed the responses of the hESC-derived neuronal networks to pharmacologic substances that act on synaptic receptors.

Materials and methods

Briefly, hESCs were differentiated towards neuronal lineage, and the effect of MEA-dish coatings on cell viability and neuronal characteristics were assessed based on live/dead assay and immunocytochemical staining. Neuronal cultures were prepared for MEA dishes and electrophysiological activity of the cultures was recorded with the MEA system. The recordings were used to assess the activity characteristics of the neuronal cells and networks. Similar analyses were conducted using pharmacologic agents that affect cell ionic and synaptic activity.

Neuronal cell differentiation

The hESC lines HS181, HS360, and HS362 derived at Karolinska Institutet (Hospital Huddinge, Stockholm, Sweden), and 06/015 derived at Regea (University of Tampere, Tampere, Finland) were used for neuronal differentiation. The ethics committee of the Karolinska Institutet approved the derivation, characterization, and differentiation of the hESC lines. The ethics committee of the Pirkanmaa Hospital District provided approval for Regea to culture the hESC lines derived at the Karolinska Institutet and to derive and culture new hESC lines. hESC lines were cultured in Knockout Dulbecco's modified eagle medium (DMEM, Invitrogen, Carlsbad, CA) with 20% serum replacement, 2 mM GlutaMax (Invitrogen), 1% non-essential amino acids (Cambrex Bio Science, New Jersey, NJ), 50 U/ml penicillin/streptomycin (Lonza Group Ltd., Switzerland), 0.1 mM 2-mercaptoethanol (Invitrogen), and 8 ng/ml basic fibroblast growth factor (bFGF, R&D Systems, Minneapolis, MN) on top of a human feeder cell layer (CRL-2429, ATCC, Manassas, CA). The undifferentiated stage of hESCs was confirmed daily by morphologic analysis and frequently by immunocytochemical stainings for the ESC markers Nanog, Oct-4, SSEA-4, and Tra-1-60.

Neural differentiation of hESCs was performed as previously described (Nat et al., 2007; Sundberg et al., 2009). Briefly, the neural differentiation was induced by dissecting hESC colonies into small clusters of approximately 3000 cells. These clusters were cultured in suspension in low attachment 6-well plates (Nunc, Thermo Fisher Scientific, Rochester, NY, USA) in 1:1 DMEM/F12/Neurobasal media (Gibco/Invitrogen) supplemented with 2 mM GlutaMax (Invitrogen), 1×B27 and 1×N2 (Gibco/Invitrogen), 25 U/ml penicillin/streptomycin and 20 ng/ml bFGF. The clusters formed hESC-derived neural aggregates that were cultured for 4 to 5 weeks with weekly mechanical passaging and medium changes 3 times/week.

Cell viability assay and immunocytochemical characterization

The effects of various coating substrates on cell viability and neuronal characteristics were assessed. Cell culture wells (24-well plates, Nunc, Roskilde, Denmark) were coated with either laminin (10 μg/ml, Sigma-Aldrich, St. Louis, MO, USA), 0.1% polyethyleneimine (PEI, Sigma-Aldrich), or PEI + laminin. PEI solution was prepared according to the directions in the MEA manual (Multi Channel Systems, 2005). Neuronal cells were seeded on coated wells (2 parallel samples/coating) and allowed to grow in an incubator (+37 °C, 5% CO_2, 95% air-humidified atmosphere) for 5 days before analysis.

For the cell viability assay, a LIVE/DEAD Viability/Cytotoxicity Kit for mammalian cells (Molecular Probes, #L3224, Invitrogen) was used. Briefly, culture medium diluted with calcein AM (0.1 μM) and ethidium homodimer-1 (0.5 μM) was added to the cells. After 30-min incubation at room temperature in a light-protected area, cells were imaged under fluorescence microscopy (IX51, Olympus, Finland), and photographed (DP71 camera, Olympus). Calcein AM stains living cells and emits green light at 515 nm, whereas ethidium homodimer-1 stains dead cells and emits red light at 635 nm. The viability assay was performed also on 3 neuronal cultures grown on PEI + laminin-coated MEA dishes for 6 weeks.

For immunocytochemical staining, cells were fixed with 4% paraformaldehyde (Sigma-Aldrich) for 20 min at room temperature. Thereafter, cells were rinsed in 2× Dulbecco's phosphate-buffered saline (PBS), blocked with 10% normal donkey serum, 0.1% TritonX-100, and 1% bovine serum albumin (BSA) in PBS (all purchased from Sigma-Aldrich) for 45 min at room temperature. After blocking, the cells were washed once with primary antibody solution (1% donkey serum, 0.1% TritonX-100, 1% BSA in PBS) prior to incubation with primary antibodies: β-tubulin$_{III}$ (mouse IgM 1:1000, Sigma-Aldrich) and microtubule-associated protein 2 (MAP-2, rabbit IgG, 1:800, Chemicon International Inc., Temecula, CA) overnight at 4 °C. On the following day, the cells were washed 3×5 min with secondary antibody solution (1% BSA in PBS) and incubated with secondary antibodies donkey anti-rabbit Alexa 488 IgG (1:400) and goat anti-mouse Alexa 568 IgG (1:400, both from Invitrogen) for 1 h at room temperature in a light-protected area. The cells were then washed 3×5 min with PBS and 2×5 min with phosphate buffer (pH 7.0, 0.01 M, Sigma-Aldrich). The cells were mounted with Vectashield Mounting Medium for Fluorescence with 4′,6-diamidino-2-phenylindole (DAPI, Vector Laboratories, Burlingame, CA), covered with a cover slip, and viewed under fluorescence microscopy.

Neuronal culture preparation on MEA dishes

Electrical activities were recorded using MEA dishes with a square array of 59 substrate-embedded titanium nitride microelectrodes (30 μm diameter, 200 μm inter-electrode distance), and an internal embedded reference electrode (200/30iR-Ti-gr, Multi Channel Systems MCS GmbH, Reutlingen, Germany). The MEA dishes were coated with PEI + laminin. Briefly, 1 ml PEI solution (0.1%) was added to the MEA dishes and incubated overnight at 4 °C. On the following day, the MEA dishes were rinsed 4× with PBS before applying a drop of laminin (10 μg/ml) to the electrode area. After 2 h incubation at +37 °C, the laminin was aspirated and dissected pieces of hESC-derived neural aggregates (n = 10–15) containing ~2000 cells each were seeded around the electrode area of the MEA dishes. The dissected neural aggregates were plated on the MEA dishes at the age of 4 to 5 weeks after the onset of differentiation in which stage they expressed only neural cell markers (Sundberg et al., 2009). Altogether, each MEA dish (n = 22) contained 20,000 to 30,000 neuronal cells. In order to enhance the *in vitro* differentiation of the neural cells to neurons, bFGF was withdrawn from the culture medium. 3 days later, the first recordings were performed and the culture medium was changed to 4 ng/ml bFGF and 5 ng/ml of brain derived neurotrophic factor (BDNF, Gibco Invitrogen) containing medium to support the neuronal maturation. Thereafter, medium composition was kept constant and all the following experiments were performed in this medium. The medium was changed 3 times per week or after every recording event.

Between the measurements, the cultures were kept in Petri dishes inside an incubator providing a +37 °C, 5% CO_2, 95% air-humidified atmosphere. At least two neuronal cultures derived from each hESC line were used for the MEA measurements.

The MEA dishes were reused several times. The dishes were thoroughly rinsed with tap water, and a neutral detergent (1% Terg-A-Zyme, Sigma-Aldrich) solution was added for overnight incubation at room temperature. Thereafter, dishes were rinsed with tap water, checked for purity under a microscope, and sterilized with 70% EtOH (15 min) in a laminar hood prior to re-coating.

Recording system

To keep the cultures sterile prior to recordings, the MEA dishes were sealed in a laminar flow hood with a semi-permeable membrane (ALA MEA-MEM, ALA Scientific Instruments Inc., Westbury, NY) that is selectively permeable to gases (O_2, CO_2), as previously described (Potter and DeMarse, 2001). The sealed MEA dishes were carefully placed into the MEA amplifier (MEA-1060BC, Multi Channel Systems) and allowed to equilibrate for 3 to 5 min before starting the recordings. The amplifier itself was placed on top of a phase-contrast microscope (IX51, Olympus) so that the neuronal cultures the electrode area could be viewed during the measurements. Imaging was performed during recording using the microscope's camera (ALTRA 20, Olympus) connected to CellD software (version 2.6, build 1210, Olympus Soft Imaging Solutions GmbH, Munich, Germany). An MEA gain of 1100 and a bandwidth of 1 to 10 kHz were utilized. Signals were sampled at 20 or 50 kHz using a data acquisition card controlled through the MC_Rack software (both from Multi Channel Systems). The culture temperature was maintained at +37 °C using a TC02 temperature controller (Multi Channel Systems). Background noise of less than 10 μV_{rms} was allowed. All the recordings were stored in a computer and visually inspected for artifacts. A high-pass filter (2nd order Butterworth filter) with a bandpass cut-off frequency set to 200 Hz was used to remove baseline fluctuations. Spike detection was performed using MC_Rack (Multi Channel Systems) with a threshold of 5.5 times the standard deviation of the noise level. NeuroExplorer (Nex Technologies, Littleton, MA) was used to visualize the processed spike data.

Cultured neuronal networks

A total of 22 neuronal cultures grown on MEA dishes were included in this study. The maximum culture follow-up time was 130 days ($n = 2$). The cultures on MEAs were measured 1 to 3 times a week, each recording lasting for 5 to 10 min. Cultures were discarded once the cells or coating detached, or upon the cessation of measurable electrical activity.

Pharmacologic testing and electrical stimulation

Each tested pharmacologic substance was first mixed with 1 ml of fresh medium. The whole medium on the MEA dish was changed to the drug containing medium, and measurements were started after 5 min incubation. Recording of 5 min was performed and the culture was washed with 1 ml of fresh medium and allowed to settle down in the incubator for 15 min before the medium containing a new substance was added.

Sodium ion channel blockade with tetrodotoxin (TTX, Sigma-Aldrich) was performed in a separate experiment with 3 cultures on MEAs. First, 5 min of baseline activity was recorded, after which the response to 50 μM TTX was measured for another 5 min. Thereafter, a washout with fresh medium and the third recording was performed.

Pharmacologic modification of post-synaptic responses was performed with 2 cultures by application of the following substances: an AMPA/kainate antagonist (6-cyano-7-nitroquinoxaline-2,3-dione; CNQX, 30 μM), an NMDA antagonist (D(−)-2-amino-5-phosphonopentanoic acid; D-AP5, 20 μM), gamma-aminobutyric acid (GABA, 100 μm), and a $GABA_A$ antagonist [(−)-bicuculline methiodide; bicuculline, 10 μM]. The reagents were purchased from Sigma. The experiment was performed after 23 days of culturing on MEAs. Each culture was photographed during measurement. First, baseline activity was measured after a fresh medium change. Next, we measured the response to CNQX, then the response to combined CNQX and D-AP5. Thereafter, a washout was performed and the culture activity was measured again in fresh medium. Next, we measured the response to GABA, after which we performed a washout as earlier. Finally, the response to the addition of bicuculline was measured.

Electrical stimulation was tested on 2 cultures 25 days after plating on MEAs, using STG2004 stimulus generator driven by the MC_Stimulus software (both from Multi Channel Systems). The stimulation paradigm was a train of 50 biphasic voltage pulses (±800 mV, 400 μsec per phase) at 300 ms intervals. The stimulation train interval varied randomly from 4 to 56 s. Only one electrode was stimulated at a time. The electrode providing the largest spontaneous network activation was selected as the stimulating electrode. The stimulated electrode was blanked for 20 ms after the stimulation in order to reduce the size of the artifacts. Additionally, ±8 ms of the signal around each stimulation time point was removed offline from all the electrodes.

Results

Neuronal cultures on MEA dishes

As a preliminary experiment, we assessed the effects of laminin, PEI, or PEI + laminin coatings on cell viability and attachment. The pH of the medium remained between 7.8 and 8.2 in all cultures regardless of the used coating. The LIVE/DEAD assay results indicated that the coating substrates did not affect cell viability (Supplementary Fig. 1). Based on the visual inspection of β-tubulin$_{III}$ and MAP-2 stainings (Supplementary Fig. 1), neuronal processes grew best on laminin- and PEI + laminin-coated wells. PEI + laminin supported long-term

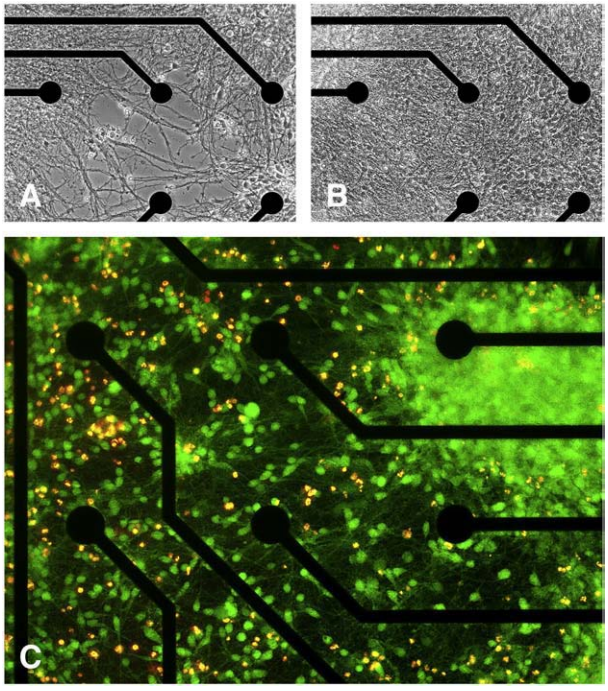

Fig. 1. Maturation of a neuronal network during the 2nd (A) and 3rd (B) weeks of culturing on MEA dish. Neuronal cells were mostly viable (green color) after 6 weeks of culturing (C). Inter-electrode distance = 200 μm.

culturing on MEA dishes. Typically, a growing neuronal network reached confluence after 2–3 weeks of culturing (Figs. 1A, B). Neuronal cells were viable after 6 weeks of culturing on MEA dishes (Fig. 1C). PEI + laminin supported neuronal growth on MEAs for over 4 months. No contamination problems were encountered, even during long culturing periods.

Spontaneous activity of the cultured neuronal networks

Spontaneous electrical activity was observed in 19 of 22 neuronal cultures on MEAs. The 3 of 22 neuronal cultures on MEAs were inactive likely due to the poor cell adhesion or viability as the cultures detached by the 1st week from the MEAs. Activity was detected as

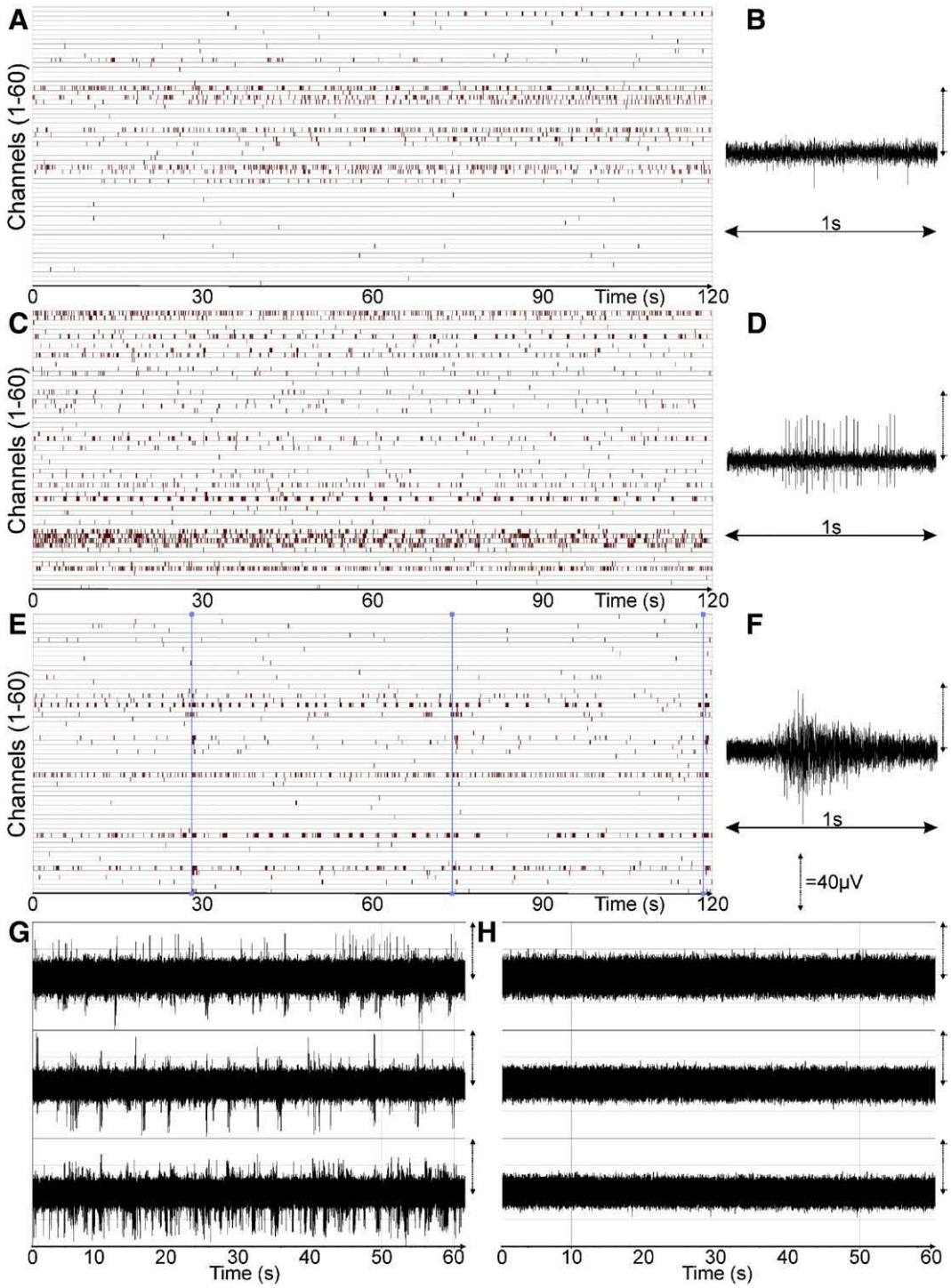

Fig. 2. Development of neuronal signaling over 4 weeks of culturing. At the first stage (1st week on MEA), single spike activity (B) was recorded only by some electrodes (A). At the second stage (weeks 2 to 3), the activity developed to spike trains (D) that were detected at multiple electrodes (C). At the third stage (from 4 weeks onwards), synchronous bursts (F) took over as the dominant kind of activity. The time points of synchronous bursts occurring in 46 s intervals in a 4 week old culture are illustrated with vertical blue lines in the raster plot (E). Neuronal activity (G) was completely inhibited when sodium ion channels were blocked by TTX (H).

early as 3 days after plating the cells on MEA dishes. In general, spontaneous activity appeared within the 1st week of culturing or did not appear at all. Typically, the first signs of electrical activity were random single spikes (Fig. 2B) which later developed to spike trains (Fig. 2D) and bursts (Fig. 2F). Here, based on visual inspection of the signals, we defined a spike train as an event of at least 5 single spikes with regular inter-spike intervals of 20 to 100 ms. Bursts were defined as events of at least 30 spikes during a 500-ms period with inter-spike interval less than 20 ms. Typically, bursts were simultaneously detected at multiple electrodes, albeit burst-like events were recorded also at single electrodes. Multiple electrode-spanning bursts are hereafter referred to as synchronous bursts (Fig. 3B).

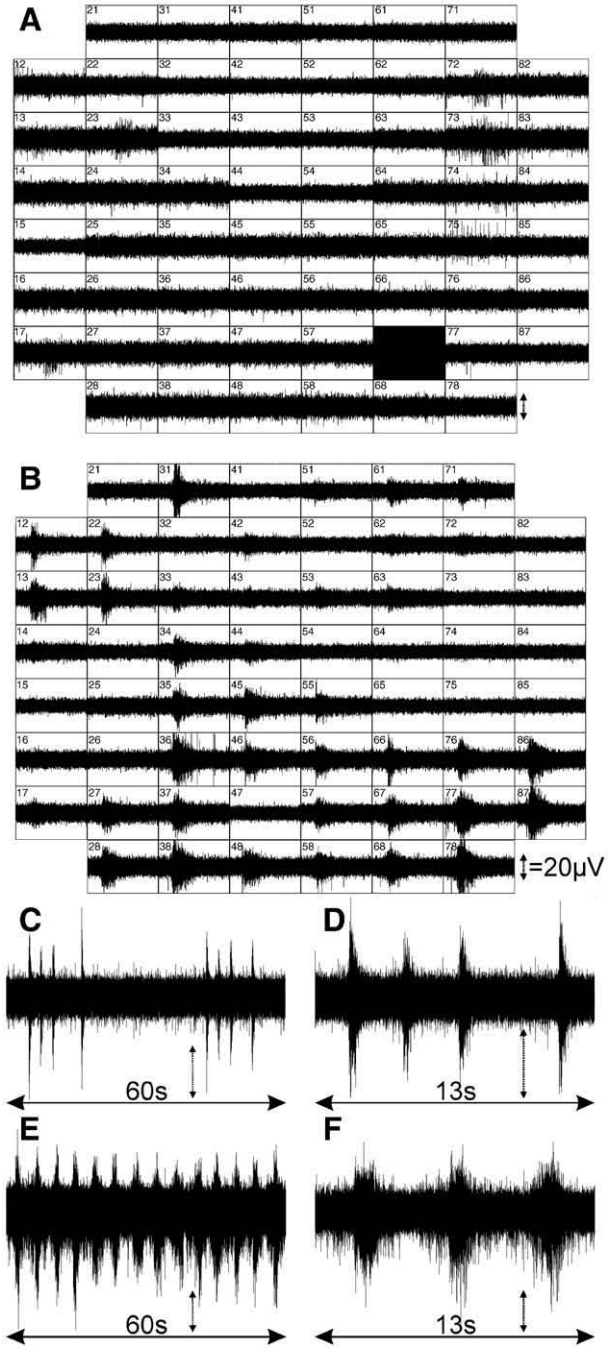

Fig. 3. A wide range of spontaneous synchronous bursts was detected. Typically, the first bursting activity occurred at only 1 to 2 electrodes after 3 to 4 weeks of culturing (A). After 4 to 6 weeks of culturing, as the culture grew denser, the bursting activity propagated over the colony and the burst profile became more bell-shaped (B). The frequency of synchronous bursts varied on different cultures. A recurring series of four bursts separated by longer rest intervals (C) and the set of four burst with closer zoom (D). Constant bursting activity (E) with closer zoom (F).

Both positive and negative monophasic, as well as biphasic spikes, were detected from the same culture. The typical spike amplitude was 20 to 40 μV, although some spike trains as high as 180 μV were recorded. Most of the activity was detected by electrodes located under dense cell layer (Fig. 1B), but some spike trains were recorded also from low-density areas containing mainly neuronal processes (Fig. 1A).

The electrical activity in cultures was confirmed to be sodium ion channel-dependent since the blockade of these ion channels using TTX completely inhibited all activity (Figs. 2G, H). The activity reappeared after washout, indicating that the inhibition was reversible (data not shown).

In 14 of the 19 MEA cultures displaying single spikes (Fig. 2A), the activity evolved into spike trains on multiple electrodes (Fig. 2C) within the first 2 weeks of culturing. Both discontinuous and constantly firing signal trains, as well as synchronous and asynchronous spikes and trains, were observed. Moreover, asynchronous signals in addition to synchronous activity could be detected from the same electrodes. Synchronous bursts (Fig. 2E, Figs. 3A–F) were detected from 6 cultures, and typically appeared after 1 month of culturing. The occurrence of synchronous bursts increased over time.

The incidence of synchronous bursts varied greatly between cultures and measurement days. The burst-envelope curve varied from indistinctly shaped (Fig. 3A) to bell-shaped (Fig. 3B). Usually, cultures with synchronous bursts also contained single spikes and spike train-type activity, but some cultures exhibited only synchronous bursts. The electrodes registering synchronous bursts located typically next to each other (Fig. 3B). The longest distance formed by adjacent burst-detecting electrodes was approximately 3.6 mm (propagation near 18 electrodes with 200 μm spacing). Recurring synchronous bursts were simultaneously detected at a maximum by 41 electrodes (41/59). Inter-burst intervals ranged from seconds to minutes. We sometimes observed rapidly repeating bursts, as previously described as superbursts by Wagenaar et al. (2006) that consisted of 3 to 4 synchronous culture-wide bursts that closely followed each other (Figs. 3C, D). In one culture, constant periodic synchronous bursts occurred at a frequency of 0.25 Hz (Figs. 3E, F).

Pharmacologic testing and responsiveness to electrical stimulation

Baseline activity is shown in Fig. 4A. Application of the AMPA/kainate antagonist CNQX (20 μM) suppressed the activity (Fig. 4B) and abolished synchronous bursts. The NMDA antagonist D-AP5 (30 μM) blocked the remaining activity (Fig. 4C), which did not return during the measurement. After a washout, the electrical activity reappeared (Fig. 4D). GABA suppressed the signaling in a dose-dependent manner (data not shown) and the addition of 100 μM of GABA completely inhibited the activity (Fig. 4E), which did not recover after a washout (Fig. 4F). Application of the $GABA_A$ receptor antagonist bicuculline (10 μM), however, induced the activity to return (Fig. 4G). Additionally, bicuculline treatment increased activity over the baseline level and induced synchronous bursting (visible as dark vertical lines in the raster plot Fig. 4H). Bicuculline treatment had similar effects on non-modulated cultures (data not shown).

In an additional experiment, we tested whether the neuronal activity patterns in hESC-derived neuronal cultures could be influenced by electrical stimulation similarly as described earlier in *in vitro* works (Ban et al., 2007; Chiappalone et al., 2007; Madhavan et al., 2007; Wagenaar et al., 2006). We used the same stimulation paradigm presented earlier by Wagenaar et al. (2006) but altered the interval between stimulations randomly (Supplementary Figs. 2A and B). Stimulation evoked synchronous bursts mainly on electrodes that already displayed spontaneous bursts before stimulations, but spikes were evoked also on other electrodes. hESC-derived neuronal

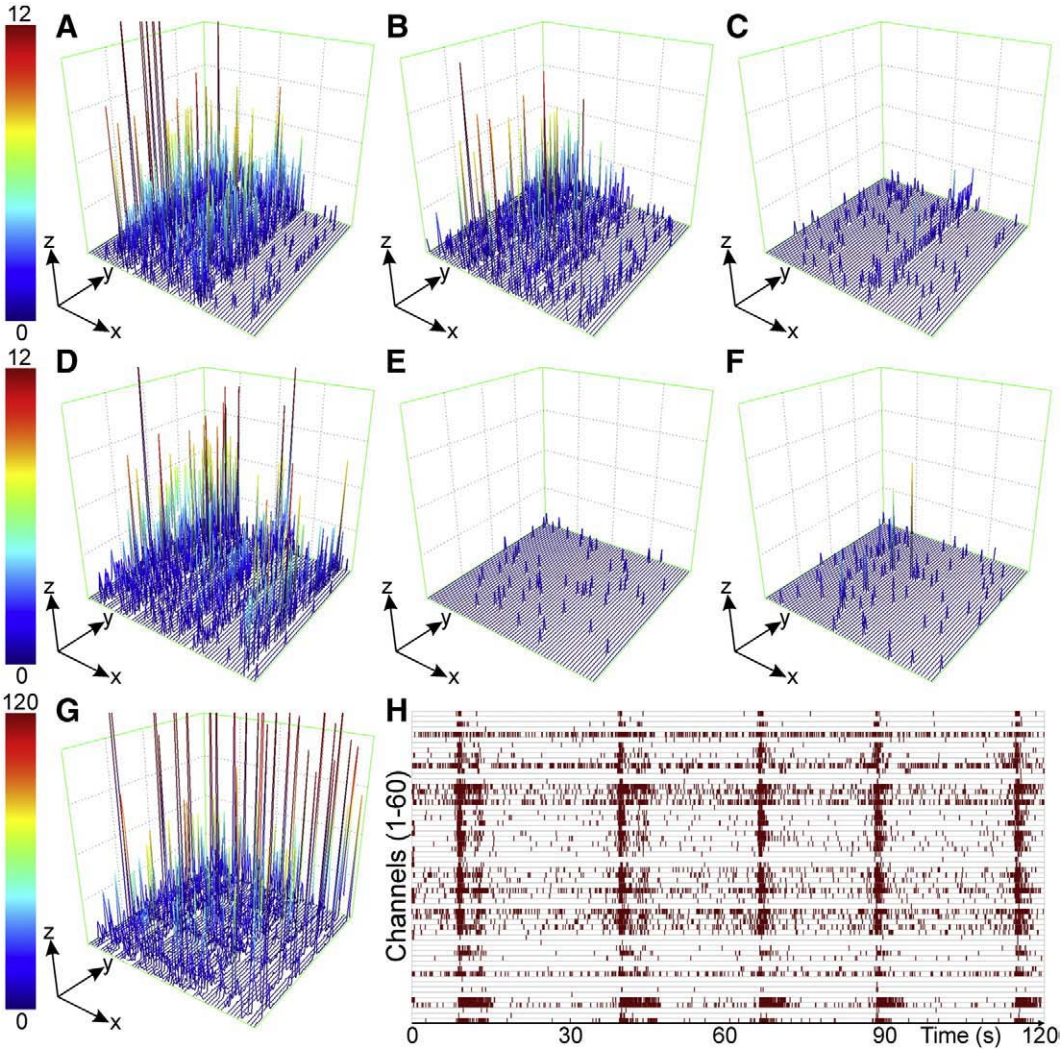

Fig. 4. Pharmacologic modulation of hESC-derived neuronal network activity. 3D-histograms (A–G) display recorded channels 1–60 along the *x*-axis. Time (in seconds; max 120) is represented by the *y*-axis. The spike count (1 s/bin) is displayed on the *z*-axis. Addition of the pharmaceuticals and recording of the network activities were performed in the following order. Baseline activity (A). The activity was partly suppressed by CNQX (B). CNQX and D-AP5 together blocked all activity (C). After a washout, activity reappeared (D). GABA inhibited all activity (E), and the activity did not return after a washout (F). The addition of bicuculline restored the activity (G) to a higher level than at the baseline (A). Note the different *z*-axis scale in G. Raster plot of the bicuculline-induced synchronous activity (H).

cultures responded to external stimulation with regularly evoked spikes. Stimulation at different electrodes produced changes in the response patterns (Supplementary Figs. 2A and B) and times (Supplementary Figs. 2C and D). For example, stimulus-induced activity, inhibited spontaneous activity, or no changes in spontaneous activity were observed on different parts of the culture.

Discussion

In this study, we provide the first evidence that hESC-derived neuronal cells can generate functional networks *in vitro*. After 5 weeks of differentiation, the functional neuronal network activity developed from single spikes to spontaneous bursts in time frame of 1 month on MEA dishes. Active neuronal cultures were followed on MEA dishes for over 4 months without any contamination.

Currently, there are many published protocols for neural differentiation of hESCs using adherent or suspension culturing, co-cultures, and various substances (retinoid acid, growth factors, noggin, etc.) that all result in at least partially pure neural populations (Hoffman and Carpenter, 2005; Nat et al., 2007). Here, we used a simple protocol for neuronal differentiation of hESCs using the suspension method as described earlier (Nat et al., 2007; Sundberg et al., 2009). The differentiated hESC-derived neural aggregates used for MEA cultures contained only neural cells at the time of plating as shown previously (Sundberg et al., 2009) and differentiated *in vitro* into MAP-2 positive neurons. The neuronal origin of the recorded activity was confirmed by the pharmacological experiments.

Previously, functionality of hESC-derived neurons has been described on the single cell level *in vitro* (Carpenter et al., 2001; Erceg et al., 2008; Johnson et al., 2007) and after transplantation *in vivo* (Reubinoff et al., 2001) using the patch clamp technique. None of the reported studies have, however, described the formation of functional networks of neuronal cells derived from hESCs as we showed here. Using the patch clamp technique, evoked action potentials of single neurons have been measurable after 4 weeks of neuronal differentiation of hESCs (Erceg et al., 2008; Johnson et al., 2007). Here, we extended these findings by showing that hESC-derived neuronal cultures start to exhibit spontaneous spikes already after 5 weeks of differentiation. Similarly, as the single hESC-derived neurons have been shown to fire spontaneously after 7 weeks and fire evoked trains of action potentials after 10 weeks of differentiation (Johnson et al., 2007), the functionality of the hESC-derived neuronal network develops from spontaneous single spikes into trains of spikes after 6 weeks and into bursting activity after 8 to 10 weeks of

differentiation. In the future, it would be very beneficial to combine the patch clamp and MEA measurements for more detailed characterization of network functionality of hESC-derived neurons.

Spontaneous neuronal activity has an important role in many aspects of neural development, including neuronal migration, differentiation, and connection patterning (Ben-Ari, 2001; Katz and Shatz, 1996; Yvert et al., 2004; Van Pelt et al., 2005). Previously, development of functional networks of mouse ESC-derived neuronal cultures has been described in a quite similar setting to that presented here (Illes et al., 2007). Interestingly, while the mouse-derived neuronal networks grown for 21 days on MEA dishes after 3 weeks of differentiation started to exhibit "bursts" of 5 ± 2 spikes within a 300-ms time period (Illes et al., 2007; Lee et al., 2000), the hESC-derived neuronal cultures expressed this kind of activity already after 7 days on MEAs after 4 to 5 weeks of differentiation. It has, however, been shown that mouse ESC (line BLC6)-derived neuronal cells can form spontaneous or evoked electrical activity 7 days after culturing *in vitro* after 4 days of differentiation (Strübing et al., 1995). The development of *in vitro* neuronal network is strongly influenced by plating density of the cells (Wagenaar et al., 2006) which may explain the differences in the maturation of functionality between different experiments. Here, we used small hESC-derived neural aggregates plated around the MEA electrode areas, which in our experience create a confluent culture faster compared to plating the cells as dissociated single cell suspension. Thus, it is very important to develop standardized culturing methods for production of structured, controlled neuronal networks for MEA environment that would enable proper comparisons between different studies and also the production of standardized testing platforms for drug screening and neurotoxicological testing.

A general characteristic of developing neuronal networks is their tendency to spontaneously discharge repetitive synchronous bursts (Corner et al., 2002; Gross et al., 1977; Kamioka et al., 1996; Maeda et al., 1995; Potter, 2008; Van Pelt et al., 2005). We recorded synchronous bursts from hESC-derived neuronal networks similar to those that typically appeared 1 month after culturing in mouse ESC-neuronal networks (Illes et al., 2007).The abundance of bursts detected resembled those observed in developing dissociated rat cortical cultures (Wagenaar et al., 2006). Burst patterns such as a recurring series of synchronous bursts separated by longer rest intervals, as well as constant bursts, were recorded.

Using reversible TTX-induced blockade of the sodium ion channels, we demonstrated that the hESC-derived neuronal network activity is dependent on voltage-gated sodium currents. The application of CNQX suppressed local spike activity compared to baseline, but not completely, in line with results in rat cortical cultures (Li et al., 2007). Interestingly, we observed also the disappearance of synchronous bursts after CNQX application. Additional blockade of NMDA receptors with co-application of D-AP5 suppressed all activity, which is consistent with findings in mouse ESC-derived (Ban et al., 2007) and rat hippocampal (Sokal et al., 2000;Ban et al., 2007) neuronal networks. The effect of CNQX + D-AP5 was reversible. The addition of GABA (100 μM) inhibited the neuronal activity similarly to mouse ESC neuronal networks (Illes et al., 2007). Interestingly, the effect was irreversible by a washout, and blunted recovery was also observed after multiple washouts (data not shown). The exogenous GABA addition can be likened to a strong culture-wide extrasynaptic 'spillover' (Trigo et al. 2008; White et al., 2000). The mechanism behind the observation remains to be clarified in future studies with receptor subtype specific agonists. Blocking of $GABA_A$ receptors with bicuculline after GABA addition resulted in a pronounced reappearance of the activity at a higher level than baseline. Bicuculline induced synchronous bursts similarly to those reported for mouse ESC-derived (Illes et al., 2007) and rat hippocampal (Sokal et al., 2000) neuronal networks. Furthermore, we observed that the amplitude of pre-existing synchronous bursts increased and periodic activity was unmasked following the addition of bicuculline to pharmacologically-naive cultures (data not shown). No morphologic changes were observed following the pharmacologic treatments. Altogether, these results indicate that the principal excitatory and inhibitory pathways of the human central nervous system are involved in the functional activity of hESC-derived neuronal networks.

Accordingly, electrical stimulation initiated or inhibited activity demonstrating that hESC-derived neuronal networks were capable of responding to external stimuli. The unresponsiveness to the stimulation directly after a spontaneous burst may result from refractoriness of the network (Maeda et al., 1995). Previous stimulation has been shown to either enhance or reduce next the stimulus response (Tateno and Jimbo, 1999). This could explain the variability in the response to our slow tetanic stimulation. More experiments are required to evaluate the role of the refractoriness in the network and the variability in the responses to the stimulation.

The findings of the present study demonstrated that the MEA measurement system is a useful tool for measuring electrical activity of hESC-derived neuronal cells. Studying the development of neuronal cell networks *in vitro* offers many advantages over *in vivo* approaches. *In vitro* systems are more accessible to microscopic imaging and pharmacologic manipulation than the human brain. Our results demonstrate that hESC-derived neuronal cells generate spontaneously active functional networks with complex patterns of activity and synchronous communication *in vitro*. Thus, these cells are suitable for use in developmental and drug screening studies and suggest a high therapeutic potential for regenerative medicine, as well.

Acknowledgments

This work was supported by the Competitive Research Funding of Pirkanmaa Hospital District, Finland; the Employment and Economic Development Center for Pirkanmaa, Finland; Arvo and Lea Ylppö Foudation, Finland and the Academy of Finland. The MEA system was funded by BioneXt Tampere, Finland. The original hESC lines were kindly provided by Prof. Outi Hovatta, Karolinska Institute, Sweden. The authors wish to thank the personnel of Regea for their technical help and support in stem cell research.

Appendix A. Supplementary data

Supplementary data associated with this article can be found, in the online version, at doi:10.1016/j.expneurol.2009.04.011.

References

Ban, J., Bonifazi, P., Pinato, G., Broccard, F.D., Studer, L., Torre, V., Ruaro, M.E., 2007. ES-derived neurons form functional networks in vitro. Stem Cells 25, 738–749.
Ben-Ari, Y., 2001. Developing networks play a similar melody. Trends Neurosci. 24, 353–360.
Carpenter, M.K., Inokuma, M.S., Denham, J., Mujtaba, T., Chiu, C.P., Rao, M.S., 2001. Enrichment of neurons and neural precursors from human embryonic stem cells. Exp. Neurol. 172, 383–397.
Chiappalone, M., Vato, A., Berdonini, L., Koudelka-Hep, M., Martinoia, S., 2007. Network dynamics and synchronous activity in cultured cortical neurons. Int. J. Neural Syst. 17, 87–103.
Corner, M.A., Van Pelt, J., Wolters, P.S., Baker, R.E., Nuytinck, R., 2002. Physiological effects of sustained blockade of excitatory synaptic transmission on spontaneously active developing neuronal networks—an inquiry into the reciprocal linkage between intrinsic biorhythms and neuroplasticity in early ontogeny. Neurosci. Biobehav. Rev. 26, 127–185.
Erceg, S., Laínez, S., Ronaghi, M., Stojkovic, P., Pérez-Aragó, M.A., Moreno-Manzano, V., Moreno-Palanques, R., Planells-Cases, R., Stojkovic, M., 2008. Differentiation of human embryonic stem cells to regional specific neural precursors in chemically defined medium conditions. PLoS ONE 3, e2122.
Gross, G.W., Rieske, E., Kreutzberg, G.W., Meyer, A., 1977. A new fixed-array multi-microelectrode system designed for long-term monitoring of extracellular single unit neuronal activity *in vitro*. Neurosci. Lett. 6, 101–106.
Hess, D.C., Borlongan, C.V., 2008. Stem cells and neurological diseases. Cell Prolif. 41, 94–114.
Hoffman, L.M., Carpenter, M.K., 2005. Human embryonic stem cell stability. Stem Cell Rev. 1, 139–144.
Illes, S., Fleischer, W., Siebler, M., Hartung, H.-P., Dihné, M., 2007. Development and pharmacological modulation of embryonic stem cell-derived neuronal network activity. Exp. Neurol. 207, 171–176.

Johnson, M.A., Weick, J.P., Pearce, R.A., Zhang, S.C., 2007. Functional neural development from human embryonic stem cells: accelerated synaptic activity via astrocyte coculture. J. Neurosci. 27, 3069–3077.
Kamioka, H., Maeda, E., Jimbo, Y., Robinson, H.P.C., Kawana, A., 1996. Spontaneous periodic synchronized bursting during formation of mature patterns of connections in cortical cultures. Neurosci. Lett. 206, 109–112.
Katz, L.C., Shatz, C.J., 1996. Synaptic activity and the construction of cortical circuits. Science 274, 1133–1138.
Lee, S.H., Lumelsky, N., Studer, L., Auerbach, J.M., McKay, R.D., 2000. Efficient generation of midbrain and hindbrain neurons from mouse embryonic stem cells. Nat. Biotechnol. 18, 675–679.
Li, X., Zhou, W., Zeng, S., Liu, M., Luo, Q., 2007. Long-term recording on multi-electrode array reveals degraded inhibitory connection in neuronal network development. Biosens. Bioelectron. 22, 1538–1543.
Lock, L.T., Tzanakakis, E.S., 2007. Stem/progenitor cell sources of insulin-producing cells for the treatment of diabetes. Tissue Eng. 13, 1399–1412.
Madhavan, R., Chao, Z., Potter, S., 2007. Plasticity of recurring spatiotemporal activity patterns in cortical networks. Phys. Biol. 4, 181–193.
Maeda, E., Robinson, H.P.C., Kawana, A., 1995. The mechanisms of generation and propagation of synchronized bursting in developing networks of cortical neurons. J. Neurosci. 15, 6834–6845.
Multi Channel Systems MCS GmbH, 2005. Microelectrode Array (MEA) User Manual. Reutlingen, Germany, pp. 20–21.
Nat, R., Nilbratt, M., Narkilahti, S., Winblad, B., Hovatta, O., Nordberg, A., 2007. Neurogenic neuroepithelial and radial glial cells generated from six human embryonic stem cell lines in serum-free suspension and adherent cultures. Glia 55, 385–399.
Otto, F., Görtz, P., Fleischer, W., Siebler, M., 2003. Cryopreserved rat cortical cells develop functional neuronal networks on microelectrode arrays. J. Neurosci. Methods 128, 173–181.
Pine, J., 1980. Recording action potentials from cultured neurons with extracellular microcircuit electrodes. J. Neurosci. Methods 2, 19–31.
Potter, S.M., DeMarse, T.B., 2001. A new approach to neural cell culture for long-term studies. J. Neurosci. Methods 110, 14–17.
Potter, S.M., 2008. How should we think about bursts? 6th Int. Meeting on Substrate-Integrated Microelectrodes. Reutlingen, Germany. ISBN 3-938345-05-5.
Reubinoff, B.E., Itsykson, P., Turetsky, T., Pera, M.F., Reinhartz, E., Itzik, A., Ben-Hur, T., 2001. Neural progenitors from human embryonic stem cells. Nat. Biotechnol. 19, 1134–1140.
Rolletschek, A., Blyszczuk, P., Wobus, A.M., 2004. Embryonic stem cell-derived cardiac, neuronal and pancreatic cells as model systems to study toxicological effects. Toxicol. Lett. 149, 361–369.
Sokal, D.M., Mason, R., Parker, T.L., 2000. Multi-neuronal recordings reveal a differential effect of thapsigargin on bicuculline- or gabazine-induced epileptiform excitability in rat hippocampal neuronal networks. Neuropharmacology 39, 2408–2417.
Strübing, C., Ahnert-Hilger, G., Shan, J., Wiedenmann, B., Hescheler, J., Wobus, A.M., 1995. Differentiation of pluripotent embryonic stem cells into the neuronal lineage in vitro gives rise to mature inhibitory and excitatory neurons. Mech. Dev. 53, 275–287.
Stummann, T.C., Bremer, S., 2008. The possible impact of human embryonic stem cells on safety pharmacological and toxicological assessments in drug discovery and drug development. Curr. Stem Cell Res. Ther. 2, 118–131.
Sundberg, M., Jansson, L., Ketolainen, J., Pihlajamäki, H., Suuronen, S., Skottman, H., Inzunza, J., Hovatta, O., Narkilahti, S., 2009. CD marker expression profiles of human embryonic stem cells and their neural derivatives, determined using flow cytometric analysis, reveal a novel CD marker for exclusion of pluripotent stem cells. Stem Cell Res. 2, 113–124.
Tateno, T., Jimbo, Y., 1999. Activity-dependent enhancement in the reliability of correlated spike timings in cultured cortical neurons. Biol. Cybern. 80, 45–55.
Thomson, J.A., Itskovitz-Eldor, J., Shapiro, S.S., Waknitz, M.A., Swiergiel, J.J., Marshall, V.S, Jones, J.M., 1998. Embryonic stem cell lines derived from human blastocysts. Science 282, 1145–1147.
Trigo, F.F., Marty, A., Stell, B.M., 2008. Axonal GABAA receptors. Eur. J. Neurosci. 28, 841–848.
Van Pelt, J., Vajda, I., Wolters, P.S., Corner, M.A., Ramakers, G.J.A., 2005. Dynamics and plasticity in developing neuronal networks in vitro. Prog. Brain Res. 147, 173–188.
Wagenaar, D.A., Pine, J., Potter, S.M., 2006. An extremely rich repertoire of bursting patterns during the development of cortical cultures. BMC Neurosci. 7, 11.
Wang, Y., Chen, S., Yang, D., Le, W.D., 2007. Stem cell transplantation: a promising therapy for Parkinson's disease. J. Neuroimmune Pharmacol. 2, 243–250.
White, J.H., McIllhinney, R.A., Wise, A., Ciruela, F., Chan, W.Y., Emson, P.C., Billinton, A., Marshall, F.H., 2000. The GABAB receptor interacts directly with the related transcription factors CREB2 and ATFx. Proc. Natl. Acad. Sci. U. S. A. 97, 13967–13972.
Wu, L., Sluiter, A.A., Guo, H.F., Balesar, R.A., Swaab, D.F., Zhou, J.N., Verwer, R.W., 2007. Neural stem cells improve neuronal survival in cultured postmortem brain tissue from aged and Alzheimer patients. J. Cell. Mol. Med. 12, 1611–1621.
Yvert, B., Branchereau, P., Meyrand, P., 2004. Multiple spontaneous rhythmic activity patterns generated by the embryonic mouse spinal cord occur within a specific developmental time window. J. Neurophysiol. 91, 2101–2109.

Available online at www.sciencedirect.com

ScienceDirect

Journal of Bionic Engineering 9 (2012) 1–10

Structured PDMS Chambers for Enhanced Human Neuronal Cell Activity on MEA Platforms

Joose Kreutzer[1,2], Laura Ylä-Outinen[2,3,4], Paula Kärnä[2,3], Tiina Kaarela[2,3], Jarno Mikkonen[5], Heli Skottman[2,3], Susanna Narkilahti[2,3,4], Pasi Kallio[1,2]

1. *Department of Automation Science and Engineering*, *Tampere University of Technology*, *Korkeakoulunkatu* 3, 33720 *Tampere*, *Finland*
2. *BioMediTech*, *Biokatu* 10, 33520 *Tampere*, *Finland*
3. *NeuroGroup*, *Institute of Biomedical Technology*, *University of Tampere*, *Biokatu* 12, 33520 *Tampere*, *Finland*
4. *The Science Center of Pirkanmaa Hospital District*, *Biokatu* 12, 33521 *Tampere*, *Finland*
5. *Department of Psychology*, *University of Jyväskylä*, *Ylistönmäentie* 33, 40500 *Jyväskylä*, *Finland*

Abstract

Structured poly(dimethylsiloxane) (PDMS) chambers were designed and fabricated to enhance the signaling of human Embryonic Stem Cell (hESC) - derived neuronal networks on Microelectrode Array (MEA) platforms. The structured PDMS chambers enable cell seeding on restricted areas and thus, reduce the amount of needed coating materials and cells. In addition, the neuronal cells formed spontaneously active networks faster in the structured PDMS chambers than that in control chambers. In the PDMS chambers, the neuronal networks were more active and able to develop their signaling into organized signal trains faster than control cultures. The PDMS chamber design enables much more repeatable analysis and rapid growth of functional neuronal network *in vitro*. Moreover, due to its easy and cheap fabrication process, new configurations can be easily fabricated based on investigator requirements.

Keywords: cell culturing, electrical activity, human embryonic stem cells, microelectrode array, poly(dimethylsiloxane)

doi: 10.1016/S1672-6529(11)60091-7

1 Introduction

Neurodegenerative diseases are a major economic burden to 21st century societies. Stroke alone is the third largest cause of death and the leading cause of long-term disability in Western industrialized countries. Neuronal cells derived from stem cells provide several potential means for reducing this burden. They can be used for understanding the disease mechanisms, developing new drugs, and treating the diseases through transplantation therapies[1–3]. However, more information and knowledge are needed to thoroughly understand the functional properties of stem cell derived neurons and neuronal networks so that these cells can be fully utilized for research and therapeutic purposes. Microelectrode Array (MEA) measurements are a widely used method to characterize the electrical activity of human-origin neuronal cells[2,4,5].

MEA platforms are commercially available in different configurations from several companies (e.g., Multi Channel Systems [MCS] GmbH, Germany; Ayanda Biosystems SA, Switzerland; Alpha Med Scientific, Inc, Japan; Axion Biosystems, NW, USA). There are, however, limitations in the cultivation chambers that impede the efficient and high-throughput analysis of stem cell derived neuronal cells on MEA platforms. Human Embryonic Stem Cells (hESC) and their neuronal derivates are especially demanding, laborious, and expensive to culture and therefore, the limitations of the cultivation chambers are more severe in studies with these cells. For example, formation of neuronal networks on top of the electrode area is not controlled and thus, the reproducible rate of similar networks is low. In addition, the growth of neuronal cells on large surfaces presents challenges by lowering the signaling rates and network formation. The large surface areas also increase

Corresponding author: Joose Kreutzer
E-mail: joose.kreutzer@tut.fi

the required amount of coating substances and cells to be seeded, and lead to more costly experiments. Thus, it is reasonable to optimize the cultivation methods on the MEA platforms to improve the attachment and maturation process of the neuronal cells and possibly reduce the costs of the experiments.

In this study we report the design of structured poly(dimethylsiloxane) (PDMS) chambers, their use on various commercially available MEA platforms, and the subsequent neuronal cell recordings. Our aim is to improve the neuronal cell attachment and maturation process, and allow more controlled growth over the electrode area without affecting the development and maturation of functional neuronal networks. The paper will discuss three chamber configurations (a one-well structure and two six-well structures) and compare their performance to a commercial chamber.

2 Materials and methods

2.1 MEA platforms

MEA technology has been used for cell network studies for decades[6–8]. MEAs are widely used in different fields of cell research and tissue engineering, from single cell recordings using Si_3N_4 cages[9] to slice cultures[10]. MEAs are used for monitoring spontaneous activity of neuronal networks[11], response to electrical and pharmaceutical stimuli[4,12], plasticity[13], and toxicological screening[5,14].

In this study, we used MEA platforms from Multi Channel Systems (MCS) GmbH (Germany). For the one-well chamber studies, we used MEA platforms with a standard electrode (200/30iR-Ti, layout 8×8) layout without a glass ring on the substrate. The same electrode layout with a glass ring served as the platform for the control study. Six-well MEA platforms (6wellMEA200/30iR-Ti-w/o, layout 6×(3×3)) were used in the six-well PDMS chambers studies.

2.2 Design and fabrication of one-well PDMS chambers

Previously, many research groups have reported cell and tissue studies utilizing PDMS microstructures[10,15–27]. Recently, PDMS has been used to fabricate microfluidic structures for hESC studies[28–37], but they have not been used with MEA platforms. PDMS is a very good material for a laboratory use and is advantageous for inexpensive prototyping applications. PDMS is resistant to most chemicals[38], gas permeable[39], optically transparent down to wavelengths of 290 nm[40], and it can be used to replicate features just a few nanometers in size[41].

A PDMS chamber including one well, hereafter referred to as the one-well chamber, was designed for the MEA platforms having all 60 electrodes in the middle of the platform. Similar to the commercial glass ring chamber produced by MCS, the one-well PDMS chamber included a reservoir to store up to 1000 μL of cell culture medium. The structured PDMS chamber featured a PDMS bottom with an open cell attachment area (4 mm in diameter, ~13 mm^2) around the electrode area (1.4 mm × 1.4 mm, ~2 mm^2) to guide the cells to grow and attach onto the electrodes, and another opening (16 mm^2) for the reference electrode as shown in Fig. 1a.

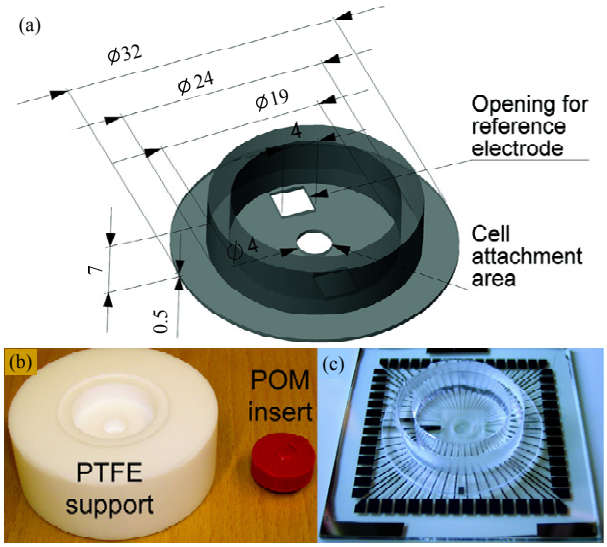

Fig. 1 (a) A one-well PDMS chamber design. Dimensions are in mm. (b) Mold for one-well PDMS chamber. (c) One-well PDMS chamber on a MEA platform.

To fabricate the one-well chambers, a mold for casting the PDMS was designed. The mold comprised of two lathe-machined parts as shown in Fig. 1b, a support made of polytetrafluoroethylene (PTFE) and an insert made of polyoxymethylene (POM). The support provides a place for the insert, which is tightly attached with a screw from the bottom. As a result, the insert can be easily exchanged to vary the shape and size of the medium chamber. In addition, the two-part approach was used to facilitate the removal of the casting from the mold. In the present study, the insert was 19 mm in di-

ameter and 7.0 mm high. The insert includes bosses 0.5 mm in height, as shown in Fig. 1b. These raised patterns leave openings in the PDMS membrane for the cell attachment area and the reference electrode.

The fabrication procedure for the one-well chamber included the following steps: preparing a mixture of PDMS, casting the PDMS mixture, degassing the mixture, placing a glass plate on top of the mold, curing the PDMS mixture, and removing the culture chamber from the mold.

The mold was used for replicating the culture chambers from PDMS. We used a two-component PDMS elastomer (Sylgard® 184, Dow Corning, purchased from Ellsworth Adhesives AB, Sweden). The base (liquid silicone rubber) and the curing agent were thoroughly mixed with a weight ratio of 10:1. After mixing, the mixture was cast to a clean mold. The mold was completely filled, covering the patterns of the insert. The mold containing the PDMS mixture was then placed into a vacuum chamber (~100 mbar absolute pressure) for 20 min to remove air bubbles that were created during the mixing and trapped in the uncured liquid silicone.

After the bubbles were removed, a clean glass plate was pressed tightly on top of the mold to contact only the bosses. Hence, these patterned areas were open after removing the PDMS structure from the mold. The glass plate also flattens the PDMS surface and thus increases the efficiency of reversible bonding to the MEA platform or other smooth surfaces. A small weight of 500 g was placed on top of the glass plate during oven curing (2 h at 70 ˚C).

Removal of the PDMS chamber from the mold was performed carefully so as to not break the thin bottom layer, which is only 0.5 mm thick. The PDMS chambers were sterilized in an autoclave before bonding to the MEA platforms. A completed PDMS chamber on a MEA platform is illustrated in Fig. 1c.

2.3 Parallel fabrication of multiple one-well chambers

A mold used for the parallel fabrication of nine one-well PDMS chambers is illustrated in Fig. 2a. The mold facilitates the production of nine preforms of one-well culturing chambers as shown in Fig. 2b. The fabrication procedure of preforms was the same as that used for a single chamber as described previously. The cured PDMS preforms were finalized by punching two holes (each 4 mm in diameter) with a biopsy punch for the cell attachment area and the reference electrode located in the middle and at the edge of the chamber, respectively. Fig. 2c illustrates a one-well PDMS culture chamber used in the experiments of this study.

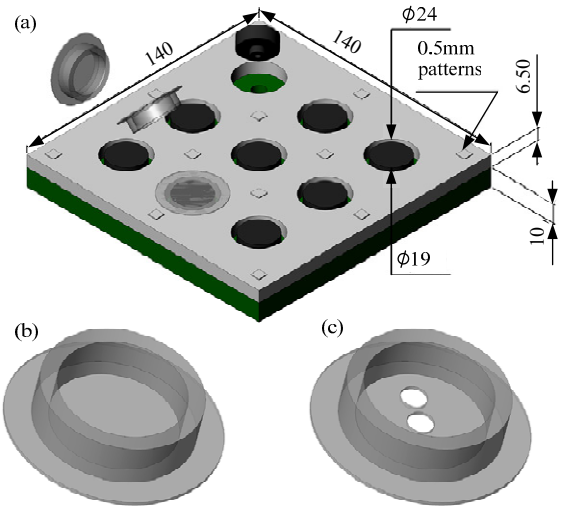

Fig. 2 (a) Mold for nine preforms of a one-well PDMS chamber. Dimensions are in mm. (b) Preform for a one-well PDMS chamber. (c) Example of a custom-made PDMS chamber.

2.4 Design and fabrication of six-well PDMS chambers

Six-well PDMS chambers were designed for MEA platforms, which included six electrode areas that each contained nine electrodes. Two chamber configurations were fabricated to demonstrate the versatility of a single MEA platform with different six-well PDMS chambers. In Configuration I, shown in Fig. 3a, each electrode area has its own medium reservoir and cell attachment area. In Configuration II, shown in Fig. 3b, all electrode areas share a larger common medium reservoir, but have their own structures to guide the cell attachment and growth. In addition to the cell guidance openings for the electrode areas, the bottom plate includes a large opening for the reference electrode in the middle. Both chamber designs are used with the same six-well MEA platform.

Configuration I with six separate medium reservoirs was designed to increase the number of parallel experiments on one MEA platform. Two different medium reservoir sizes, volumes of 150 µL and 250 µL, were fabricated to determine the appropriate volume of medium required for a practical medium change interval of three times per week.

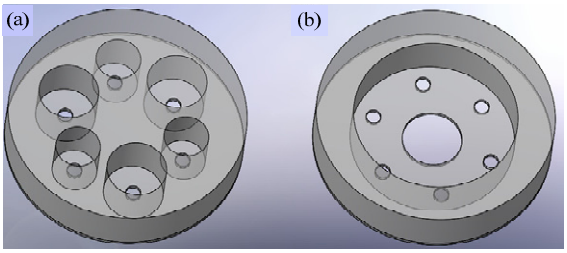

Fig. 3 (a) A six-well PDMS chamber with separate medium reservoirs called as configuration I. (b) A six-well PDMS chamber with common medium reservoir called as configuration II.

Configuration I (Fig. 3a) was fabricated from two parts. The top part, providing the walls of the containers, was punched out from a bulk (thickness 6.5 mm) PDMS sheet using a 32 mm diameter custom-made punch. Thereafter, three 6 mm ∅ holes and three 8 mm ∅ holes were punched through the disk for the medium reservoirs using custom-made punches. The bottom part was punched out from a bulk (thickness 0.5 mm) PDMS sheet with the 32 mm (in diameter) punch. The two parts were bonded irreversibly using an oxygen plasma treatment (Vision 320 Mk II, Advanced Vacuum Scandinavia AB, Sweden) with the following parameters: O_2 flow rate of 30 sccm, pressure of 30 mTorr, power of 30 W, and time of 15 s. Finally, the six openings for the cell attachment areas (2 mm ∅, ~3 mm^2) were punched through the membrane using the biopsy punch.

Configuration II (Fig. 3b) utilized a common medium reservoir to increase the number of replicates in the same culture conditions. This design also comprised of two parts. The top part (32 mm ∅) was punched out from the bulk (thick 6.5 mm) PDMS sheet, and a 22 mm ∅ hole was punched in the middle. A thin bottom membrane was fabricated and bonded as in Configuration I. Six 2 mm ∅ openings for the cell attachment areas and one 8 mm ∅ opening for the common reference electrode in the middle were also punched.

2.5 Assembly and cleaning

A smooth PDMS surface forms a reversible bond with a flat surface due to Van der Waals interaction that can seal structures water tightly[42]**.** In this study, PDMS chambers were reversibly bonded on MEA platforms. The bond strength was sufficient for long-term cell culture, and could also sustain the mechanical forces that were encountered during the installation of covers before measurements under a microscope.

The PDMS chambers and the MEA platforms were cleaned with detergent solution (1% (w/v) Terg-A-Zyme, Sigma-Aldrich, St. Louis, MO, US) after every experiment. After an overnight bath in detergent solution, components were washed carefully with de-ionized water and then sterilized using 70% ethanol, or an autoclave. Thereafter, components were ready for the next experiment.

2.6 Cell source and culturing

The cells used in the experiment were hESC-derived neuronal cells from lineages Regea 08/023 and Regea 06/015. Regea has ethical approval to derivate, culture, and differentiate the hESCs (Skottman, R05116) as well as permission for human stem cell research from Valvira (1426/32/300/05). First, the hESCs were mechanically cut into small pieces and the cell aggregates were placed into neural differentiation medium containing Dulbecco's Modified Eagle's Medium/F12 (Gibco, Invitrogen, Finland) and Neurobasal medium (Gibco) 1:1, supplemented with 2 mM GlutaMax (Gibco, USA), 1 × B27 (Gibco) and 1 × N2 (Gibco), 20 $ng{\cdot}mL^{-1}$ basic fibroblast growth factor (bFGF, R&D Systems, Minneapolis, MN), and penicillin/streptomycin (25 $U{\cdot}mL^{-1}$, Cambrex, Belgium). In this medium, the hESCs formed neurospheres in a suspension culture, as previously described[43]. The medium was changed three times per week and spheres were mechanically dissected on a weekly basis. After ~8 weeks of differentiation in the suspension culture, cells turned into neuronal cells[43] and were ready to be seeded onto MEAs.

To assess the quality of the cells to be seeded, mycoplasma tests, hESC karyotyping, and gene and protein expression analyses of neuronal cells were routinely performed. Cells used in this study had a normal karyotype, were mycoplasma free, and had a normal neuronal phenotype.

2.7 Surface coating and cell seeding

The PDMS chambers were first bonded reversibly onto the MEA platforms, as described above. The cell attachment areas were then coated using a two-step coating procedure as previously described[4]. Briefly, polyethyleneimide (PEI, 0.05% w/v, Sigma-Aldrich) solution was pipetted onto the electrode area and incubated overnight at +4 ˚C. The MEA platforms were

rinsed three times with sterile water and allowed to dry. Thereafter, a laminin solution (40 µL, 20 µg·mL^{-1} human laminin, Sigma-Aldrich) was added to the cell attachment area and incubated overnight at +4 ˚C. In control experiments including the glass ring chambers, the same two-step coating procedure was used, but 1000 µL of PEI and laminin solutions were added to uniformly cover the entire surface.

Cells were seeded onto the MEA platform as very small aggregates (~50 µm–100 µm ∅). In total, approximately ten aggregates per one-well chamber (PDMS chambers and glass ring chambers) were seeded onto the electrode area. In six-well designs, cells were plated both as aggregates and as single cell suspensions to evaluate the suitability of commonly used seeding methods for PDMS chambers. In the aggregate plating, 1 to 2 small aggregates were placed to each well. In the suspension plating, cell aggregates were enzymically dissociated into single cell suspensions with TrypLE Select (Invitrogen) for 15 min. Cells were washed with cell culture medium and 20 000 cells were plated to each well. Neural differentiation medium without the basic fibroblast growth factor (bFGF) was used in the beginning of the seeding. After three days, the brain-derived neurotrophic factor (BDNF, 5 ng·mL^{-1}, Gibco) and bFGF (4 ng·mL^{-1}) were added into the cell culture medium to enhance the neuronal maturation. MEA platforms were stored in Petri dishes inside an incubator (+37 ˚C, 5% CO_2) between the MEA recordings, and the medium was changed three times per week.

2.8 Covers

Before the cell recordings, the MEA chambers were sealed inside a laminar flow hood. The one-well chambers were sealed with a semipermeable membrane[44] (ALA MEA-MEM, ALA Scientific Instruments Inc., Westbury, NY) installed over a PTFE cap (MCS). The six-well PDMS chambers were sealed with a 3 mm thick PDMS membrane.

2.9 Data acquisition and analysis

A MEA amplifier (MEA-1060 Amplifier, MCS) was used for signal filtering and amplification. The amplifier was placed on top of a phase-contrast microscope (XI51, Olympus, Finland) for simultaneous imaging. The temperature on the MEA was maintained with a specific controller (TC02, MCS) and a heating element (set to 38.5 ˚C, He-Inv25, MCS) was placed under the MEA platform. Data was recorded using the MC_Rack program. Post-recording analysis was performed with MC_Rack, MC_DataTool (both from MCS), MATLAB (MathWorks, Natick, MA), and NeuroExplorer (Nex Technologies, Littleton, MA). Spikes in the recorded signals were detected with MC_Rack. The spike detection threshold was set to a level of −5× standard deviation of the noise in each channel.

2.10 Statistical analysis

All statistical analyses were performed with IBM SPSS-software (version 19, IBM, Armonc, NY, USA). Statistical analysis was performed using nonparametric Kruskall-Wallis test followed by Mann-Whitney U test. The p-value ≤ 0.05 was considered significant.

3 Experiments and results

To quantify and demonstrate the performance of the cell signaling in the different cultivation chambers, two performance measurements were defined. The influence of the cultivation chamber on the cells was evaluated by investigating the attachment of the cells and the development of functional neuronal networks.

The cell attachment was studied by evaluating whether the cells attach and start to form networks within two days after seeding. The development of functional networks was measured by recording the electrical activity using the MEAs for 15 days and counting the number of active electrode channels and the number of spikes in the active channels. A channel was defined as active when at least five neuronal spikes were recorded per 250 s recording period. The number of active channels describes portion of the network that is electrically active and the number of spikes describes the quality of the activity.

In the experiments, the performance in the one-well PDMS chambers and in the two types of six-well PDMS chambers was compared to the control - the commercial one-well glass chamber.

3.1 Cell attachment

A successful cell attachment was counted if a seeded cell aggregate attached, started to grow, and formed a network within two days after seeding.

The results indicate that the cell aggregates attach equally well in the one-well PDMS chambers (success

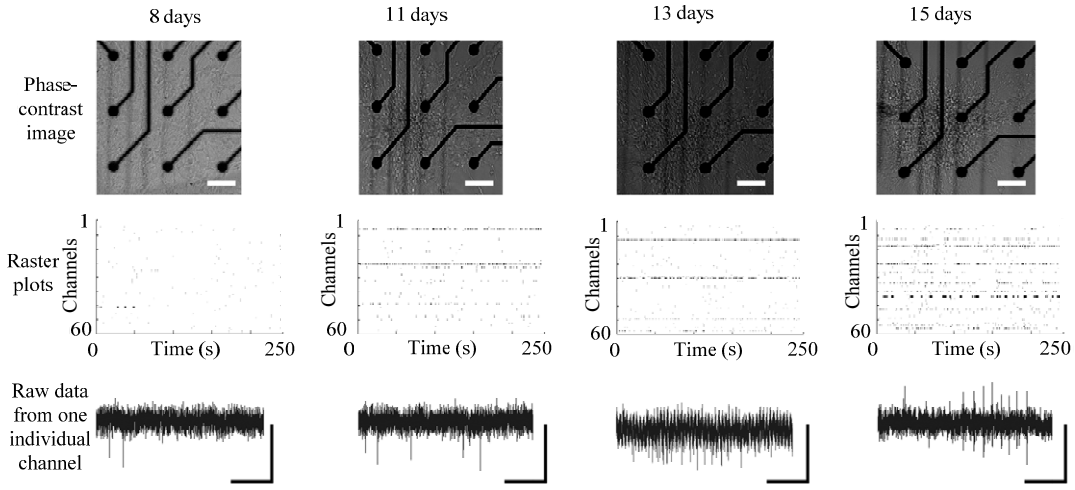

Fig. 4 Spontaneous network activities in MEAs were measured at 8, 11, 13, and 15 DID. The phase-contrast images show the growth of neuronal networks. Phase-contrast images were taken from the same PDMS-MEA platform and same location on different days. The scale bar is 100 μm. In raster plots all 60 channels are presented over a 250 s measuring period and the raster is presented if spike/spikes are detected at 1 s bin. The raw data plots were taken from one channel for 1 s. Scale bars: for *x*-axis= 250 μs, for *y*-axis=20 μV. Representative phase-contrast microscopy images shows the growth of the cells in MEA platform, and raster-plots of the activity and raw data plots show maturation of neuronal networks at both networks and the one channel levels for each time-point.

rate 32/36 = 89%) as in the glass ring chambers (success rate 35/41 = 85%). In the six-well designs, the attachment rate was similar (success rate 35/40 = 88% for Configuration I, and 18/20 = 90%, for configuration II).

3.2 Development of functional networks in one-well designs

Typically, hESC-derived neuronal signaling develops in three stages: 1) initially some individual single spikes occur sporadically, 2) after two weeks, more organized signal trains appear, and 3) finally signaling develops to synchronous bursting activity[4]. In the experiments of this study, the same neuronal network maturation patterns were detected in the cultures in the PDMS chambers (Fig. 4).

Fig. 4 shows representative phase-contrast images of networks, raster plots, and raw data of neuronal networks at 8, 11, 13, and 15 days in dish (DID). The raster plots show the network activities of all 60 MEA channels over the 250 s recording time, and the raw data plots show detailed signal development from single spiking (8 DID) to prominent training activity (15 DID).

As described earlier, in this study the activity of a neuronal network was evaluated by measuring the active number of MEA channels and the number of spikes in the neuronal signals. The number of active channels in a MEA and the average number of spikes in an active channel/MEA are shown in Fig. 5. The development of the signaling is shown at time points of 8, 11, 13, and 15 DID. Typically, neuronal networks in the PDMS chambers were more active compared to those in the control chambers. This was evaluated by counting the number of the active channels at all time points. Thus, at 8 and 11 DID there was a significantly higher number of active channels in neuronal networks growing in the PDMS chambers (p = 0.047 and 0.014, respectively) compared to the controls. In addition, the number of spikes was higher in the PDMS chambers than in the glass chambers at same time points (p = 0.028 and p = 0.009, respectively) compared to controls.

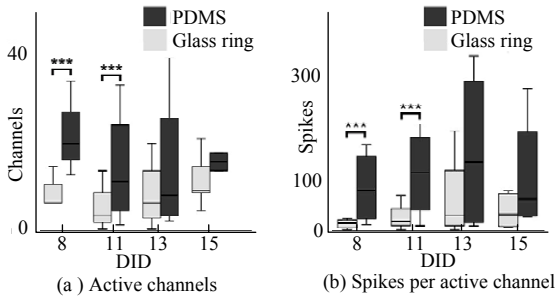

Fig. 5 (a) Number of active channels from aggregate cultures of neuronal cells in glass-ring MEAs and PDMS chamber MEAs at time-points 8, 11, 13, and 15 DID. (b) Number of detected spikes per active channel from aggregate cultures and in glass-ring MEAs and PDMS chamber MEAs at time-points 8, 11, 13, and 15 DID. For graphs, spikes were detected from 250 s measurement period and the results from at least 5 MEAs per group (n=8) were plotted. Data is plotted as box plot were median, quartiles and minimum and maximum values are shown. *** = $p < 0.05$.

3.3 Development of functional networks in six-well designs

MEA platforms with configuration I were used to compare single cell and aggregate seeding methods and measure activities up to 49 DID. Both seeding methods resulted in active networks, although the maturation time varied. The maturation of the single cell plated networks was significantly slower compared to the aggregate cultures at 7 to 35 DID follow up time. The comparison of maturation speed of neuronal networks between aggregate and single cell suspension method is shown in Fig. 6. Both network types eventually developed into training-like activity, in 9 or 49 DID, for aggregates and single cell culture, respectively.

When compared to one-well chambers, the networks in the six-well designs developed similarly, as shown in Fig. 7. The results also show that the use of the separate small medium chambers (150 µL and 250 µL) does not affect the signal quality and provides easy and targeted cell seeding. Even the smaller medium reservoir (150 µL) in the six-well design was large enough for sufficient nutrient exchange in static cultivation in an incubator, and the standard medium exchange cycle (every three days) was sufficient.

4 Discussion

The results presented in the previous section demonstrate the benefits of the structured PDMS chambers in MEA recordings of neuronal networks derived from hESC. In the PDMS chambers, strong signaling and maturing networks formed in a shorter period of time than on the glass ring chambers. The networks in the PDMS chambers became active earlier and developed significantly more prominent training activities when compared to the glass ring chambers. This shows that neuronal networks can mature faster, and consequently cultures can be prepared for experimental measurements sooner. Similar amounts of aggregates were adequate for network formation in both chambers. However, with the six-well PDMS designs, an extremely small number of cells (1–2 aggregates or 20 000 cells in suspension) was sufficient to support growth of viable neuronal networks. Importantly by using either culturing method, functional neuronal networks were formed although it took significantly more time for the single cell cultures to maturate compared to the aggregate cultures. Depending on the application, both types

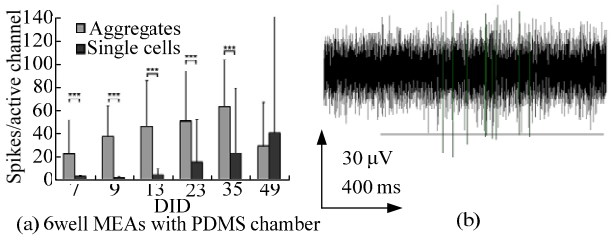

Fig. 6 (a) Cells either plated as single cell suspension or as aggregates into six-well Configuration I. Spikes per active channel were plotted as mean, and error bars shows standard deviation. (b) Typical training activity was developed in both single cell and aggregate plated networks. Faster development was detected from aggregate plated networks. *** = $p < 0.05$.

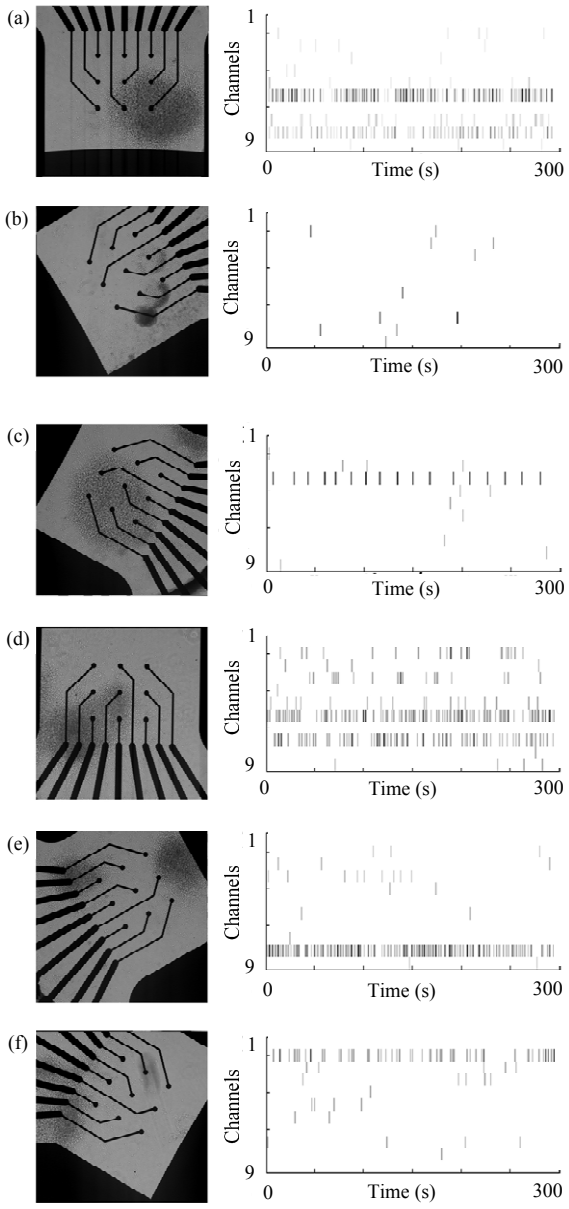

Fig. 7 Representative phase-contrast microscopy images and raster plots from cells on six-well MEA with Configuration I PDMS chamber. They formed good networks and expressed spontaneous signaling at 16 DID in all separate wells. All six wells presented in (a)-(f) are on one MEA.

of seeding methods/cultures can be grown in six-well PDMS designs.

Preparing the mature cultures faster is not the only advantage of using the structured PDMS chambers. With the PDMS chambers, the volume of the coating solution (human laminin in neuronal studies) can be reduced from 1000μl to 40μl, which results in significant cost savings in high-throughput experiments.

In the medium change (every three days), a manual aspirating pipette is used with fast suction. In the PDMS chambers, the cells do not experience fluid-induced shear stress since the structured PDMS chamber protects them. Therefore, the requirement for precisely positioning the pipette tip is not as important in the PDMS chambers providing an easier and faster medium change. The smaller cell attachment area also offers more repeatable and efficient cell seeding and thus, increases the number of successful experiments.

The versatile use of the relatively expensive MEA platforms is also one of the advantages we propose in this study. For example, the six-well chamber with separate medium reservoirs is useful for pharmacological and toxicological experiments in the MEA platform[2]. The six-well chamber with a common medium reservoir, in turn, increases the number of replicates for experiments in which the same environment is essential. The same MEA platform can be utilized for both purposes simply by changing the PDMS structure on top. This is not possible with the fixed chambers.

The PDMS chamber is easy to position accurately and attach reversibly to commercial MEA platforms. The reversible bond is watertight and stable for long-term cell culturing. The bond strength is sufficient to keep the PDMS chamber on a MEA platform during all steps in the measurement procedure, including multiple reattachments of the sealing cap. However, the reversibly bonded PDMS chambers can be simply detached by peeling them from the MEA platforms. Moreover, the separate parts are easy to clean because both parts (the PDMS chamber and the MEA platform) can be sterilized separately in an autoclave or with ethanol and/or UV-light.

5 Conclusions

In this study, we developed structured PDMS cultivation chambers that enhance the maturation process and spontaneous activity of hESC-derived neuronal cells. These cells formed strongly signaling, dense, and functional networks faster in our structured PDMS chambers than in control MEA platforms with a fixed glass ring.

Using the PDMS structures with the limited cell attachment area, the amount of coating materials, the initial number of cells, and the amount of culturing medium can be reduced significantly in MEA studies. Reversible bonding to a MEA platform makes the PDMS chamber easy to detach, clean, sterilize, and replace. Therefore, single PDMS chamber can be used with different MEA configurations or single MEA platform with different PDMS chamber configurations to enhance the versatility of MEA platforms.

Acknowledgment

The study was part of the project STEMFUNC funded by the Academy of Finland. This study was also financially supported by the Competitive Research Funding of the Tampere University Hospital (Grant 9L064). We wish to thank the personnel of IBT for their support of stem cell research.

References

[1] Goldman S. Stem and progenitor cell-based therapy of the human central nervous system. *Nature Biotechnology*, 2005, **23**, 862–871.

[2] Johnstone A F, Gross G W, Weiss D G, Schroeder O H, Gramowski A, Shafer T J. Microelectrode arrays: A physiologically based neurotoxicity testing platform for the 21st century. *Neurotoxicology*, 2010, **31**, 331–350.

[3] Schmidt C E, Leach J B. Neural tissue engineering: Strategies for repair and regeneration. *Annual Review of Biomedical Engineering*, 2003, **5**, 293–347.

[4] Heikkilä T J, Ylä-Outinen L, Tanskanen J M, Lappalainen R S, Skottman H, Suuronen R, Mikkonen J E, Hyttinen J A, Narkilahti S. Human embryonic stem cell-derived neuronal cells form spontaneously active neuronal networks in vitro. *Experimental Neurology*, 2009, **218**, 109–116.

[5] Ylä-Outinen L, Heikkilä J, Skottman H, Suuronen R, Äänismaa R and Narkilahti S. Human cell-based micro electrode array platform for studying neurotoxicity. *Front Neuroeng*, 2010, **3**, 1–9.

[6] Pine J. Recording action potentials from cultured neurons with extracellular microcircuit electrodes. *Journal of Neuroscience Methods*, 1980, **2**, 19–31.

[7] Thomas C A, Jr., Springer P A, Loeb G E, Berwald-Netter Y, Okun L M. A miniature microelectrode array to monitor the bioelectric activity of cultured cells. *Experimental Cell Re-*

search, 1972, **74**, 61–66.

[8] Gross G W, Rieske E, Kreutzberg G W, Meyer A. A new fixed-array multi-microelectrode system designed for long-term monitoring of extracellular single unit neuronal activity in vitro. *Neuroscience Letters*, 1977, **6**, 101–105.

[9] Erickson J, Tooker A, Tai Y C, Pine J. Caged neuron MEA: A system for long-term investigation of cultured neural network connectivity. *Journal of Neuroscience Methods*, 2008, **175**, 1–16.

[10] Berdichevsky Y, Sabolek H, Levine J B, Staley K J, Yarmush M L. Microfluidics and multielectrode array-compatible organotypic slice culture method. *Journal of Neuroscience Methods*, 2009, **178**, 59–64.

[11] Wagenaar D A, Pine J, Potter S M. An extremely rich repertoire of bursting patterns during the development of cortical cultures. *BMC Neuroscience*, 2006, **7**, 151–156.

[12] Illes S, Fleischer W, Siebler M, Hartung H P, Dihne M. Development and pharmacological modulation of embryonic stem cell-derived neuronal network activity. *Experimental Neurology*, 2007, **207**, 171–176.

[13] van Pelt J, Vajda I, Wolters P S, Corner M A, Ramakers G J. Dynamics and plasticity in developing neuronal networks in vitro. *Progress in Brain Research*, 2005, **147**, 173–188.

[14] van Vliet E, Stoppini L, Balestrino M, Eskes C, Griesinger C, Sobanski T, Whelan M, Hartung T, Coecke S. Electrophysiological recording of re-aggregating brain cell cultures on multi-electrode arrays to detect acute neurotoxic effects. *Neurotoxicology*, 2007, **28**, 1136–1146.

[15] van Kooten T G, Whitesides J F, von Recum A. Influence of silicone (PDMS) surface texture on human skin fibroblast proliferation as determined by cell cycle analysis. *Journal of Biomedical Materials Research*, 1998, **43**, 1–14.

[16] Leclerc E, Sakai Y, Fujii T. Cell culture in 3-dimensional microfluidic structure of PDMS (polydimethylsiloxane). *Biomedical Microdevices*, 2003, **5**, 109–114.

[17] Lee J N, Jiang X, Ryan D, Whitesides G M. Compatibility of mammalian cells on surfaces of poly(dimethylsiloxane). *Langmuir*, 2004, **20**, 11684–11691.

[18] Tourovskaia A, Figueroa-Masot X, Folch A. Differentiation-on-a-chip: A microfluidic platform for long-term cell culture studies. *Lab Chip*, 2005, **5**, 14–19.

[19] Rhee S W, Taylor A M, Tu C H, Cribbs D H, Cotman C W, Jeon N L. Patterned cell culture inside microfluidic devices. *Lab Chip*, 2005, **5**, 102–107.

[20] Kim S J, Lee J K, Kim J W, Jung J W, Seo K, Park S B, Roh K H, Lee S R, Hong Y H, Kim S J, Lee Y S, Kim S J, Kang K S. Surface modification of polydimethylsiloxane (PDMS) induced proliferation and neural-like cells differentiation of umbilical cord blood-derived mesenchymal stem cells. *Journal of Materials Science*: *Materials in Medicine*, 2008, **19**, 2953–2962.

[21] Kim Y C, Kang J H, Park S-J, Yoon E-S, Park J-K. Microfluidic biomechanical device for compressive cell stimulation and lysis. *Sensors and Actuators B*: *Chemical*, 2007, **128**, 108–116.

[22] Dworak B J, Wheeler B C. Novel MEA platform with PDMS microtunnels enables the detection of action potential propagation from isolated axons in culture. *Lab Chip*, 2009, **9**, 404–410.

[23] Park J, Koito H, Li J, Han A. Microfluidic compartmentalized co-culture platform for CNS axon myelination research. *Biomedical Microdevices*, 2009, **11**, 1145–1153.

[24] Teixeira A I, Ilkhanizadeh S, Wigenius J A, Duckworth J K, Inganas O, Hermanson O. The promotion of neuronal maturation on soft substrates. *Biomaterials*, 2009, **30**, 4567–4572.

[25] Adewola A F, Lee D, Harvat T, Mohammed J, Eddington D T, Oberholzer J, Wang Y. Microfluidic perifusion and imaging device for multi-parametric islet function assessment. *Biomedical Microdevices*, 2010, **12**, 409–417.

[26] Liu L, Luo C, Ni X, Wang L, Yamauchi K, Nomura S M, Nakatsuji N, Chen Y. A micro-channel-well system for culture and differentiation of embryonic stem cells on different types of substrate. *Biomedical Microdevices*, 2010, **12**, 505–511.

[27] Agastin S, Giang U B, Geng Y, Delouise L A, King M R. Continuously perfused microbubble array for 3D tumor spheroid model. *Biomicrofluidics*, 2011, **5**, 24110.

[28] Khademhosseini A, Ferreira L, Blumling J, 3rd, Yeh J, Karp J M, Fukuda J, Langer R. Co-culture of human embryonic stem cells with murine embryonic fibroblasts on microwell-patterned substrates. *Biomaterials*, 2006, **27**, 5968–5977.

[29] Abhyankar V V, Beebe D J. Spatiotemporal micropatterning of cells on arbitrary substrates. *Analytical Chemistry*, 2007, **79**, 4066–4073.

[30] Gerecht S, Bettinger C J, Zhang Z, Borenstein J T, Vunjak-Novakovic G, Langer R. The effect of actin disrupting agents on contact guidance of human embryonic stem cells. *Biomaterials*, 2007, **28**, 4068–4077.

[31] Ungrin M D, Joshi C, Nica A, Bauwens C, Zandstra P W. Reproducible, ultra high-throughput formation of multicellular organization from single cell suspension-derived human embryonic stem cell aggregates. *PLoS One*, 2008, **3**, e1565.

[32] Cimetta E, Figallo E, Cannizzaro C, Elvassore N, Vunjak-Novakovic G. Micro-bioreactor arrays for controlling cellular environments: Design principles for human em-

bryonic stem cell applications. *Methods*, 2009, **47**, 81–89.

[33] Kamei K, Guo S, Yu Z T, Takahashi H, Gschweng E, Suh C, Wang X, Tang J, McLaughlin J, Witte O N, Lee K B, Tseng H R. An integrated microfluidic culture device for quantitative analysis of human embryonic stem cells. *Lab Chip*, 2009, **9**, 555–563.

[34] Korin N, Bransky A, Dinnar U, Levenberg S. Periodic "flow-stop" perfusion microchannel bioreactors for mammalian and human embryonic stem cell long-term culture. *Biomedical Microdevices*, 2009, **11**, 87–94.

[35] Kreutzer J, Lappalainen R S, Ylä-Outinen L, Narkilahti S, Mikkonen J E, Kallio P. Laminin coated PDMS surfaces for long-term measurements of hESC-derived neural networks. *Proceedings of the symposium on Microelectrode Arrays in Tissue Engineering*, Tampere, Finland, 2009, 23–25.

[36] Serena E, Figallo E, Tandon N, Cannizzaro C, Gerecht S, Elvassore N, Vunjak-Novakovic G. Electrical stimulation of human embryonic stem cells: Cardiac differentiation and the generation of reactive oxygen species. *Experimental Cell Research*, 2009, **315**, 3611–3619.

[37] Villa-Diaz L G, Torisawa Y S, Uchida T, Ding J, Nogueira-de-Souza N C, O'Shea K S, Takayama S, Smith G D. Microfluidic culture of single human embryonic stem cell colonies. *Lab Chip*, 2009, **9**, 1749–1755.

[38] Mata A, Fleischman A J, Roy S. Characterization of polydimethylsiloxane (PDMS) properties for biomedical micro/nanosystems. *Biomedical Microdevices*, 2005, **7**, 281–293.

[39] Merkel T C, Bondar V I, Nagai K, Freeman B D, Pinnau I. Gas sorption, diffusion, and permeation in poly(dimethylsiloxane). *Journal of Polymer Science Part B*: *Polymer Physics*, 2000, **38**, 415–434.

[40] Shih T-K, Chen C-F, Ho J-R, Chuang F-T. Fabrication of PDMS (polydimethylsiloxane) microlens and diffuser using replica molding. *Microelectronic Engineering*, 2006, **83**, 2499–2503.

[41] Xia Y, Whitesides G M. Soft lithography. *Angewandte Chemie International Edition*, 1998, **37**, 550–575.

[42] McDonald J C, Duffy D C, Anderson J R, Chiu D T, Wu H, Schueller O J, Whitesides G M. Fabrication of microfluidic systems in poly(dimethylsiloxane). *Electrophoresis*, 2000, **21**, 27–40.

[43] Lappalainen R S, Salomaki M, Yla-Outinen L, Heikkila T J, Hyttinen J A, Pihlajamaki H, Suuronen R, Skottman H, Narkilahti S. Similarly derived and cultured hESC lines show variation in their developmental potential towards neuronal cells in long-term culture. *Regenerative Medicine*, 2010, **5**, 749–762.

[44] Potter S M, DeMarse T B. A new approach to neural cell culture for long-term studies. *Journal of Neuroscience Methods*, 2001, **110**, 17–24.

frontiers in
NEUROENGINEERING

ORIGINAL RESEARCH ARTICLE
published: 30 September 2010
doi: 10.3389/fneng.2010.00111

Human cell-based micro electrode array platform for studying neurotoxicity

Laura Ylä-Outinen[1], Juha Heikkilä[1], Heli Skottman[1], Riitta Suuronen[1,2,3], Riikka Äänismaa[1] and Susanna Narkilahti[1]*

[1] *Regea – Institute for Regenerative Medicine, University of Tampere and Tampere University Hospital, Tampere, Finland*
[2] *Department of Eye, Ear, and Oral Diseases, Tampere University Hospital, Tampere, Finland*
[3] *Department of Biomedical Engineering, Tampere University of Technology, Tampere, Finland*

Edited by:
Antonio Novellino, ett s.r.l., Italy

Reviewed by:
Leandro Lorenzelli, Fondazione Bruno Kessler, Italy
Hari S. Sharma, Uppsala University, Sweden

Correspondence:
Susanna Narkilahti, Regea – Institute for Regenerative Medicine, University of Tampere, Biokatu 12, 33520 Tampere, Finland.
e-mail: susanna.narkilahti@regea.fi

At present, most of the neurotoxicological analyses are based on *in vitro* and *in vivo* models utilizing animal cells or animal models. In addition, the used *in vitro* models are mostly based on molecular biological end-point analyses. Thus, for neurotoxicological screening, human cell-based analysis platforms in which the functional neuronal networks responses for various neurotoxicants can be also detected real-time are highly needed. Microelectrode array (MEA) is a method which enables the measurement of functional activity of neuronal cell networks *in vitro* for long periods of time. Here, we utilize MEA to study the neurotoxicity of methyl mercury chloride (MeHgCl, concentrations 0.5–500 nM) to human embryonic stem cell (hESC)-derived neuronal cell networks exhibiting spontaneous electrical activity. The neuronal cell cultures were matured on MEAs into networks expressing spontaneous spike train-like activity before exposing the cells to MeHgCl for 72 h. MEA measurements were performed acutely and 24, 48, and 72 h after the onset of the exposure. Finally, exposed cells were analyzed with traditional molecular biological methods for cell proliferation, cell survival, and gene and protein expression. Our results show that 500 nM MeHgCl decreases the electrical signaling and alters the pharmacologic response of hESC-derived neuronal networks in delayed manner whereas effects can not be detected with qRT-PCR, immunostainings, or proliferation measurements. Thus, we conclude that human cell-based MEA platform is a sensitive online method for neurotoxicological screening.

Keywords: human embryonic stem cell, neuronal network, microelectrode array, neurotoxicology, methyl mercury chloride

INTRODUCTION

Neurotoxicity of various chemicals is currently tested solely with *in vivo* methods due to the lack of proper, validated *in vitro* cell models. Cells such as primary cultures of rat cerebellar granule cells have been used as a possible *in vitro* model (Harry et al., 1998; van Vliet et al., 2007; Bal-Price et al., 2009; Hogberg et al., 2009) for both developmental and adult neurotoxicity testing. Recently also human-derived cells, e.g., neural progenitor cells and umbilical cord blood-derived neural stem cells have been tested for neurotoxicity studies (Zeng et al., 2006; Buzanska et al., 2009a,b; Moors et al., 2009; Bal-Price et al., 2010). In addition to the need of developing human cell-based *in vitro* models that would enable better interpretation of neurotoxicological responses in humans and help to replace and reduce animal tests, more relevant *in vitro* toxicological models are needed. Currently used *in vitro* neuronal models are mostly based on molecular biological end-point analyses such as gene expression, cell proliferation and differentiation, and neurite outgrowth. It has, however, become clear that in addition to traditional cell viability testing, the testing pattern should include various general cell function tests and especially concentrate on neuron-specific aspects such as the neuronal network's electrical functionality and its alterations due to toxic compounds in subcytotoxic levels (van Vliet et al., 2007; Bal-Price et al., 2010). Validation of all these tests is of high importance for development of routinely usable *in vitro* neurotoxicology testing platforms.

Thus, there is a clear need of human cell-based neurotoxicity models with which the toxicological effects can be monitored online. With non-invasive microelectrode array (MEA), the functional activity of neuronal cell networks can be measured *in vitro* for long periods of time and can be used as an additional real-time analysis method (Pine, 1980; Ben-Ari, 2001; Wagenaar et al., 2006; Illes et al., 2007; Heikkilä et al., 2009). As MEA technologies offer indeed a proper way to measure the electrical activity of the networks and further allow the detection of network responses to extrinsic factors these technologies are seen as a promising way to rapid and sensitive screening of neurotoxicity testing as discussed in recent review by Johnstone et al. (2010).

Human pluripotent, e.g., embryonic stem cells are an excellent source to produce the main cells types of the human brain: neurons, astrocytes, and oligodendrocytes (Reubinoff et al., 2001; Zhang et al., 2001; Erceg et al., 2008; Lappalainen et al., 2010; Sundberg et al., 2010). These cells follow the *in vivo* neural development closely and the produced neuronal cells have electrical properties of their brain counter parts (Carpenter et al., 2001; Itsykson et al., 2005; Johnson et al., 2007; Erceg et al., 2008). Importantly, these cells can form spontaneously active functional neuronal networks (Heikkilä et al., 2009) the activity development of which resembles that of rodent primary and embryonic stem cell-derived neuronal cultures (Wagenaar et al., 2006; Illes et al., 2007). Methyl mercury is

a well known neurotoxicant for both developing and adult central nervous system (Kaur et al., 2006) affecting microtubule disruption, oxidative stress, and neurotransmitter deregulation (Castoldi et al., 2001) and causing focal damage in particular brain areas leading to manifestation of paresthesia, ataxia, constriction of visual field, and hearing loss in adult humans (Clarkson, 1993). During life span, humans are most sensitive to methyl mercury during the prenatal period which results in several severities range of mental retardation (Clarkson, 1993).

In this study we exposed spontaneously active human embryonic stem cell (hESC)-derived neuronal networks cultured in MEA's to methyl mercury chloride (MeHgCl) at various concentrations and recorded both acute and delayed networks responses to this toxicant. We show that at subcytotoxic levels, the human neuronal networks' response to this exposure can be detected with MEA but not with classical molecular biological analyses.

MATERIALS AND METHODS

REAGENTS

Methyl mercury II chloride (MeHgCl), polyethyleneimine (PEI), mouse laminin, paraformaldehyde, γ-aminobutyric acid (GABA), and bicuculline methiobromide were purchased from Sigma-Aldrich (St. Louis, MO, USA). 6-cyano-7-nitroquinoxaline-2,3-dione (CNQX) and D(-)-2-amino-5-phosphonopentanoic acid (D-AP5) were from Ascent Scientific (Bristol, UK). B27 supplement, N2 supplement, DMEM/F12 and Neurobasal media, Glutamax, and brain-derived neurotrophic factor (BDNF) were from Invitrogen (Carlsbad, CA, USA). Basic fibroblast growth factor (bFGF) was from R&D Systems (Minneapolis, MN, USA). Penicillin/streptomycin and phosphate buffered saline (dPBS) were from Lonza Group Ltd (Switzerland). 48-well and 96-well plates were from Nunc (ThermoFisher Scientific, Rochester, NY, USA).

Rabbit anti-microtubule associated protein 2 polyclonal antibody (MAP-2, 1:600), and monoclonal mouse anti-galactocerebroside (GalC, 1:400) were purchased from Chemicon. Monoclonal mouse anti-beta-tubulin isotype III (β-tubulin$_{III}$, 1:1250) was purchased from Sigma and sheep anti-human glial fibrillary acidic protein antibody (GFAP, 1:800) was purchased from R&D systems.

CELL CULTURE

The hESCs grown as colonies were mechanically cut into aggregates containing approximately 3000 cells and placed into suspension culture in neural differentiation medium as recently reported (Lappalainen et al., 2010). Culture medium consisted of 1:1 DMEM/F12 and Neurobasal media supplemented with 2 mM GlutaMax, 1 × B27, 1 × N2, and 25 U/ml penicillin/streptomycin. During neurosphere culture, constant supply of bFGF (20 ng/ml) was provided. The aggregates were differentiated for 8 weeks during which they formed round, constant neurospheres and expressed typical neural markers as described in the earlier studies (Hicks et al., 2009; Lappalainen et al., 2010). The medium was changed three times per week and growing spheres were manually cut into smaller spheres once a week.

After differentiation period cells were plated down onto MEA plates (Multi Channel Systems, Germany). Each standard MEA plate contains 59 titanium nitride measurement electrodes in diameter 30 and 200 μm inter-electrode distances. In addition, also 6-well MEA plates were used, which consists of 6 separated 9 electrode areas (diameter 30 mm, inter-electrode distance 200 μm). In both MEA types, electrode areas were separated with in-house designed Poly(dimethyl siloxane) (PDMS) structures (designed and manufactured by J. Kreutzer and P. Kallio, Tampere University of Technology, Department of Automation Science and Engineering, Finland). Cell plating on MEA's was performed as previously described (Heikkilä et al., 2009). First, MEA plates were coated with two step coating procedure; overnight incubation with PEI (0.05% w/v, incubation +4°C) followed by washing with sterile water, and overnight incubation with mouse laminin (20 μg/ml, incubation +4°C). Thereafter, neurospheres were cut into small aggregates (∅ ~200 μm) and plated onto coated MEA plates. Neuronal differentiation medium supplemented with 4 ng/ml bFGF and 5 ng/ml BDNF was applied to cells during MEA culture. The cells and networks were grown for 3 weeks before MeHgCl exposure.

MeHgCl EXPOSURE

MeHgCl was dissolved into sterile dPBS in stock concentration 1 mM and thereafter diluted into neuronal differentiation medium (containing bFGF and BDNF) freshly just before use. Next, the medium containing either 0, 0.5, 50, or 500 nM MeHgCl was changed to neuronal networks growing on MEA's (n = 4/each concentration) or in standard 48- and 96-well plates. The cells were cultured in MeHgCl containing medium for 72 h where after it was washed away.

ELECTROPHYSIOLOGICAL MEASUREMENTS

Measurements were performed with MEA1060-Inv-BC-amplifier with integrated TPC Temperature controller adjusted to +37°C and data was recorded with MC_Rack software (all from Multichannel systems, Reutlingen, Germany). Prior to measurements, MEA plates were sealed with semi-permeable membrane (standard MEAs) or PDMS discs (6-well MEAs) in laminar hood to keep the cultures sterile for repeated measurements as reported earlier (Potter and DeMarse, 2001).

Prior to MeHgCl exposure, the spontaneous baseline electrical activities of each MEA were measured (300 s/MEA) and only MEA cultures demonstrating spike train activity (at least 300 spikes detected at least from one channel per measurement period) were selected to experiment. One MEA from each MeHgCl concentration was recorded for 1 h to detect the acute response. Thereafter, each MEA was recorded at time points of 24, 48, and 72 h for 300 s for delayed response. After 72 h MEA cultures were washed with fresh medium and recovery responses were measured 72 h after washout.

Post-recording data was processed with MC_DataTool (MCS), MATLAB (MathWorks, Natick, MA, USA), Excel (Microsoft), and NeuroExplorer (NexTechnologies, Littleton, MA, USA). Peaks from MEA raw data were detected using threshold limit STD × (-5). From each MEA, total spikes/MEA, total spike number/active channel, and spiking rate/s were calculated. Spike number data was normalized with respect to baseline activity to each MEA separately. For pharmacological response analysis, data was normalized against the mean of baseline activity period. Thereafter, each datapoint was smoothened with Gaussian smoother over ±25 timepoints and plotted into graph.

PHARMACOLOGIC TESTING

Pharmacological response to specific agonists and antagonists of AMPA/kainite, NMDA, and GABA receptors were tested with CNQX, D-AP5, GABA, and bicuculline in concentrations 30 μM, 20 μM, 100 mM, and 20 μM, respectively. Response test were performed immediately after the 72 h exposure period.

QUANTITATIVE RT-PCR ANALYSIS

Samples for qRT-PCR analysis were collected from MEAs immediately after 72 h MeHgCl exposure into lysis buffer and RNA was extracted using NucleoSpin® RNA XS kit according to the manufacturer's instructions (Machery-Nagel GmbH & Co, Düren, Germany). Next, 200 ng of total RNA was reverse-transcribed into cDNA in reaction volume of 20 μl. The qRT-PCR was performed with standard protocol using ABI Prism 7300 instrument (Applied Biosystems, CA, USA) and TaqMan® Gene Expression assays (all from Applied Biosystems) for musashi (ID Hs01045894), neurofilament-68 (NF-68, ID Hs00196245), and GAPDH (ID 4331182) according to manufacturer's instructions with TaqMan® Universal PCR master mix. All samples were performed as four technical replicates. Briefly, the expression levels of musashi, NF-68, and GFAP were evaluated using GAPDH as an internal control. Ct values were determined for every reaction and the relative quantification was calculated using $2^{-\Delta\Delta Ct}$ method (Livak and Schmittgen, 2001). Values of the control sample (not exposed to MeHgCl) were used as a calibrator.

TIME-LAPSE IMAGING

For time-lapse imaging of the neuronal cultures during MeHgCl exposure, a subset of neurospheres were replated on mouse laminin (10 μg/ml, Sigma-Aldrich, St. Louis, MO, USA) coated 48-well plates (8 parallel wells/MeHgCl concentration). The cells were allowed to grow as in MEA plates for 3 weeks until MeHgCl exposure. Thereafter, the well plate was transferred into a time-lapse imaging system (Cell-IQ®, Chip-man Technologies Ltd., Tampere, Finland) which allows for continuous monitoring of selected cells as described previously (Narkilahti et al., 2007). Briefly, sealed culture well plate was placed in a chamber (+36.5°C) with 5% CO_2 gas supply. The cells of interest were selected for monitoring in 500 μm × 670 μm size areas or in grid areas 2 × 2 (1500 × 2010 μm) using an all-in-focus imaging system (Tarvainen et al., 2002) and gained images were stored for later use in JPEG-format. All areas of interest were imaged at 45-min interval for the total exposure time of 72 h. The cells were then fixed for immunocytochemical analysis.

IMMUNOCYTOCHEMISTRY

The samples for immunocytochemical analyses were fixed with cold 4% paraformaldehyde for 20 min either after 72 h MeHgCl exposure or 72 h after washout. The fixed samples were blocked against non-specific antibody binding for 45 min in room temperature (RT) using 10% normal donkey serum (NDS), 0.1% Triton X-100, and 1% bovine serum albumin (BSA) in phosphate buffered saline (PBS). Next, the cells were washed with 1% NDS, 0.1% Triton X-100, and 1% BSA in PBS and incubated overnight at +4°C with primary antibodies diluted to the same buffer. The used antibodies were MAP-2 and ß-tubulin$_{III}$ for neuronal cells, GFAP for astrocytes, and GalC for oligodendrocytes. In the following day the cells were washed with 1% BSA in PBS and incubated with secondary antibodies (anti-mouse, anti-rabbit, or anti-sheep conjugated to Alexa Fluor-488 or 568, Molecular Probes, Invitrogen) diluted to the washing buffer for 1 h at RT. Finally, the cells were repeatedly washed with PBS and phosphate buffer, mounted with Vectashield with 4′6-diamidino-2-phenylindole (DAPI, Vector Laboratories, Peterborough, UK), and cover-slipped. For double-labeling, two primary antibodies and two secondary antibodies were applied simultaneously. When primary antibodies were omitted (negative control), no positive labeling was detected. Cells were imaged using an Olympus microscope (IX51, Olympus, Finland) equipped with a fluorescence unit and camera (DP30BW, Olympus, Finland).

CELL PROLIFERATION MEASUREMENTS

BrdU

The proliferation rate of the neuronal cultures was measured 72 h after MeHgCl washout using a colorimetric enzyme-linked immunosorbent assay (ELISA) for 5-bromo-2′-deoxyuridine (BrdU) (Roche, Basel, Switzerland), which is based on the BrdU incorporation into the DNA during strand synthesis. The manufacturer's protocol was used with small modifications. Briefly, the networks were incubated with BrdU labeling reagent (100 μM) for 20 h at +37°C in 5% CO_2. The cells were then collected and replated into 96-well plate wells (Nunc) at a density of 5000 cells/well. Ten parallel samples/group were prepared. The well plates were centrifuged at 300 × g for 10 min at RT after which the medium was tapped off the wells. The cells were dried for 15 min and fixed with FixDenat solution for 30 min at RT. The FixDenat solution was tapped off and anti-BrdU monoclonal antibody conjugated with peroxidase was added and incubated for 90 min at RT. The plates were then washed three times with dPBS and the substrate solution was added for 5 min. The reaction was stopped with H_2SO_4 and absorbance was measured at a 450-nm wavelength using a Viktor^2 1420 Multilabel Counter (PerkinElmer-Wallac). The background absorbance (measured from negative controls) was subtracted from the measured sample absorbances.

Wst-1 analysis

Cell proliferation capacity was also measured with WST-1 reagent by evaluating succinate-tetrazolium reductase activity. Wst-1 Cell proliferation Assay (Takara Bio Inc., Shiga, Japan) was performed with ELISA from 12 parallel 96-wells/sample. Briefly, cells were once washed with PBS and ready-to-use solution of WST-1 was diluted into PBS and added to the cells. Cells were incubated for 4 h in +37°C, 5% CO_2 after which the measurement was performed with Viktor^2 1420 Multilabel Counter at a 450-nm wavelength. The background absorbance (measured from negative controls) was subtracted from the measured sample absorbances.

RESULTS

HUMAN EMBRYONIC STEM CELL-DERIVED NEURAL CELLS SPONTANEOUSLY FORM ELECTRICALLY ACTIVE NETWORKS

HESC-derived neuronal cell networks stay viable and active in MEA plates for several months and their activity can be measured repeatedly (Heikkilä et al., 2009). The spontaneous activity

develops in 3 weeks to a stage where the networks exhibit train-like activity repeatedly from several channels. **Figure 1A** shows MEA plate with spontaneously active neuronal network. A raster plot showing prominent training activity of the network is represented in **Figure 1B**. For MeHgCl exposure only MEA plates with spontaneously active networks were selected.

MeHgCl DOES NOT HAVE ACUTE EFFECT ON NETWORK ACTIVITY

Immediately after adding the cell culture medium containing 0, 0.5, 50, or 500 nM MeHgCl one MEA/each group was measured for the first hour continuously to detect possible acute effects. No acute toxic effects were observed. The same natural fluctuation on spiking activity was detected in all MEAs and MeHgCl concentration-dependent alteration could not be observed during the measurement period (**Figure 2**).

MeHgCl EXPOSURE DECREASES NETWORK ACTIVITY IN A DELAYED MANNER

The used subtoxic doses of MeHgCl did not have acute effects but during longer exposure clear effects on spontaneous activity was detected. The activity of neuronal networks prominently decreased with each MeHgCl concentration when compared to 0 nM MeHgCl controls after 72 h exposure (**Figures 3A,C**).

MeHgCl EXPOSED NETWORKS SHOW ALTERATION IN THEIR RESPONSE TO PHARMACOLOGICAL SUBSTANCES

To evaluate the neuronal receptor actions in neuronal networks the pharmaceutical testing was performed. Control networks (0 nM MeHgCl) responded as expected as D-AP5, CNQX, and GABA inhibited but bicuculline excited the network activity. MeHgCl at concentrations 0.5 and 50 nM did not have effect on pharmaceutical response (data not shown). Alteration was detected on GABA and bicuculline response, however, with networks exposed to 500 nM MeHgCl as the signaling of the exposed networks was not completely silenced by GABA and the response to bicuculline was stronger when compared to the control networks. (**Figure 3B**).

TRADITIONAL MOLECULAR BIOLOGICAL ANALYSES DID NOT SHOW MeHgCl-DEPENDENT EFFECTS ON THE NEURONAL NETWORKS

QRT-PCR analysis of the cells collected at the end of the MeHgCl exposure (72 h) did not show MeHgCl-related variation. *Musashi* was equally expressed by the cells treated with 0.5, 50, or 500 nM MeHgCl (**Figure 4A**). *NF-68* was prominently expressed by the cells exposed to 0.5 or 50 nM MeHgCl (**Figure 4A**) but overall the expression of *NF-68* in cells exposed to 500 nM MeHgCl was similar as in unexposed cells.

Immunocytochemical staining and analysis verified the similarity of the neuronal networks regardless of the used MeHgCl concentration. MAP-2 and ß-tubulin$_{III}$ positive neuronal cells were detected throughout the network (**Figure 4B**). Also, some GFAP positive astrocytes were detected in each group. In addition to neuronal cells and astrocytes few cells among the networks stained positive for oligodendrocytic marker GalC (**Figure 4B**).

Time-lapse imaging was performed during MeHgCl exposure and it further verified that the unexposed cells or cells exposed to MeHgCl grew and proliferated in a similar fashion (**Figure 5A**).

Due to not detecting molecular biological differences between the unexposed or exposed cells we maintained a subset of cells for additional 72 h after removing the MeHgCl. These cells were analyzed for their proliferation capacity and protein expression using immunostaining. Proliferation of unexposed or MeHgCl exposed cells 72 h after MeHgCl washout was similar according to BrdU and WST-1 analyses (**Figure 5B**). Moreover, the network phenotype was similar as in the previous staining (data not shown).

DISCUSSION

Here we have provided the first proof-of-principle that human ESC-derived neuronal cells are suitable for neurotoxicological screening in MEA platform. The known neurotoxic substance, MeHgCl, caused alterations in functionality in spontaneously active human neuronal networks under subcytotoxic levels. This study underlines the need to develop more sensitive methods for neurotoxicology testing platforms and shows that MEA-based technologies are suitable for that purpose.

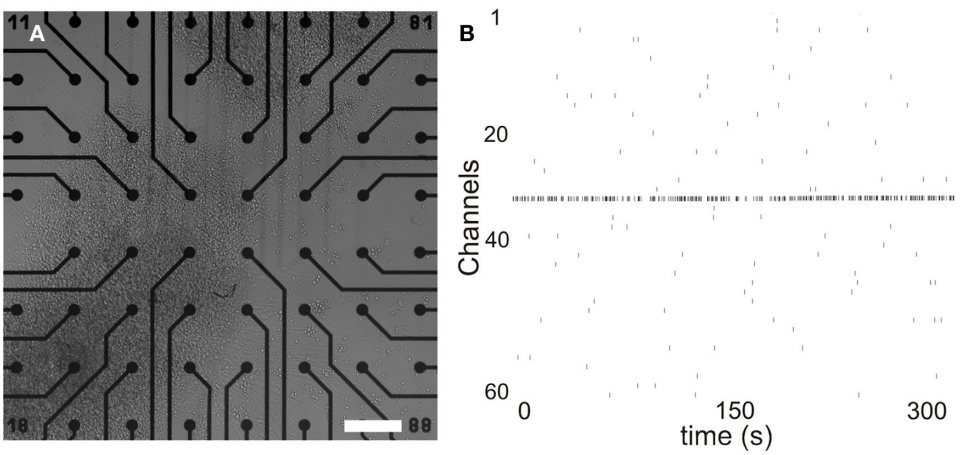

FIGURE 1 | Spontaneously active neuronal networks in MEA. (A) HESC-derived neuronal cells form networks *in vitro* in MEA. **(B)** Formed networks show training activity within 3 weeks of culturing. Scale 200 µm. *x*-Axis time: 300 s, *y*-axis represents each channel.

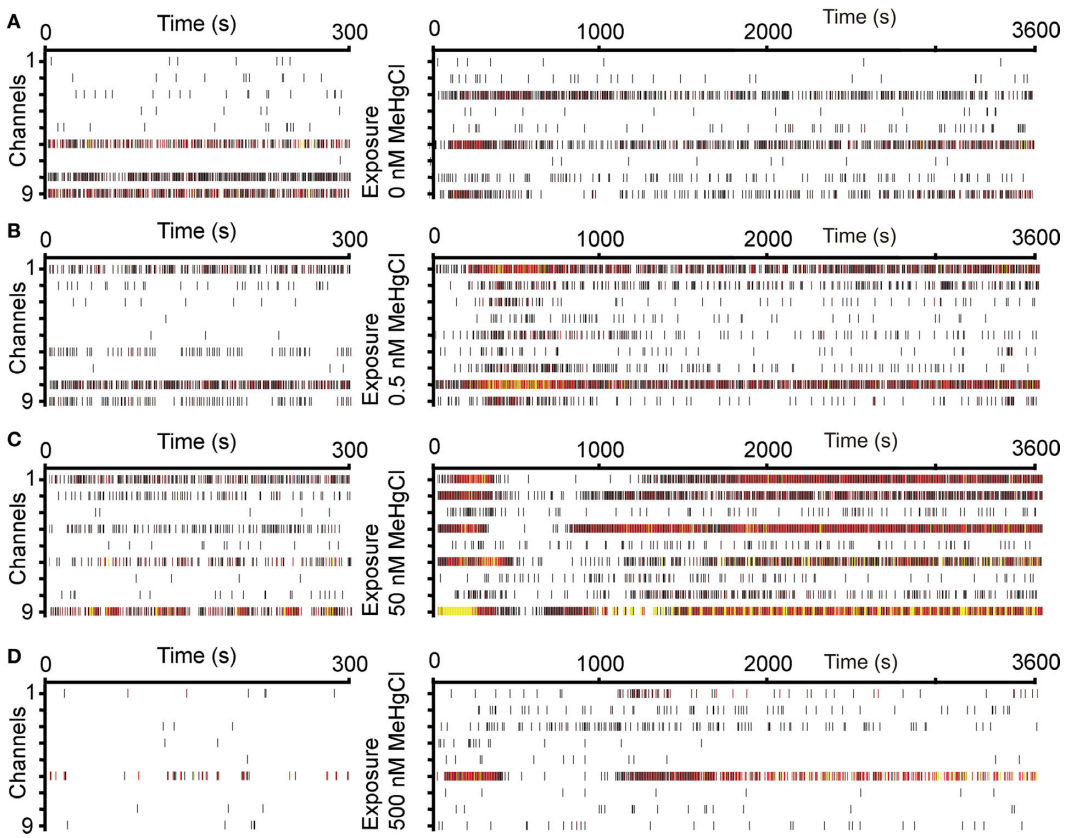

FIGURE 2 | Acute effect of MeHgCl exposure to neuronal network activity. The baseline activity (on the left) of one MEA in each group: **(A)** 0 nM MeHgCl, **(B)** 0.5 nM MeHgCl, **(C)** 50 nM MeHgCl, **(D)** 500 nM MeHgCl exposure, and activity immediately after MeHgCl exposure (1 h, on the right). x-Axis time: baseline 300 s, acute response 600 s, y-axis represents each channel. Spikes are marked as rasters and heated colors represent increased activity rate.

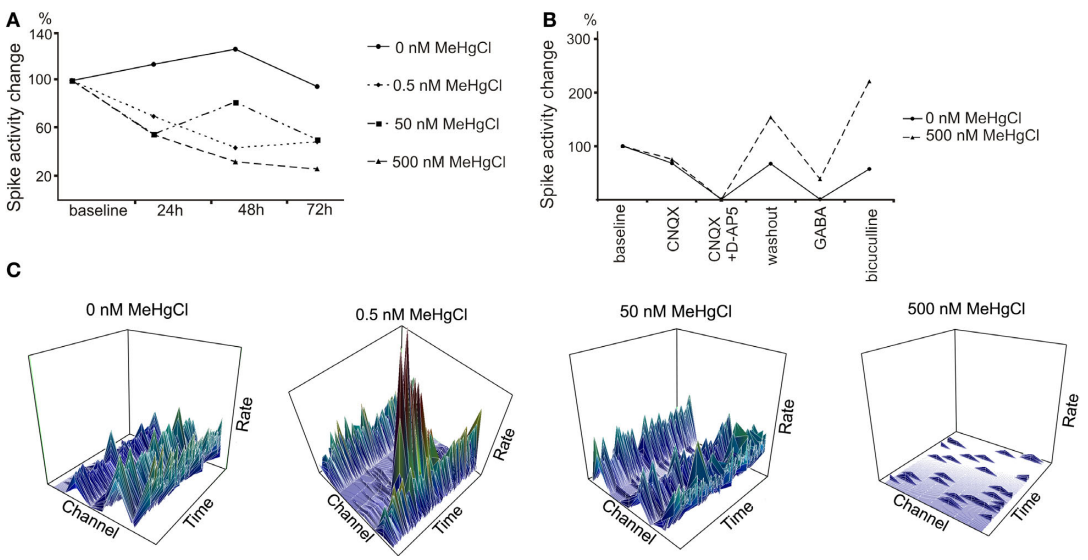

FIGURE 3 | Delayed effect of MeHgCl exposure to neuronal network activity. (A) The activity of neuronal networks decreased toward 72 h of MeHgCl exposure in a concentration-dependent manner. The activity was measured from four parallel MEAs for 300 s at each timepoint. **(B)** 500 nM MeHgCl exposure altered the networks' response to pharmacological substances. **(C)** Representative 3D plots of the activity rate/s (*z*-axis)/time (*x*-axis)/channel (*y*-axis) from one MEA/MeHgCl concentration at 72 h timepoint. Scales: activity rate/s 0–7 (bin = 1 s), time 300 s, channels 1–9. All data was gained as number of spikes/MEA which was normalized to the number of spikes at baseline.

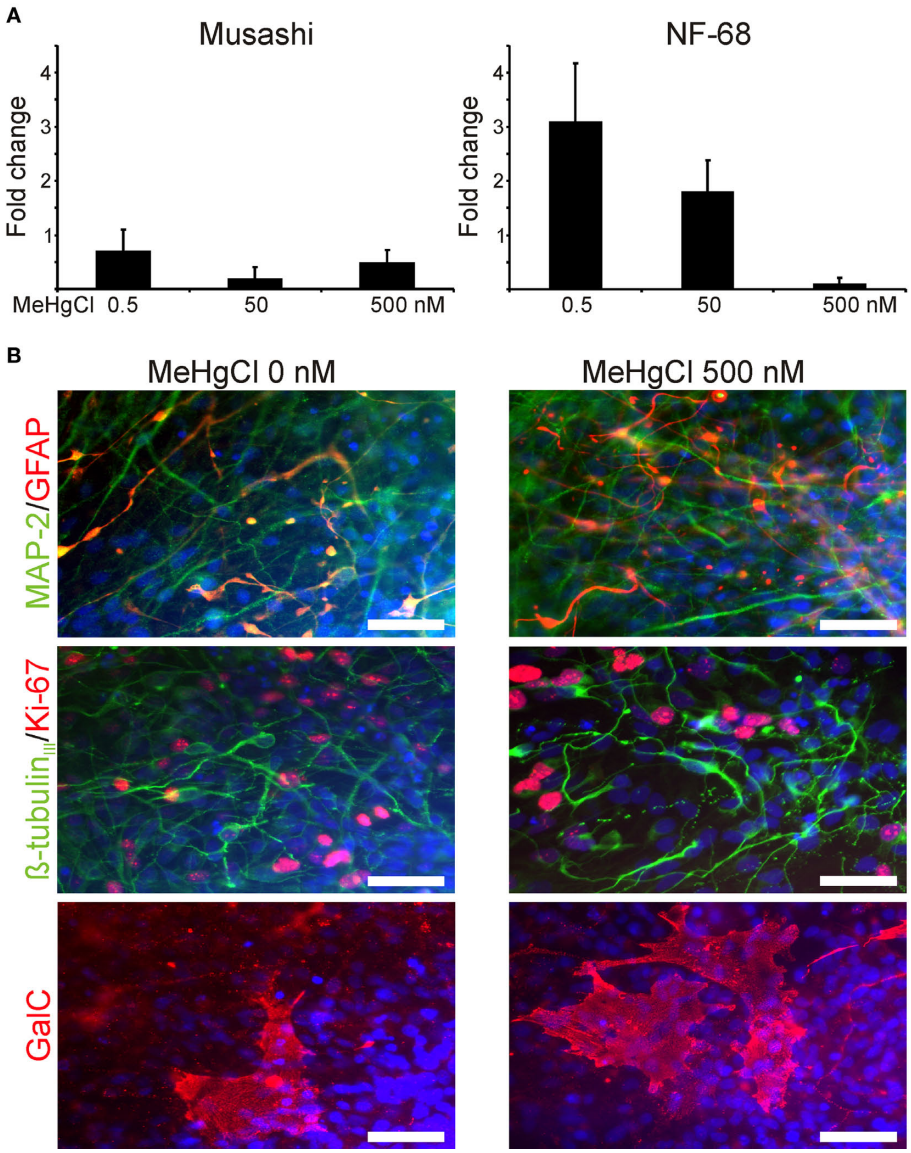

FIGURE 4 | Molecular biological analyses of the cells after MeHgCl exposure. (A) The relative *musashi* and *NF-68* mRNA expression of neuronal cells exposed to 0, 0.5, 50, or 500 nM MeHgCl did not show prominent variation. The data was normalized to the expression of house-keeping gene GAPDH, and values of unexposed cells were used as a calibrator set to 0 at y-axis. **(B)** The neuronal cell phenotypes appeared similar regardless of the MeHgCl concentration and stained positive for MAP-2, ß-tubulin$_{III}$, GFAP, and GalC **(B)**. Scale 50 µm.

The development of human-based cell models is highly needed for toxicological testing and drug screening studies. For neurotoxicological studies, fetal human brain-derived cells have been used (Fritsche et al., 2005; Moors et al., 2009). These cells hold, however, limiting features such as origin and culturing time which makes their large scale use challenging. Other possible human-based cell sources considered for neurotoxicological studies are, e.g., SH-SY5Y human neuroblastoma cells (Biedler et al., 1973) or NT2 human teratocarcinoma cells (Bliss et al., 2006) which can be differentiated toward CNS cell types. These cells are, however, different from "normal" healthy cells by genetics and physiologics which raise questions on their behavior when exposed to toxic substances. The development of hESC culture methods (Thomson et al., 1998) and their neural differentiation (Carpenter et al., 2001; Reubinoff et al., 2001; Zhang et al., 2001) opened up a new era for neurotoxicological field. Neuronal cells derived from hESCs most likely resemble the counterpart cells in the developing and adult human brain (Zeng et al., 2006). Thus, these cells could be used both for developmental and adult neurotoxicity testing as shown for 1-methyl-4-phenylpyridinium (MPP^+) toxicity to hESC-derived dopaminergic neurons (Zeng et al., 2006). Here, we used hESC-derived neurosphere cultures which have been characterized for expression of neural markers previously (Heikkilä et al., 2009; Hicks et al., 2009; Sundberg et al., 2009; Lappalainen et al., 2010). In addition, these cultures were shown to contain MAP-2 or β-tubulin$_{III}$ positive neurons and GFAP positive astrocytes after 4 week culturing on MEA dishes.

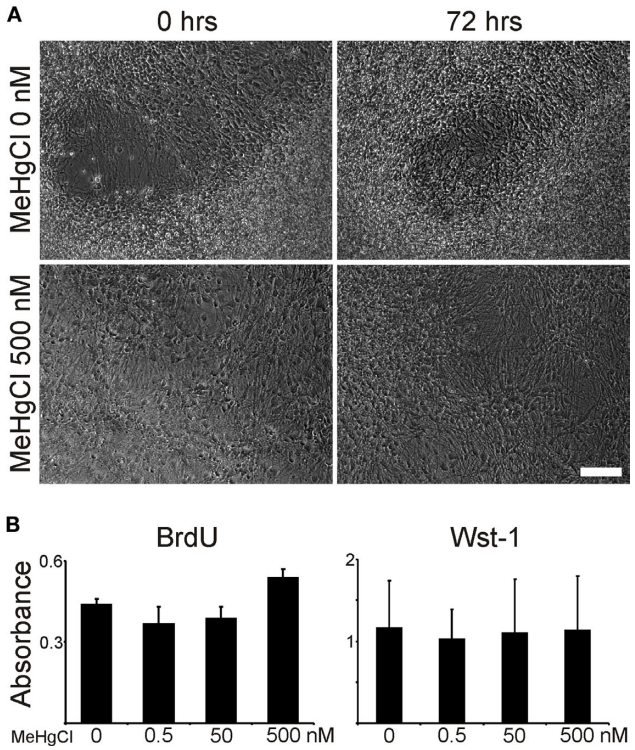

FIGURE 5 | Time-lapse and proliferation analyses. (A) Time-lapse imaging verified the viability of the neuronal networks as no differences could be observed on morphologies during the 72 h of MeHgCl exposure. **(B)** Both BrdU and Wst-1 analyses asserted that all neuronal networks proliferated similarly 72 h after MeHgCl washout. Scale 100 μm.

Here, we focused to study the MeHgCl effects on reported subcytotoxic levels (>1 μM *in vitro*) (van Vliet et al., 2008) to spontaneously active hESC-derived neuronal networks. The results showed that MeHgCl at 0.5–500 nM range caused concentration depended decrease in total spike activity during 72 h exposure compared to the control cultures. Previous, it has been reported that MeHgCl exposure caused decrease the evoked field potential amplitudes in rat primary telencephalon cultures in a concentration depended manner at 1–100 μM range whereas the effects on the spontaneous network activities were not reported (van Vliet et al., 2007). In addition to changes observed in functional level, we did not detected major changes caused by MeHgCl on cell morphology, proliferation, gene or protein expression on the studied concentrations. It has been shown that MeHgCl at a slightly higher concentration (750 nM) caused decrease in amount of differentiating β-tubulin$_{III}$ positive cells, and cell migration at 500 nM to 10 μM in human fetal brain cells which showed cytotoxicity to MeHgCl at 10 μM concentration (Moors et al., 2009). Although we did not study cell migration in more detail, the time-lapse imaging of treated cultures did not implicate that hESC-derived neuronal cell migration would be affected at studied MgHgCl concentrations (0.5–500 nM).

In this study we could show that MeHgCl at subcytotoxic levels clearly decreased the electrical functionality of hESC-derived networks. Harmful effects were not detected with traditional molecular biological methods. This clearly clarifies the advantage of MEA setup which is more sensitive to detect differences between groups treated with subcytotoxic concentrations. These results underline the need to study the subcytotoxic effects of different substances more carefully since they may reveal effects on functional properties which may or may not be acute, long-lasting, or even permanent. The MeHgCl exposed hESC-derived neuronal networks also showed distinct responses to pharmacologic substances. The network signaling decreased when treated with AMPA/kainate (CNQX) and NMDA (D-AP5) receptor antagonist and GABA agonist treatments as in control networks whereas the response for $GABA_A$ receptor antagonist bicuculline was substantially stronger when compared to untreated networks. Thus it is possible, that 72 h MeHgCl exposure had an effect on GABA receptor subunit expression on the hESC-derived neuronal cells. Interestingly, Bal-Price and colleagues reported also changed responses to bicuculline in their study where primary rat cortical cultures were exposed to domoic acid (Hogberg et al., 2010). Unfortunately, due to small amounts of RNA gained from MEAs more detailed GABA receptor subunit analysis with qRT-PCR could not be performed here. Thus, this will require further studies in the future.

Here we have showed that hESC-derived neuronal networks are indeed suitable for toxicological screening studies. The MEA platform is especially eligible for screening functional responses in spontaneously active neuronal networks that are missed with traditional molecular biology end-point analyses. We have shown that hESC-derived neural cells are capable of forming spontaneously active networks exhibiting signaling from sporadic single spiked to more mature synchronous bursting activity (Heikkilä et al., 2009). This setup is in routine use in our laboratory, thus it is highly applicable also for neurotoxicological studies. Regardless of the usability and enormous research possibilities MEA setup also holds its cons. The controllability of the networks is plating-dependable thus batch to batch variation is expected. Also, standard glass MEA plates are not favored by hESC-derived neuronal cells and coatings are crucial for network forming capability. Also, the gained data is a large package to handle and analysis of it is challenging (Wagenaar et al., 2006; Illes et al., 2007; Heikkilä et al., 2009) and more standardized analysis methods should be developed. Also more structured networks gained by different surface patterning and guiding applications would enable more standardized functional networks instead of the used spontaneously self organizing cultures that would increase the repeatability of the tests. In the future, the MEA setup offers an intriguing possibility to study neuronal networks derived from human patients' induced pluripotent stem cells (iPSCs) as we recently reported (Äänismaa et al., 2010). In deed, there are almost limitless possibilities to model genetic neurological deficiencies *in vitro* as well as perform, e.g., drug screening with these iPSC-derived neural cells. We conclude that MEA platform is highly suitable for neurotoxicological testing and would be a valuable addition to current analysis patterns.

ACKNOWLEDGMENTS

This study was funded by Academy of Finland (projects 122959 and 123233), BioneXt Tampere, and Competitive Research Funding of Pirkanmaa Hospital District. We want to acknowledge the personnel of Regea for the support in stem cell research and J. Kreutzer and P. Kallio, Tampere University of Technology, for PDMS designs.

REFERENCES

Äänismaa, R., Ylä-Outinen, L., Heikkilä, J., Suuronen, R., Skottman, H., and Narkilahti, S. (2010). *Neural Differentiation of Human Induced Pluripotent Stem Cells: Formation of Functional Neuronal Networks.* Conference Proceedings of the 7th International Meeting on Substrate-Integrated Micro Electrode Arrays, Reutlingen, 90–91.

Bal-Price, A. K., Hogberg, H. T., Buzanska, L., and Coecke, S. (2010). Relevance of in vitro neurotoxicity testing for regulatory requirements: challenges to be considered. *Neurotoxicol. Teratol.* 32, 36–41.

Bal-Price, A. K., Hogberg, H. T., Buzanska, L., Lenas, P., van Vliet, E., and Hartung, T. (2009). In vitro developmental neurotoxicity (DNT) testing: relevant models and endpoints. *Neurotoxicology*. doi: 10.1016/j.neuro.2009.11.006.

Ben-Ari, Y. (2001). Developing networks play a similar melody. *Trends Neurosci.* 24, 353–360.

Biedler, J. L., Helson, L., and Spengler, B. A. (1973). Morphology and growth, tumorigenicity, and cytogenetics of human neuroblastoma cells in continuous culture. *Cancer Res.* 33, 2643–2652.

Bliss, T. M., Kelly, S., Shah, A. K., Foo, W. C., Kohli, P., Stokes, C., Sun, G. H., Ma, M., Masel, J., Kleppner, S. R., Schallert, T., Palmer, T., and Steinberg, G. K. (2006). Transplantation of hNT neurons into the ischemic cortex: cell survival and effect on sensorimotor behavior. *J. Neurosci. Res.* 83, 1004–1014.

Buzanska, L., Ruiz, A., Zychowicz, M., Rauscher, H., Ceriotti, L., Rossi, F., Colpo, P., Domanska-Janik, K., and Coecke, S. (2009a). Patterned growth and differentiation of human cord blood-derived neural stem cells on bio-functionalized surfaces. *Acta Neurobiol. Exp. (Wars)* 69, 24–36.

Buzanska, L., Sypecka, J., Nerini-Molteni, S., Compagnoni, A., Hogberg, H. T., del Torchio, R., Domanska-Janik, K., Zimmer, J., and Coecke, S. (2009b). A human stem cell-based model for identifying adverse effects of organic and inorganic chemicals on the developing nervous system. *Stem Cells* 27, 2591–2601.

Carpenter, M. K., Inokuma, M. S., Denham, J., Mujtaba, T., Chiu, C. P., and Rao, M. S. (2001). Enrichment of neurons and neural precursors from human embryonic stem cells. *Exp. Neurol.* 172, 383–397.

Castoldi, A. F., Coccini, T., Ceccatelli, S., and Manzo, L. (2001). Neurotoxicity and molecular effects of methylmercury. *Brain Res. Bull.* 55, 197–203.

Clarkson, T. W. (1993). Mercury: major issues in environmental health. *Environ. Health Perspect.* 100, 31–38.

Erceg, S., Lainez, S., Ronaghi, M., Stojkovic, P., Perez-Arago, M. A., Moreno-Manzano, V., Moreno-Palanques, R., Planells-Cases, R., and Stojkovic, M. (2008). Differentiation of human embryonic stem cells to regional specific neural precursors in chemically defined medium conditions. *PLoS ONE* 3, e2122. doi: 10.1371/journal.pone.0002122.

Fritsche, E., Cline, J. E., Nguyen, N. H., Scanlan, T. S., and Abel, J. (2005). Polychlorinated biphenyls disturb differentiation of normal human neural progenitor cells: clue for involvement of thyroid hormone receptors. *Environ. Health Perspect.* 113, 871–876.

Harry, G. J., Billingsley, M., Bruinink, A., Campbell, I. L., Classen, W., Dorman, D. C., Galli, C., Ray, D., Smith, R. A., and Tilson, H. A. (1998). In vitro techniques for the assessment of neurotoxicity. *Environ. Health Perspect.* 106(Suppl. 1), 131–158.

Heikkilä, T. J., Ylä-Outinen, L., Tanskanen, J. M., Lappalainen, R. S., Skottman, H., Suuronen, R., Mikkonen, J. E., Hyttinen, J. A., and Narkilahti, S. (2009). Human embryonic stem cell-derived neuronal cells form spontaneously active neuronal networks in vitro. *Exp. Neurol.* 218, 109–116.

Hicks, A. U., Lappalainen, R. S., Narkilahti, S., Suuronen, R., Corbett, D., Sivenius, J., Hovatta, O., and Jolkkonen, J. (2009). Transplantation of human embryonic stem cell-derived neural precursor cells and enriched environment after cortical stroke in rats: cell survival and functional recovery. *Eur. J. Neurosci.* 29, 562–574.

Hogberg, H. T., Kinsner-Ovaskainen, A., Hartung, T., Coecke, S., and Bal-Price, A. K. (2009). Gene expression as a sensitive endpoint to evaluate cell differentiation and maturation of the developing central nervous system in primary cultures of rat cerebellar granule cells (CGCs) exposed to pesticides. *Toxicol. Appl. Pharmacol.* 235, 268–286.

Hogberg, H. T., Novellino, A., Sobanski, T., and Bal-Price, A. K. (2010). *Application of Micro Electrode Arrays (MEAs) as an Emerging Technology for Developmental Neurotoxicity*. Conference Proceeding of the 7th International Meeting on Substrate-Integrated Micro Electrode Arrays, Reutlingen, 142–144.

Illes, S., Fleischer, W., Siebler, M., Hartung, H. P., and Dihne, M. (2007). Development and pharmacological modulation of embryonic stem cell-derived neuronal network activity. *Exp. Neurol.* 207, 171–176.

Itsykson, P., Ilouz, N., Turetsky, T., Goldstein, R. S., Pera, M. F., Fishbein, I., Segal, M., and Reubinoff, B. E. (2005). Derivation of neural precursors from human embryonic stem cells in the presence of noggin. *Mol. Cell. Neurosci.* 30, 24–36.

Johnson, M. A., Weick, J. P., Pearce, R. A., and Zhang, S. C. (2007). Functional neural development from human embryonic stem cells: accelerated synaptic activity via astrocyte coculture. *J. Neurosci.* 27, 3069–3077.

Johnstone, A. F., Gross, G. W., Weiss, D. G., Schroeder, O. H., Gramowski, A., and Shafer, T. J. (2010). Microelectrode arrays: a physiologically based neurotoxicity testing platform for the 21st century. *Neurotoxicology* 31, 331–350.

Kaur, P., Aschner, M., and Syversen, T. (2006). Glutathione modulation influences methyl mercury induced neurotoxicity in primary cell cultures of neurons and astrocytes. *Neurotoxicology* 27, 492–500.

Lappalainen, R. S., Salomäki, M., Ylä-Outinen, L., Heikkilä, T. J., Hyttinen, J. A., Pihlajamäki, H., Suuronen, R., Skottman, H., and Narkilahti, S. (2010). Similarly derived and cultured hESC lines show variation in their developmental potential towards neuronal cells in long-time culture. *Regen. Med.* (in press).

Livak, K. J., and Schmittgen, T. D. (2001). Analysis of relative gene expression data using real-time quantitative PCR and the 2(-Delta Delta C(T)) method. *Methods* 4, 402–408.

Moors, M., Rockel, T. D., Abel, J., Cline, J. E., Gassmann, K., Schreiber, T., Schuwald, J., Weinmann, N., and Fritsche, E. (2009). Human neurospheres as three-dimensional cellular systems for developmental neurotoxicity testing. *Environ. Health Perspect.* 117, 1131–1138.

Narkilahti, S., Rajala, K., Pihlajamaki, H., Suuronen, R., Hovatta, O., and Skottman, H. (2007). Monitoring and analysis of dynamic growth of human embryonic stem cells: comparison of automated instrumentation and conventional culturing methods. *Biomed. Eng. Online* 6, 11.

Pine, J. (1980). Recording action potentials from cultured neurons with extracellular microcircuit electrodes. *J. Neurosci. Methods* 2, 19–31.

Potter, S. M., and DeMarse, T. B. (2001). A new approach to neural cell culture for long-term studies. *J. Neurosci. Methods* 110, 17–24.

Reubinoff, B. E., Itsykson, P., Turetsky, T., Pera, M. F., Reinhartz, E., Itzik, A., and Ben-Hur, T. (2001). Neural progenitors from human embryonic stem cells. *Nat. Biotechnol.* 19, 1134–1140.

Sundberg, M., Jansson, L., Ketolainen, J., Pihlajamaki, H., Suuronen, R., Skottman, H., Inzunza, J., Hovatta, O., and Narkilahti, S. (2009). CD marker expression profiles of human embryonic stem cells and their neural derivatives, determined using flow-cytometric analysis, reveal a novel CD marker for exclusion of pluripotent stem cells. *Stem Cell Res.* 2, 113–124.

Sundberg, M., Skottman, H., Suuronen, R., and Narkilahti, S. (2010). Production and isolation of NG2(+) oligodendrocyte precursors from human embryonic stem cells in defined serum-free medium. *Stem Cell Res.* 5, 91–103.

Tarvainen, J., Saarinen, M., Laitinen, J., Korpinen, J., and Viitanen, J. (2002). Creating images with high data contents for microworld applications. *Ind. Syst. Rev.* 1, 17–23.

Thomson, J. A., Itskovitz-Eldor, J., Shapiro, S. S., Waknitz, M. A., Swiergiel, J. J., Marshall, V. S., and Jones, J. M. (1998). Embryonic stem cell lines derived from human blastocysts. *Science* 282, 1145–1147.

van Vliet, E., Morath, S., Eskes, C., Linge, J., Rappsilber, J., Honegger, P., Hartung, T., and Coecke, S. (2008). A novel in vitro metabolomics approach for neurotoxicity testing, proof of principle for methyl mercury chloride and caffeine. *Neurotoxicology* 29, 1–12.

van Vliet, E., Stoppini, L., Balestrino, M., Eskes, C., Griesinger, C., Sobanski, T., Whelan, M., Hartung, T., and Coecke, S. (2007). Electrophysiological recording of re-aggregating brain cell cultures on multi-electrode arrays to detect acute neurotoxic effects. *Neurotoxicology* 28, 1136–1146.

Wagenaar, D. A., Pine, J., and Potter, S. M. (2006). An extremely rich repertoire of bursting patterns during the development of cortical cultures. *BMC Neurosci.* 7, 11. doi: 10.1186/1471-2202-7-11.

Zeng, X., Chen, J., Deng, X., Liu, Y., Rao, M. S., Cadet, J. L., and Freed, W. J. (2006). An in vitro model of human

dopaminergic neurons derived from embryonic stem cells: MPP+ toxicity and GDNF neuroprotection. *Neuropsychopharmacology* 31, 2708–2715.

Zhang, S. C., Wernig, M., Duncan, I. D., Brustle, O., and Thomson, J. A. (2001). In vitro differentiation of transplantable neural precursors from human embryonic stem cells. *Nat. Biotechnol.* 19, 1129–1133.

Conflict of Interest Statement: The authors declare that the research was conducted in the absence of any commercial or financial relationships that could be construed as a potential conflict of interest.

Received: 28 July 2010; paper pending published: 29 July 2010; accepted: 30 August 2010; published online: 30 September 2010. Citation: Ylä-Outinen L, Heikkilä J, Skottman H, Suuronen R, Äänismaa R and Narkilahti S (2010) Human cell-based micro electrode array platform for studying neurotoxicity. Front. Neuroeng. ***3****:111. doi: 10.3389/fneng.2010.00111*

The Journal of Tissue Engineering and Regenerative Medicine

Three dimensional growth matrix for human embryonic stem cell-derived neuronal cells

Laura Ylä-Outinen[a,b,c], Tiina Joki[a,b,c], Mari Varjola[a,b], Heli Skottman[a,b], Susanna Narkilahti[a,b,c]

[a]*NeuroGroup, Institute of Biomedical Technology, University of Tampere, Tampere, Finland*

[b]*BioMediTech, Tampere, Finland*

[b]*The Science Center of Pirkanmaa Hospital District, Tampere University Hospital, Tampere, Finland*

Keywords: Astrocytes, Encapsulation, Hydrogel, Neural tissue engineering, Neuronal network activity, Oligodendrocytes, PuraMatrix™

Short title: 3D culturing matrix for human neuronal cells

Corresponding author: Susanna Narkilahti

Address: Institute of Biomedical Technology

University of Tampere

Biokatu 12, 33520 Tampere, Finland

Telephone:+ 358 40 708 5113

Fax: + 358 3 3551 8498

Email: susanna.narkilahti@uta.fi

ABSTRACT:

The future tissue engineering applications for neuronal cells will require supportive 3D matrix. This particular matrix should be soft, elastic, and supportive for cell growth. Here, we characterize the suitability of the 3D synthetic hydrogel matrix, PuraMatrix™, as a growth platform for human embryonic stem cell (hESC)-derived neural cells. The viability of the cells grown on the top of, inside, and under the hydrogel was monitored. The maturation and the electrical activity of the neuronal networks inside the hydrogel were further characterized.

We showed that cells stayed viable on the top of the PuraMatrix™-surface and the growth of the neural cells and neural processes was good. Further, hESC-derived neurons, astrocytes, and oligodendrocytes all grew, matured, and migrated when cultured inside the hydrogel. Importantly, neuronal cells were able to form electrically active connections that were verified using microelectrode array. Thus, as a conclusion, the PuraMatrix™ is a good supportive growth matrix for human neural cells and may serve as a matrix for neuronal scaffolds in neural tissue engineering.

1. INTRODUCTION:

Currently, a lot of hope is seen in cell therapies for the central nervous system (CNS) deficits. Especially, stem cells are foreseen as a potential source for new regenerative therapies. Human embryonic stem cells (hESC) are considered to have huge potential in transplantation therapies in the future and they have been successfully differentiated into neuronal cells, astrocytes, and oligodendrocytes (Lappalainen *et al.* 2010; Sundberg *et al.* 2010). In addition to transplantation therapies, these cells can be used for *in vitro* toxicity and drug testing and developmental studies (Johnstone *et al.* 2010; Ylä-Outinen *et al.* 2010; Zeng *et al.* 2006). Another potential cell source for neural applications are human induced pluripotent stem (hiPS) cells. These cells are pluripotent like hESCs and are derived/created directly from the patients own somatic cells (Hu *et al.* 2010; Takahashi *et al.* 2007). HIPS cells are seen potential for patient specific drug screening platforms as well as for future treatments (Hu *et al.* 2010). These cells have been successfully differentiated into neuronal cells that can form spontaneously active neuronal networks and thus resemble their hESC-derived counterparts (Hu *et al.* 2010; Äänismaa *et al.* 2011). For all these purposes, neural cells *in vitro* should be studied in more tissue-like environment, that is in 3D, in order to mimic as native cell behavior as possible.

In vivo experiments have shown that cell transplantations solely are not enough to support the regeneration in the host tissue. After transplantations, the viability of the cells is often poor (Hicks *et al.* 2009; Oizumi *et al.* 2008) or vice versa as unwanted cell types like undifferentiated cells causing teratomas or tumors can outgrow from the cell grafts (Amariglio *et al.* 2009). Typically, after severe CNS trauma, the injury site has a cavity that does not support the viability of transplanted cells and is slowly filled with glial scar preventing regeneration of the functional tissue (Hejcl *et al.* 2008; Nisbet *et al.* 2008; Zhong *et al.* 2008). Therefore, the presence of a structural support preventing the scar formation on the injury site

is also important, which has been shown to be achievable with biomaterials (Hejcl *et al.* 2008; Nisbet *et al.* 2008). In addition, in case of allogenous cell grafts the transplantation is associated with graft rejection that is currently avoided with relatively heavy immunosuppressive medication that may cause harmful side-effects (Li *et al.* 2009). Thus, more sophisticated tissue engineering designs combining both cells and supportive biomaterial scaffold most likely will offer solution to overcome most of the challenges seen in the current cell transplantation methods.

Biomaterials for neural tissue engineering should be non-toxic, three dimensional, support the growth of wanted cell type, and allow the nutrition flux (Holmes *et al.* 2000; Thonhoff *et al.* 2008). In regenerative medicine, the materials should also allow the cell migration and interaction with the host tissue. Material scaffold could also be engineered to release cell supportive substances such as growth factors and needed immunosuppression could be provided by local release of immunosuppressant's (Lindvall *et al.* 2010; Zhong *et al.* 2008) Hydrogels are potential materials for CNS deficits because they are highly porous, can form 3D structures *in vitro* and/or *in vivo* and can fill the cavity and thus prevent the formation of glial scar (Hejcl *et al.* 2008). Few hydrogels in 3D format such as Matrigel (Thonhoff *et al.* 2008), PuraMatrix™ (Gelain *et al.* 2006; Thonhoff *et al.* 2008), hyaluronic acid (Brännvall *et al.* 2007), Poly(ethylene glygolide)-derivatives (Freudenberg *et al.* 2009), and chitosan (Leipzig *et al.* 2010) have been studied in combination with neuronal cells. Although these materials are shown to support the growth of neuronal cells not all of them are suitable for clinical use e.g. Matrigel that is of mouse origin and not defined natural product.

In case of hyaluronic acid and chitosan, these materials have only been tested with animal derived neural cells and not with human neural cells (Brännvall *et al.* 2007; Leipzig *et al.* 2010). PM and Matrigel, on the other hand, have been shown to be biocompatible with human fetal stem cell-derived neuronal cells (Thonhoff *et al.* 2008). PM is synthetic, peptide

nanofibrous hydrogel the composition of which is fully known and controlled (Zhang *et al.* 2005). It consists of peptide sequence RADA16 and its modification with functional groups has also been studied (Zhang 2002). Still, whether PM actually supports survival of encapsulated human neuronal cells long term and whether those cells are able to maturate into functional neurons, has not been addressed.

Here, our aim was to study whether hESC-derived neurons, astrocytes, and oligodendrocytes survive on the top, encapsulated in, or under the PM for prolonged periods. We also addressed whether these cells can maturate into spontaneously active neurons/neuronal networks inside of the 3D structure. Our results show both proper cell survival and functionality with PM hydrogel.

2. MATERIALS AND METHODS

2.1 hESC and neural differentiation

Two hESC lines derived at Regea–Institute for Regenerative Medicine, Regea 06/040 and Regea 08/023, were used in this study. Regea has ethical approval from Pirkanmaa Hospital District to derivate, culture, and differentiate the human embryonic stem cells (Skottman, R05116) and the permission from the National Authority for Medicolegal Affairs (Valvira, 1426/32/300/05) to conduct human stem cell research.

The hESCs grown as colonies were mechanically cut into smaller pieces and placed into suspension culture in differentiation media as described previously (Lappalainen *et al.* 2010). Neuronal and astrocytic differentiation was performed as previously described (Lappalainen *et al.* 2010). Briefly, neural differentiation medium (NMD) that contains 1:1 Dulbecco's Modified Eagle's Medium/F12 (Gibco, Invitrogen, Finland) and Neurobasal medium supplemented with 2 mM GlutaMax, 1× B27, 1× N2 (all from Gibco), 20 ng/ml fibroblast growth factor (bFGF, R&D Systems, Minneapolis, MN, USA), and penicillin/streptomycin (25 U/ml, Cambrex, Belgium) was used. The small cell aggregates formed neurospheres in suspension culture as previously described (Lappalainen *et al.* 2010). The medium was changed 3 times per week and the spheres were mechanically dissected once a week. Neurospheres were cultured for 8 weeks to gain pure neuronal population and for 20 weeks to gain astrocytic population. During these differentiation periods, the cell populations were differentiated into neuronal or astrocytic lineages (Lappalainen *et al.* 2010; Sundberg *et al.* 2009). Moreover, additional hESC colony pieces were cultured as suspension culture in oligodendrocyte precursor cell (OPC) differentiation medium (OPCDM). The OPC differentiation procedure has been described earlier (Sundberg *et al.* 2010). Shortly, OPC

differentiation was initiated in suspension culture in N2 medium [DMEM/F-12 medium with 1× N2, 2 mM GlutaMax, 0.6% glucose, 5 mM Hepes, 2 μg/ml heparin (Sigma-Aldrich), 25 U/ml penicillin and streptomycin] supplemented with 10 ng/ml human ciliary neurotrophic factor (CNTF), 20 ng/ml human epithelial growth factor (EGF), and 20 ng/ml bFGF (R&D Systems Europe) for 4 weeks. Thereafter, for the following 3 weeks the cells were cultured in N2 medium containing 10 ng/ml CNTF, 20 ng/ml EGF, 10 ng/ml bFGF, 100 ng/ml insulin-like growth factor-1 (Sigma-Aldrich), 20 ng/ml platelet-derived growth factor-AA (Peprotech Inc.), and 1 μg/ml laminin (Sigma-Aldrich). After this, the cells were encapsulated to PM scaffold and thereafter, OPCDM [N2 medium supplemented with 200 μM L-ascorbic acid 2-phosphate (Sigma-Aldrich), 10 ng/ml CNTF, and 40 ng/ml 3,3′,5-triiodo-L-thyronine (Sigma-Aldrich)] was used as the culture medium for OPCs.

2.2. Preparation of the hydrogels and cell culturing setups

Synthetic self-assembled PM (BD Bioscience, Sparks, MD, USA) was used as hydrogel scaffold. The hydrogel was used in concentrations of 0.25, 0.15, 0.10, and 0.05%.

Cells were seeded either 1) on the top of the gelled material, 2) under the hydrogel (the cells first grown on the top of the laminin for one week and the hydrogel then added on the top of the cells), or 3) encapsulated into the hydrogel. Moreover, the results from the 3D cultures were compared to 2D control in which the cells were cultured on the laminin (10 μg/ml, Sigma-Aldrich) surface, a standard culture matrix of these cells (Lappalainen *et al.* 2010). The non-coated cell-culture polystyrene (CCPS) was used as a negative control.

After differentiation periods, the cells were either dissociated into single cell suspension with Trypsin (Sigma-Aldrich) or cut into smaller cell aggregates (Ø ~100 μm) mechanically.

Shortly, for single cell suspension, 1× Trypsin was added onto top of the neurospheres and incubated for 5 minutes. Trypsin was inactivated with 5% human serum (Sigma-Aldrich) and single cell suspension was washed with NDM or OPCDM. Cell aggregates were cut with scalpel and placed to NDM or OPCDM.

2.2.1. Preparation of the hydrogel surfaces

The PM was gelated according to manufacturer's instructions. Shortly, the stock solutions were diluted into appropriate concentrations (0.05%, 0.10%, 0.15%, or 0.25%) with sterile water and added to the cell culture wells (140 µl/cm^2). Cell culture medium was gently added on the top and the solution was let to form a gel at +37 °C for 30 min. During that period, cell culture medium was changed three times. After gelation, single cell suspension or cell aggregates were plated onto hydrogel surfaces for 2D culturing on the top of the hydrogel.

2.2.2. Preparation of the encapsulated cells

For encapsulation, cells were mixed with PM resulting in final cell density of 1×10^6 cells in one ml of 0.10% hydrogel. First, the cells were mixed with 10% sucrose. This solution was mixed in 1:1 ratio with PM that was first diluted to 0.20% solution in 20% sucrose. Then, cell culture medium was pipetted carefully on top of cell/PM solution to initiate gelation process. The spontaneously formed gels have un-uniform layer height ranging from 1 000 µm (edges of the well) to 500 µm (centre of the well).

2.2.3. Preparation of the cells embedded with the hydrogel

First, cells were plated onto 10 µg/ml laminin coated CCPS in small cell aggregates and cultured in NDM for 3 days. In that time neuronal outgrowth of population was prominent. The hydrogel solution was prepared as before to sterile water before adding it on the top of the cells. Gelation was initiated by gently adding NDM.

In addition, cells were seeded onto laminin (10 µg/ml) coated CCPS wells, which served as a positive growth matrix control. Cells seeded on non-treated wells were used as a negative growth matrix control. Cells were cultured with described manners for 4 weeks in total.

2.3. Time-lapse monitoring

For time-lapse imaging, the well plate was transferred into a Cell-IQ® imaging system (Chip-man Technologies Ltd., Tampere, Finland) which allows for continuous monitoring of selected cells as described previously (Narkilahti *et al.* 2007). The sealed culture well plate was placed in a chamber (+36.5°C) with 5% CO_2 gas supply and imaged continuously except during medium changing periods (less than 15 min three times per week). Cells grown on top of, in, or under the hydrogel were monitored for up to 2 weeks with this system.

2.4. Cytotoxicity analysis

After 7 days of culturing, the cells on the top or under of the hydrogels, or 2D controls were stained using the Live/Dead Viability/Cytotoxicity Kit for mammalian cells (Molecular Probes/Invitrogen, Finland). Briefly, the kit stains live cells with the green fluorescence dye

calcein-AM (emission at 488 nm) and dead cells with the red fluorescence dye ethidium homodimer-1 (emission at 568 nm). Cells were incubated with calcein-AM (0.1 μM) and ethidium homodimer-1 (0.5 μM) for 30 minutes and immediately imaged with Olympus IX51 inverted microscope combined with Olympus DB71 digital camera (Olympus, Finland).

2.5. Immunostaining

For immunocytochemistry, cells were fixed with 4% paraformaldehyde (Fluka, Italy) after 4 weeks of culturing and stained with neural markers. Briefly, unspecific staining was blocked with 10% normal donkey serum (NDS, Sigma-Aldrich), 0.1% Triton-X 100 (Sigma-Aldrich), and 1% bovine serum albumin (BSA, Sigma-Aldrich) for 45 min at room temperature. The cells were then washed once with 1% NDS, 0.1% Triton-X, and 1% BSA. Thereafter, the primary antibodies; rabbit anti-microtubule associated protein (MAP-2 1:800, Chemicon International, Millipore, Massachusetts, MA), mouse anti-neurofilament 200 kD (Sigma-Aldrich), monoclonal mouse anti- β -tubulin isotype III (β-tub, 1:1250 Sigma-Aldrich), or sheep anti-human glial fibrillary acidic protein antibody (GFAP, 1:800 R&D systems), Chondroitin Sulfate Proteoglycan (NG-2, 1:200, Chemicon, protocol without Triton-X), and galactocerebrocide (GalC, 1:400 Chemicon, protocol without Triton-X) in 1% NDS, 0.1% Triton-X, and 1% BSA were incubated with cells at +4°C overnight. The following day the cells were washed three times with 1% BSA and secondary antibodies, Alexa Fluor 488 conjugated to anti-rabbit, anti-mouse or anti-sheep (1:400, Molecular Probes) in 1% BSA were added for 1 h at room temperature. Finally, cells were washed three times with PBS and twice with phosphate buffer and mounted with Vectashield containing 4',6-diamidino-2-phenylindole (DAPI, Vector Laboratories, England).

2.6. Confocal imaging

The encapsulated cells were cultured 4 weeks prior to confocal imaging. Confocal images were taken with LSM 700 confocal microscope (Carl Zeiss, Jena, Germany) using a 40× air objective. The stack images were taken in 1 µm range, totally 70 µm thick. The visualization of confocal data was performed with Zen2009 (Carl Zeiss) or BioImageXD (www.bioimagexd.net).

2.7. Electrophysiological measurements

In addition, differentiated neuronal cells encapsulated into hydrogel matrix were plated onto microelectrode array (MEA) plates (Multi Channel Systems, MCS, Reutlingen, Germany). With MEA, extracellular field potentials from electrically active neural cells can be measured. MEA is non-invasive, suitable for prolonged and continuous measurements, and allows the measurements from neuronal network level. Thus, MEAs provide activity information of the neural cell population both in spatial and temporal levels (Potter *et al.* 2001; Wagenaar *et al.* 2006).

Each standard MEA plate contains 59 titanium nitride measurement electrodes (diameter of 30 µm, 200 µm inter-electrode distance). For liquid container and cell seeding area, the electrode areas were separated with in-house designed Poly(dimethyl siloxane) (PDMS) structures designed and manufactured by J. Kreutzer and P. Kallio, Tampere University of Technology,

Department of Automation Science and Engineering, Finland. The control MEA plates were coated with two step coating procedure; overnight incubation with polyethyleneimine (PEI, Sigma-Aldrich, 0.05% w/v, incubation +4°C) followed by washing with sterile water, and overnight incubation with mouse laminin (Sigma-Aldrich, 20 µg/ml, incubation +4°C). Thereafter, neuronal cells were plated as aggregates onto laminin coated MEA plates for 2D standard controls. The cell culture medium was changed three times per week, and MEAs were measured with MEA1060-Inv-BC amplifier (MCS). To keep the temperature at 37°C during measurements, TC02 Temperature controller (MCS) was integrated into system. The data was recorded with MC_Rack-software (MCS). Continuous extracellular field potential data was collected for 20 kHz sampling rate and post-acquisition filtered with 200 Hz high-pass filter. MEA data shows electrical activity of neuronal cells in network level also spatially. Collected spatio-temporal field potential data was post-recording processed with MC_Datatool (MCS) and MATLAB (MathWorks, Natick, MA, USA).

2.8. Statistical analysis

For the statistical analysis, cells were calculated from at least 3 parallel samples, at least 5 images per sample, and at least 50 cells were counted/figure (except in non-coated CCPS where attached cell amount was extremely small). Counted data was statistically analysed with SPSS 19 software (SPSS Inc., Chicago, USA) using Kruskal-Wallis non-parametric test followed by *post-hoc* comparison by Mann-Whitney U-test. A p-value (corrected with alpha spending function) of less than 0.05 was allowed for significance.

3. RESULTS

3.1. Cells cultured in different hydrogel concentrations

To optimize the hydrogel concentration to support the hESC-derived neuronal and astroglial cells, four different hydrogel concentrations was used: 0.05%, 0.10%, 0.15%, and 0.25% (Figure 1 A and B, C and D, E and F, G and H, respectively). Moreover, the cells were cultured on laminin surface (Figure 1 I and J) and non-coated CCPS (Figure 1 K and L). The cells were cultured for 2 weeks on the top of the hydrogel and thereafter either stained with Live/Dead kit or immunostained against MAP-2 and GFAP. The viability of the cells was good on the top of the hydrogel (Figure 1 A, C, E, G,) compared to laminin surface (Figure 1 I). On the non-coated CCPS, the cells did not attach and thus there were only few dead cells left (Figure 1 K). Statistical analysis showed significant difference between non-coated CCPS and all other conditions (gels in density 0.25 %, 0.15 %, 0.10 % or 0.05 %, or 2D laminin surface) in cell survival (Figure 2A). Cell survival was, however, equally good in all conditions when compared to 2D laminin control (Figure 2 A). According to Figure 1 G and H, it is seen that the 0.25% does not support the neural migration as prominently as lower concentrations. The best outgrowth can be seen on 0.10% hydrogel (Figure 1, C and D).

For more detailed characterization, the cells were seeded on top of the gels in density 0.25 %, 0.15 %, 0.10 %, or 0.05 % and were allowed to grow and differentiate for 2 wks. Thereafter, cells were stained against MAP-2 (for neuronal cells) and GFAP (for glial cells), and percentages of neurons vs. glial cells in the gels were calculated. The best neuronal cell ratio and cell survival was found in 0.10% gel structure (Figure 2B). Also, 0.10 % and 0.05% gels supported neuronal cell maturation significantly more than astrocytic maturation (Figure 2C). According to these results, 0.10% PM was chosen for the next experiments.

3.2. The viability of the cells under the hydrogel

The viability of the neuronal cells under the hydrogel was evaluated with Live/Dead-kit. The cells were plated on laminin-coated cell culture wells and cultured for one week during which time the cells were viable and neuronal outgrowth was prominent in all the wells in the study. Thereafter, the 0.10 % PM hydrogel was added on the top of the cells and cells were stained after one week. According to cell viability analysis, cell survival was poorer under the hydrogel (Figure 3A) compared to 2D culturing control on laminin (Figure 3B). However, the neuronal neurites did not withdraw under the gel compared to those without gel (Figure 3C vs. D). Moreover, live cells spread from the cell aggregates and grew long neurites also under the hydrogel.

3.3. 3D growth and maturation of encapsulated cells

In 3D culture, the cells were fully surrounded by hydrogel material thus providing more *in vivo*-like environment for the cells. This affects the migration of the cells as well as the probability for cell-cell interactions and therefore the neuronal network forming capacity. We evaluated the maturation of the cells inside the hydrogel with fluorescence microscopy as well as with confocal microscopy. The neurons seemed to have more *in vivo* -like phenotype including more branched and thicker dendritic processes inside the hydrogel (Figure 3E) compared to laminin surface grown cells (Figure 3F). The cells were spread all over the hydrogel. Figure 3 G shows layer-by-layer reconstruction of stack image that illustrates the cells in various z-levels. Moreover, rendered confocal z-stack image in orthogonal sections

(Figure 3H) shows that during prolonged culturing time in 3D, the neuronal somas translocated in near surface of the PM scaffold while intensive MAP-2 positive neuronal process networks was visible allover the hydrogel structure.

3.4. Suitability of the hydrogel matrix for glial cell types

The different glial cell types of hESC-origin; astrocytes and oligodendrocytes were cultured inside the PM hydrogel. Even though there was quite substantial cell death seen in long term 3D cultures (total of 4 wks), both cell types were able to stay alive inside the hydrogel (Figure 4 A-B). More detailed phenotypical analysis of astroglial and oligodendrocyte precursor markers shows that cells keep their phenotype in gel (Figure 4 C-D).

3.5. Neuronal network forming capability inside the 3D hydrogel

We evaluated the neuronal network forming capability inside the PM gel with MEA platform. The action potentials of the cells were detected with 59 small electrodes on the bottom of the cell culture dish (Figure 5A). The neurons inside the gel were able to form active spontaneously firing networks (Figure 5B) similarly to 2D cultures (Figure 5C). The forming of spontaneous network activity inside the gel took ~4 wks to develop into spike train-like activity whereas in control this activity level was achieved already in 2 weeks. None of the cultures monitored here, however, did develop into synchronous busting level activity that is considered as the final maturation stage of *in vitro* cultured neuronal networks. Both cultures showed training-like electrical activity (Heikkilä *et al.* 2009) after 4 weeks culturing in MEA plates (Figure 5B-C).

4. DISCUSSION

In this study we show for the first time the functionality of the human-derived neuronal cells in 3D *in vitro* environment. We evaluated the viability, growth, maturation, and electrical activity of clinically relevant human neural cell types in prolonged 3D cultures. We showed that neural cells, that is neurons, astrocytes, and oligodendrocytes, were viable under the PM hydrogel. In 3D environment, neuronal cells developed more branched neurite structures compared to 2D culture and thus appeared to resemble better their *in vivo* counterparts. Moreover, 3D cultured neurons were able to form spontaneously functional networks inside the 3D matrix.

During few recent years, the 3D cultures have been developed for *in vitro* models and for the studies related to transplantation therapies. Interconnected neuronal networks in 3D mimic better the *in vivo* environment compared to 2D cultures (Pautot *et al.* 2008). Thus, they can be used in developmental brain research, in development of tissue based biosensors or neurotoxicological and pharmacological *in vitro* models (Preynat-Seauve *et al.* 2009; Xu *et al.* 2009). As brain is relatively soft tissue with elastic modulus of ~500 Pascal (PA) (Lu *et al.* 2006) it is already shown that the used 3D matrix should have similar characteristics in order to support neural growth and differentiation (Saha *et al.* 2008; Teixeira *et al.* 2009). Further, hydrogels offer good option for reconstructing 3D environment suitable for neuronal cells (Brännvall *et al.* 2007; Gelain *et al.* 2006) and it has already been shown that animal-derived neuronal cells stay viable, grow, and mature in 3D hydrogel environment (Brännvall *et al.* 2007; Freudenberg *et al.* 2009; Leipzig *et al.* 2010). We tested PM in concentration ratio from 0.05% to 0.25% to find the optimal 3D culturing parameters. Earlier, it has been shown that 0.25% PM supports neuronal differentiation of human fetal stem cells (Thonhoff *et al.* 2008)

whereas for hESC-derived neuronal cells the optimal concentration seems to be to 0.10% according to our results. This concentration relates approximately to the elastic modulus of 1200 Pa according to earlier studies (Leon *et al.* 1998; Yamaoka *et al.* 2006). We did never, however, reached better culturing in 3D compared to 2D as suggested in recent study using same material and immortalized human fetal stem cells (Ortinau *et al.* 2011). This could be explained by the much more longer follow up time in our study and also by the composition of the cell population which in our case contained mainly neurons vs. glial cells that was opposite in study by Ortinau and colleagues (2011).

In previous studies, neural 3D cultures using hydrogels have been prepared by growing the cells under or top of the hydrogel or within the hydrogel (Gelain *et al.* 2006; Thonhoff *et al.* 2008). Here, we showed that hESC-derived neuronal cells were viable under, top, and inside the 0.10% PM hydrogel. In contrast to recent study (Ortinau *et al.* 2011) we did not see any benefit of functionalization of hydrogel with laminin (data not shown) which we have not either seen in functionalization of polylactide meshes for hESC-derived neuronal cultures (Ylä-Outinen *et al.* 2010). This suggests that the thin, nanoscale mesh-like structure is enough to support growth and maturation of these hESC-derived neuronal cells. Culturing cells encapsulated inside the hydrogel is especially important when designing products for transplantations as the graft should be injectable to enable easy surgical operation to the CNS tissue (Zhong *et al.* 2008). The 0.10% PM supported also growth of encapsulated glial cells, that is astrocytes and oligodendrocytes, which is beneficial for developing multiple cell type 3D *in vitro* models or cell grafts (Park *et al.* 2009; Taylor *et al.* 2005).

There has been few papers comparing the differences of 2D and 3D culturing in genotype - (Li *et al.* 2007), morphological -, and phenotypical level (Crompton *et al.* 2007; Ortinau *et al.* 2011; Thonhoff *et al.* 2008) and very few describing the functional properties of 3D cultured neurons (Mahoney *et al.* 2006; Xu *et al.* 2009). Unfortunately, it is hard to estimate the

differences between 2D and 3D cultures if the control 2D cells have been cultured in plain polystyrene and not on laminin or other coated surface that favors neuronal attachment and growth. Also, the 3D culturing times have been relative short that does not favor neuronal maturation (Ortinau *et al.* 2011) and thus longer follow-up periods are clearly needed (Pautot *et al.* 2008). In our study we follow the formation of neuronal networks inside the PM gel for up to 4 weeks. Importantly, the neurons did stay alive and were able to form networks that were spontaneously active inside the gel as described earlier in 2D (Heikkilä *et al.* 2009). The confocal imaging revealed that neurons did re-organize them selves during 4 weeks as the somas aligned near to the upper surface close to the medium whereas neurites formed intensive networks inside the gel. Moreover, most of the encapsulated cell differentiated into neurons. This further suggests that hESC-derived neuronal cells grown in 3D PM would be suitable source for transplantation that would results in reconstruction of lost neuronal circuits.

Acquisition of an optimal and as much tissue-like environment as possible to neuronal cells for regeneration therapies is highly needed. Matrigel, used in some of the studies, consists of the basal membrane proteins of the mouse cells (Uemura *et al.* 2010). It contains variety of extracellular proteins and thus supports the growth of many cell types including neuronal cells (Thonhoff *et al.* 2008). It is, however, of animal origin and its composition is not defined, and thus is not appropriate for transplantation therapies. PM, on the other hand, has a potential to be used for clinical applications as there is also Good Manufacturing Practice (GMP) level product available (www.puramatrix.com). Neuronal cells have been cultured also with other 3D hydrogels such as hyaluronic acid (Brännvall *et al.* 2007) and chitosan (Leipzig *et al.* 2010). The suitability of those hydrogels as matrixes for clinically relevant human neural cells has not been studied. In addition to our study, two papers (Ortinau *et al.* 2011; Thonhoff *et al.* 2008) have described the suitability of PM as growth matrix for human derived neural cells

suggesting that this material should be further studied for that purpose. Of course, there are still some challenges related to combination of material and cells like drastic pH changes during gelation as well as taking this process into injectable GMP-level form.

In conclusion the cell-biomaterial matrix created in this study can be used for drug screening purposes, toxicological studies due the non-invasive, repetitive functionality analysis of 3D cultured cells as well as for providing new information for tissue engineering and stem cell research.

Acknowledgement

This study was financially supported by the Academy of Finland (Grant 123233), the Competitive Research Funding of the Tampere University Hospital, the Finnish Cultural Foundation/ Pirkanmaa Regional Fund, and the Finnish Funding Agency for Technology and Innovation (StemInClin-project). The MEA system was founded by BioNext Tampere. Authors wish to thank personnel of IBT for their support in stem cell research and particularly, Riikka Äänismaa, PhD and Maria Sundberg, PhD are acknowledged.

Figure legends:

Figure 1. Effect of tested hydrogel concentrations to cells viability and differentiation. Neuronal cells cultured on the top of the PuraMatrix™-hydrogel with concentrations 0.05% (A, B), 0.10% (C,D), 0.15% (E,F), 0.25% (G,H). Cells cultured on the top of laminin coating (I,J) and non-coated cell culture plastic (K,L) were used as reference. In each condition, Live/Dead-analysis (A,C,E,G,I,K) and Immunostaining (B,D,F,H,J,L) was performed. In Immunostaining: MAP-2 = green, GFAP= red, and DAPI=blue. The scalebar is 100 μm.

Figure 2. The viability and phenotype of the cells inside the PuraMatrix hydrogel and control conditions. Live/dead analysis shows the proportions of the viable cells from each population (A). Significant difference is detected between negative control (un-treated polystyrene surface) and other conditions (different gel concentrations and laminin treated surface). The total amount of attached cells and percentages of different neural cell types are illustrated according to gel concentration (0.25%, 0.15%, 0.10%, and 0.05%) or control conditions (non-coated well-plate surface and laminin-treated surface) (B). The percentages of different cell types in correlation to cell density (C). Significant differences detected between MAP-2 positive cells and GFAP and non-neural cell types in densities 0.10% and 0.05 %. Bars are average values and error bars represent standard deviation for all illustrations. For significance: ***: $p<0.05$

Figure 3. Cell survival under the hydrogel and maturation inside the hydrogel. Cells that are cultured first on the top of laminin (one week) and then covered by PuraMatrix™ (after 7 days C) and stained with live/dead kit (A). Laminin cultured cells as a control in live/dead analysis (B) and after 2 weeks of culturing (D). The network formation and morphology of the 4 weeks cultured cells inside the hydrogel (E) and on top of the laminin coating (F). Layer-by-layer reconstruction from MAP-2 positive cells shows cells growing in different z-levels (G) inside the gel. Confocal imaging analysis by orthogonal sectioning from 4 weeks cultured neuronal cells (H). In confocal image, stack with 1 μm interval and total of 70 μm thickness of hydrogel scaffold structure. Scalebars= 100 μm.

Figure 4. Glial cell culturing inside the hydrogel. Astrocytes (A) and oligodendrocyte precursor cells (B) can be cultured inside the PuraMatrix™-hydrogel. Both cell types retain

their typical morphology (enlarged images) in the hydrogel. (C) Immunocytochemical characterization of the astroglial cells with MAP-2 (for neuronal cells) and GFAP (for astrocytic cells) inside the gel. (D) Immunocytochemical characterization of the oligodendroglial cells with NG-2 and GalC inside the gel. Scalebars for background images are 100 μm.

Figure 5. Microelectrode array dish (A). Microelectrode array dish is a cell culture well containing substrate embedded tiny electrodes on the bottom. Cells encapsulated to hydrogel were added on the top of the electrodes and were cultured for several weeks. Array wide raster plot is shown from the cells inside the gel (B) and from laminin surface cultured cells (C). In raster plot each recorded channel is represented in y-axis and time (300s) in x-axis. Each raster shows the detected spike. Both networks in raster plots (B, C) show typical training-like activity in several channels.

References:

Amariglio N, Hirshberg A, Scheithauer BW, Cohen Y, Loewenthal R, Trakhtenbrot L, Paz N, Koren-Michowitz M, Waldman D, Leider-Trejo L, Toren A, Constantini S and Rechavi G. 2009, Donor-derived brain tumor following neural stem cell transplantation in an ataxia telangiectasia patient, *PLoS Med* **6**: e1000029.

Brännvall K, Bergman K, Wallenquist U, Svahn S, Bowden T, Hilborn J and Forsberg-Nilsson K. 2007, Enhanced neuronal differentiation in a three-dimensional collagen-hyaluronan matrix, *J Neurosci Res* **85**: 2138-46.

Crompton KE, Goud JD, Bellamkonda RV, Gengenbach TR, Finkelstein DI, Horne MK and Forsythe JS. 2007, Polylysine-functionalised thermoresponsive chitosan hydrogel for neural tissue engineering, *Biomaterials* **28**: 441-9.

Freudenberg U, Hermann A, Welzel PB, Stirl K, Schwarz SC, Grimmer M, Zieris A, Panyanuwat W, Zschoche S, Meinhold D, Storch A and Werner C. 2009, A star-PEG-heparin hydrogel platform to aid cell replacement therapies for neurodegenerative diseases, *Biomaterials* **30**: 5049-60.

Gelain F, Bottai D, Vescovi A and Zhang S. 2006, Designer self-assembling peptide nanofiber scaffolds for adult mouse neural stem cell 3-dimensional cultures, *PLoS One* **1**: e119.

Heikkilä TJ, Ylä-Outinen L, Tanskanen JM, Lappalainen RS, Skottman H, Suuronen R, Mikkonen JE, Hyttinen JA and Narkilahti S. 2009, Human embryonic stem cell-derived neuronal cells form spontaneously active neuronal networks in vitro, *Exp Neurol* **218**: 109-16.

Hejcl A, Lesny P, Pradny M, Michalek J, Jendelova P, Stulik J and Sykova E. 2008, Biocompatible hydrogels in spinal cord injury repair, *Physiol Res* **57 Suppl 3**: S121-32.

Hicks AU, Lappalainen RS, Narkilahti S, Suuronen R, Corbett D, Sivenius J, Hovatta O and Jolkkonen J. 2009, Transplantation of human embryonic stem cell-derived neural precursor cells and enriched environment after cortical stroke in rats: cell survival and functional recovery, *Eur J Neurosci* **29**: 562-74.

Holmes TC, de Lacalle S, Su X, Liu G, Rich A and Zhang S. 2000, Extensive neurite outgrowth and active synapse formation on self-assembling peptide scaffolds, *Proc Natl Acad Sci U S A* **97**: 6728-33.

Hu BY, Weick JP, Yu J, Ma LX, Zhang XQ, Thomson JA and Zhang SC. 2010, Neural differentiation of human induced pluripotent stem cells follows developmental principles but with variable potency, *Proc Natl Acad Sci U S A* **107**: 4335-40.

Johnstone AF, Gross GW, Weiss DG, Schroeder OH, Gramowski A and Shafer TJ. 2010, Microelectrode arrays: a physiologically based neurotoxicity testing platform for the 21st century, *Neurotoxicology* **31**: 331-50.

Lappalainen RS, Salomaki M, Yla-Outinen L, Heikkila TJ, Hyttinen JA, Pihlajamaki H, Suuronen R, Skottman H and Narkilahti S. 2010, Similarly derived and cultured hESC lines show variation in their developmental potential towards neuronal cells in long-term culture, *Regen Med* **5**: 749-62.

Leipzig ND, Wylie RG, Kim H and Shoichet MS. 2010, Differentiation of neural stem cells in three-dimensional growth factor-immobilized chitosan hydrogel scaffolds, *Biomaterials* **32**: 57-64.

Leon EJ, Verma N, Zhang S, Lauffenburger DA and Kamm RD. 1998, Mechanical properties of a self-assembling oligopeptide matrix, *J Biomater Sci Polym Ed* **9**: 297-312.

Li GN, Livi LL, Gourd CM, Deweerd ES and Hoffman-Kim D. 2007, Genomic and morphological changes of neuroblastoma cells in response to three-dimensional matrices, *Tissue Eng* **13**: 1035-47.

Li SC and Zhong JF. 2009, Twisting immune responses for allogeneic stem cell therapy, *World J Stem Cells* **1**: 30-35.

Lindvall O and Kokaia Z. 2010, Stem cells in human neurodegenerative disorders--time for clinical translation?, *J Clin Invest* **120**: 29-40.

Lu YB, Franze K, Seifert G, Steinhauser C, Kirchhoff F, Wolburg H, Guck J, Janmey P, Wei EQ, Kas J and Reichenbach A. 2006, Viscoelastic properties of individual glial cells and neurons in the CNS, *Proc Natl Acad Sci U S A* **103**: 17759-64.

Mahoney MJ and Anseth KS. 2006, Three-dimensional growth and function of neural tissue in degradable polyethylene glycol hydrogels, *Biomaterials* **27**: 2265-74.

Narkilahti S, Rajala K, Pihlajamaki H, Suuronen R, Hovatta O and Skottman H. 2007, Monitoring and analysis of dynamic growth of human embryonic stem cells: comparison of automated instrumentation and conventional culturing methods, *Biomed Eng Online* **6**: 11.

Nisbet DR, Crompton KE, Horne MK, Finkelstein DI and Forsythe JS. 2008, Neural tissue engineering of the CNS using hydrogels, *J Biomed Mater Res B Appl Biomater* **87**: 251-63.

Oizumi H, Hayashita-Kinoh H, Hayakawa H, Arai H, Furuya T, Ren YR, Yasuda T, Seki T, Mizuno Y and Mochizuki H. 2008, Alteration in the differentiation-related molecular expression in the subventricular zone in a mouse model of Parkinson's disease, *Neurosci Res* **60**: 15-21.

Ortinau S, Schmich J, Block S, Liedmann A, Jonas L, Weiss DG, Helm CA, Rolfs A and Frech MJ. 2011, Effect of 3D-scaffold formation on differentiation and survival in human neural progenitor cells, *Biomed Eng Online* **9**: 70.

Park J, Koito H, Li J and Han A. 2009, Microfluidic compartmentalized co-culture platform for CNS axon myelination research, *Biomed Microdevices* **11**: 1145-53.

Pautot S, Wyart C and Isacoff EY. 2008, Colloid-guided assembly of oriented 3D neuronal networks, *Nat Methods* **5**: 735-40.

Potter SM and DeMarse TB. 2001, A new approach to neural cell culture for long-term studies, *J Neurosci Methods* **110**: 17-24.

Preynat-Seauve O, Suter DM, Tirefort D, Turchi L, Virolle T, Chneiweiss H, Foti M, Lobrinus JA, Stoppini L, Feki A, Dubois-Dauphin M and Krause KH. 2009, Development of human nervous tissue upon differentiation of embryonic stem cells in three-dimensional culture, *Stem Cells* **27**: 509-520.

Saha K, Keung AJ, Irwin EF, Li Y, Little L, Schaffer DV and Healy KE. 2008, Substrate modulus directs neural stem cell behavior, *Biophys J* **95**: 4426-38.

Sundberg M, Jansson L, Ketolainen J, Pihlajamaki H, Suuronen R, Skottman H, Inzunza J, Hovatta O and Narkilahti S. 2009, CD marker expression profiles of human embryonic stem cells and their neural derivatives, determined using flow-cytometric analysis, reveal a novel CD marker for exclusion of pluripotent stem cells, *Stem Cell Res* **2**: 113-24.

Sundberg M, Skottman H, Suuronen R and Narkilahti S. 2010, Production and isolation of NG2+ oligodendrocyte precursors from human embryonic stem cells in defined serum-free medium, *Stem Cell Res* **5**: 91-103.

Takahashi K, Tanabe K, Ohnuki M, Narita M, Ichisaka T, Tomoda K and Yamanaka S. 2007, Induction of pluripotent stem cells from adult human fibroblasts by defined factors, *Cell* **131**: 861-72.

Taylor AM, Blurton-Jones M, Rhee SW, Cribbs DH, Cotman CW and Jeon NL. 2005, A microfluidic culture platform for CNS axonal injury, regeneration and transport, *Nat Methods* **2**: 599-605.

Teixeira AI, Ilkhanizadeh S, Wigenius JA, Duckworth JK, Inganas O and Hermanson O. 2009, The promotion of neuronal maturation on soft substrates, *Biomaterials* **30**: 4567-72.

Thonhoff JR, Lou DI, Jordan PM, Zhao X and Wu P. 2008, Compatibility of human fetal neural stem cells with hydrogel biomaterials in vitro, *Brain Res* **1187**: 42-51.

Uemura M, Refaat MM, Shinoyama M, Hayashi H, Hashimoto N and Takahashi J. 2010, Matrigel supports survival and neuronal differentiation of grafted embryonic stem cell-derived neural precursor cells, *J Neurosci Res* **88**: 542-51.

Wagenaar DA, Pine J and Potter SM. 2006, An extremely rich repertoire of bursting patterns during the development of cortical cultures, *BMC Neurosci* **7**: 151–156.

Xu T, Molnar P, Gregory C, Das M, Boland T and Hickman JJ. 2009, Electrophysiological characterization of embryonic hippocampal neurons cultured in a 3D collagen hydrogel, *Biomaterials* **30**: 4377-83.

Yamaoka H, Asato H, Ogasawara T, Nishizawa S, Takahashi T, Nakatsuka T, Koshima I, Nakamura K, Kawaguchi H, Chung UI, Takato T and Hoshi K. 2006, Cartilage tissue engineering using human auricular chondrocytes embedded in different hydrogel materials, *J Biomed Mater Res A* **78**: 1-11.

Ylä-Outinen L, Heikkilä J, Skottman H, Suuronen R, Äänismaa R and Narkilahti S. 2010, Human cell-based micro electrode array platform for studying neurotoxicity, *Front Neuroeng* **3**: 1-9.

Ylä-Outinen L, Mariani C, Skottman H, Suuronen R, Harlin A and Narkilahti S. 2010, Electrospun Poly(L,D-lactide) Scaffolds Support the Growth of Human Embryonic Stem Cell-derived Neuronal Cells, *The Open Tissue Engineering and Regenerative Medicine Journal* **3**: 1-9.

Zeng X, Chen J, Deng X, Liu Y, Rao MS, Cadet JL and Freed WJ. 2006, An in vitro model of human dopaminergic neurons derived from embryonic stem cells: MPP+ toxicity and GDNF neuroprotection, *Neuropsychopharmacology* **31**: 2708-15.

Zhang S. 2002, Emerging biological materials through molecular self-assembly, *Biotechnol Adv* **20**: 321-39.

Zhang S, Gelain F and Zhao X. 2005, Designer self-assembling peptide nanofiber scaffolds for 3D tissue cell cultures, *Semin Cancer Biol* **15**: 413-20.

Zhong Y and Bellamkonda RV. 2008, Biomaterials for the central nervous system, *J R Soc Interface* **5**: 957-75.

Äänismaa R, Ylä-Outinen L, Mikkonen JE and Narkilahti S (2011). Human pluripotent stem cell-derived neuronal networks: their electrical functionality and usability for modelling and toxicology, InTech.

Figure 1.

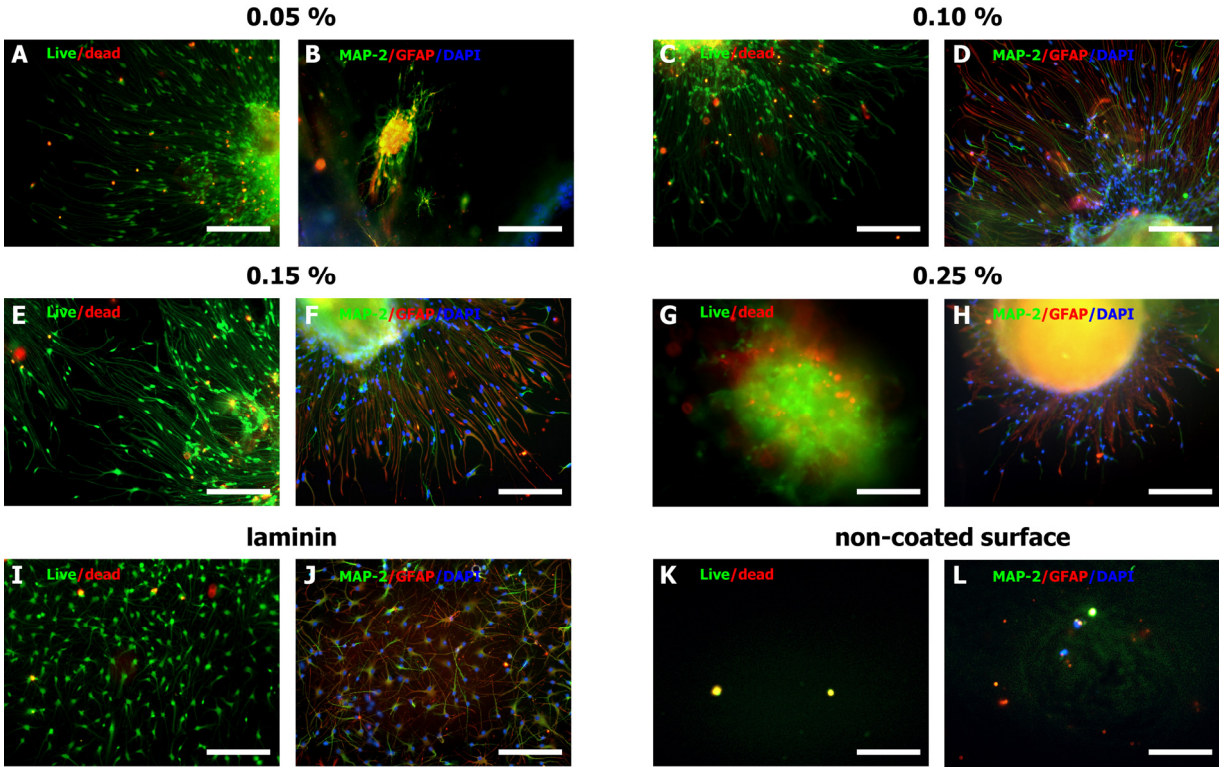
0.05 %
A Live/daad
B MAP-2/GFAP/DAPI
0.10 %
C Live/dead
D MAP-2/GFAP/DAPI
0.15 %
E Live/dead
F MAP-2/GFAP/DAPI
0.25 %
G Live/dead
H MAP-2/GFAP/DAPI
laminin
I Live/dead
J MAP-2/GFAP/DAPI
non-coated surface
K Live/dead
L MAP-2/GFAP/DAPI

Figure 2.

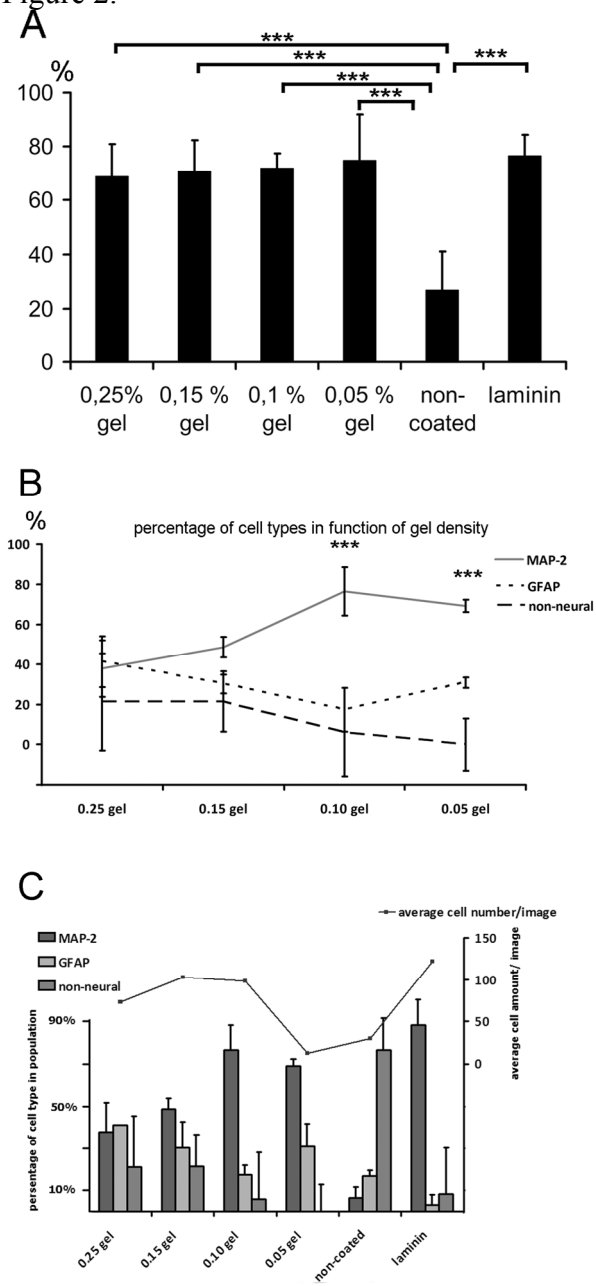
A
%
100
80
60
40
20
0
***
***
***
***
***
0,25% gel
0,15 % gel
0,1 % gel
0,05 % gel
non-coated
laminin
B
%
percentage of cell types in function of gel density
MAP-2
GFAP
non-neural
***
***
0.25 gel
0.15 gel
0.10 gel
0.05 gel
C
average cell number/image
MAP-2
GFAP
non-neural
persentage of cell type in population
average cell amount/ image
90%
50%
10%
150
100
50
0
0.25 gel
0.15 gel
0.10 gel
0.05 gel
non-coated
laminin

Figure 3.

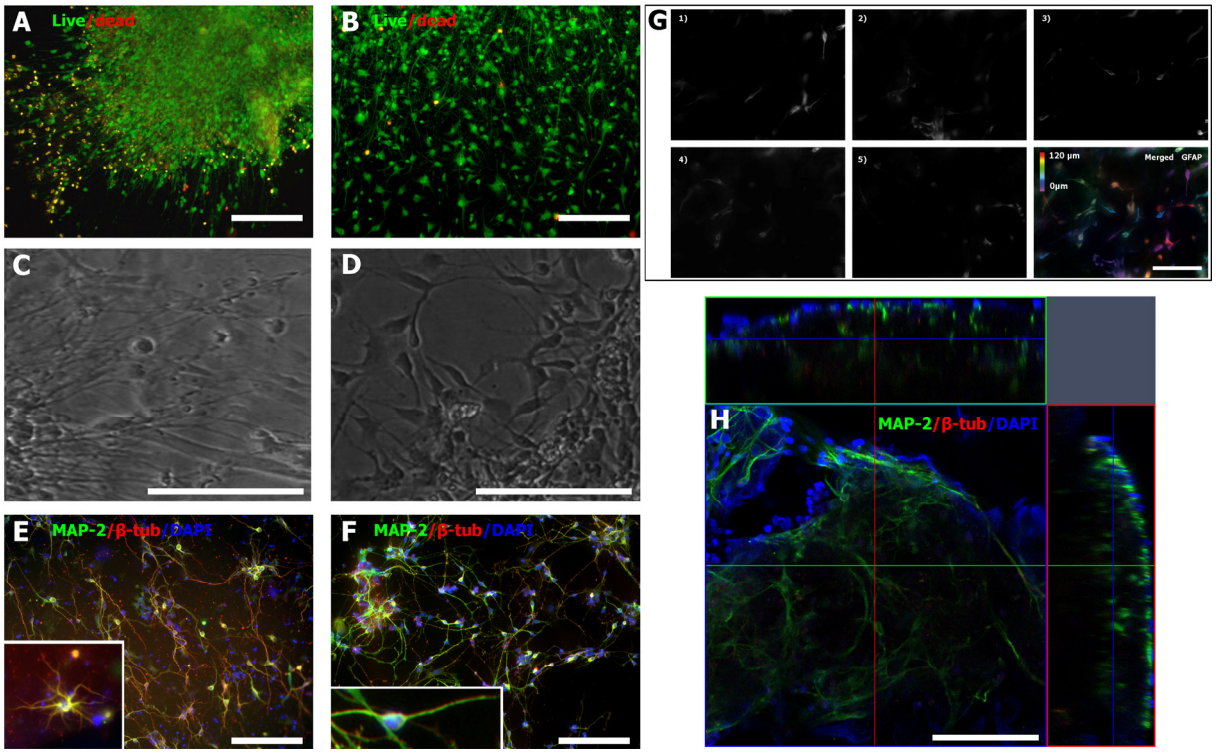
A
Live/dead
B
Live/dead
C
D
E
MAP-2/β-tub/DAPI
F
MAP-2/β-tub/DAPI
G
1)
2)
3)
4)
5)
120 µm
0µm
Merged GFAP
H
MAP-2/β-tub/DAPI

Figure 4.

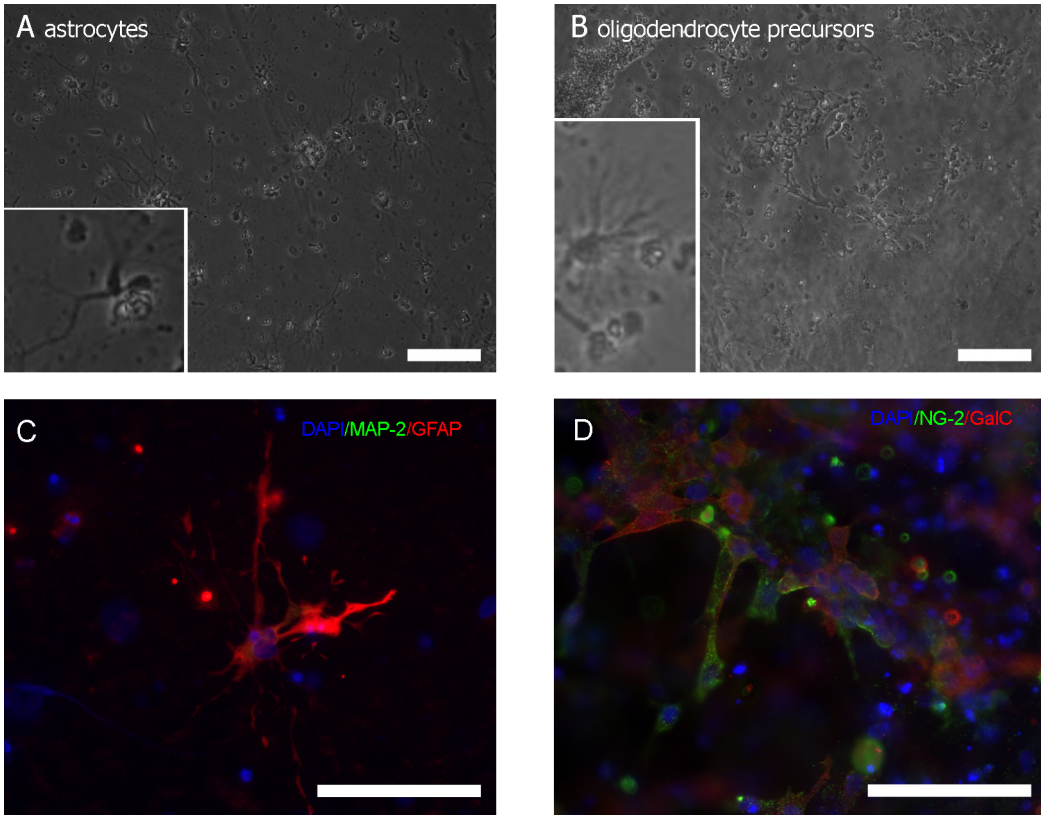
A astrocytes
B oligodendrocyte precursors
C
DAPI/MAP-2/GFAP
D
DAPI/NG-2/GalC

Figure 5.

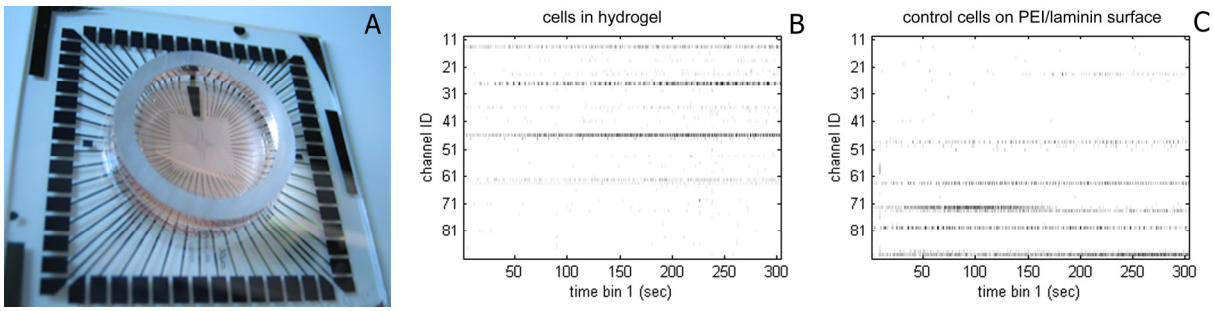
A
cells in hydrogel
B
control cells on PEI/laminin surface
C
channel ID
11
21
31
41
51
61
71
81
50
100
150
200
250
300
time bin 1 (sec)